# Niemann-Pick Type C disease: protective mechanisms from neurodegeneration and targets for therapeutic intervention

by

Chan Chung

A dissertation submitted in partial fulfillment
of the requirements for the degree of
Doctor of Philosophy
(Molecular and Cellular Pathology)
in the University of Michigan
2016

Doctoral Committee:

Professor Andrew P. Lieberman, Chair
Associate Professor David B. Lombard
Professor Jack M. Parent
Assistant Professor Vikram G. Shakkottai
Professor Joel A. Swanson

# Dedication

This dissertation is dedicated to all Niemann-Pick disease patients and their families, especially the patient's family who shared the progress of a disease in 2011 NPC conference. Whenever I was faced with an unexpected difficulty in my research, I remembered they were fighting a disease and I could get over a difficulty.

## Acknowledgements

Firstly, I would like to express my sincere gratitude to my mentor, Prof. Andy Lieberman, not only for the continuous support of my Ph.D. study but also for his patience and motivation. His guidance helped me in all the time of research and writing of this thesis. I could not have imagined having a better mentor for my Ph.D. study. In future, I wish to be a mentor like him. Also, due to his deep consideration, I could kill two birds (research and marriage).

Besides my mentor, I would like to thank my thesis committee members: Prof. Jack Parent, Prof. David Lombard, Prof. Vikram Shakkottai, and Prof. Joel Swanson, for their insightful comments and encouragement as well as for deep questions which incented me to widen my research from various perspectives. Your expertise helped guide my growth as a scientist during my Ph.D. study.

My sincere thanks also goes to Prof. Zaneta Nikolovska-Coleska, and Mrs. Laura Labut, for their kind assistance and support in the Department of Pathology. Especially, I thank Prof. Nicholas Lukacs, who is a former director of Molecular and Cellular Pathology graduate program. Without his tremendous advice and help, I could not survive from tight first-year Ph.D. coursework.

I take this opportunity to express gratitude to all current and former labmates, Mark Schultz, Prasanth Puthanveetil**,** Kelsey Krus, Satya Reddy**,** Zhigang Yu**,** Varuna Banduseela, Kotaro Komori, Samir Nath, Ting Yu, Matthew Elrick, Brittany Dixon, and Elisa Giorgetti. Without their precious support, it would not be possible to conduct this research. In particular, I

am grateful to Mark and Prasanth for scientific and non-scientific discussion to expand my intellectual horizon. I also appreciate Ting and Matt for showing me many new and valuable experimental methods. In addition, I would like to thank James Dell'Orco and Brian Gregorka. My completion of this project could not have been accomplished without their collaboration.

To my caring, loving, and supportive wife, Boyoung: my deepest gratitude. When the times got rough, your encouragement was much appreciated. It was a great comfort and relief to know that you were willing to provide management of our household activities and to take care of me and our son while I completed my work. Owing to your unwavering love, patience and support, I could follow my interest as a scientist without worry. My heartfelt thanks. And, I thank my son, Sunwoo, for giving me the opportunity to be a father and the supreme happiness.

Last but not the least, I would like to thank my family: my mother, parents-in-law, sister, brother-in-law, nieces, uncles and aunts for supporting me spiritually throughout writing this thesis and my life in general. Without their unceasing encouragement, support and attention, it would be impossible to keep studying what I longed for. And, I am sorry to my father and grandmother because I was not with them when they passed away.

I am also grateful to my friends. In particular, I thank Geunyoung, who stuck by me during difficult times or good times.

Finally, I am grateful to the God for the good health and well-being that were necessary to complete Ph.D. study.

# Table of Contents

# List of Figures

**Figure**

# List of Tables

**Table**

## List of Abbreviations

17-allylamino-17-demethoxygeldanamycin (17-AAG)

1-methyl-4-phenylpyridinium (MPP)

4',6-diamidino-2-phenylindole (DAPI)

Acid sphingomyelinase (ASM)

Adeno-associated virus serotype 2 (AAV2)

Adenosine triphosphate (ATP)

Apoptotic protease-activating factor (Apaf-1)

Ask1 (apoptosis signal regulated kinase 1)

Avidin-Biotin Complex (ABC)

Bis (monoacylglycero) phosphate (BMP)

Bovine serum albumin (BSA)

CA-074 methyl ester (CA-074ME)

CNS (Central nervous system)

Cystatin B (CSTB)

Daxx (Death-Domain Associated Protein)

Deoxyribonucleic acid (DNA)

Diacylglycerol (DAG)

Dimethyl sulfoxide (DMSO)

Endoplasmic reticulum (ER)

Feline immunodeficiency virus (FIV)

Fetal bovine serum (FBS)

Gene ontology (GO)

GFAP (Glial fibrillary acidic protein)

Glyceraldehyde-3-Phosphate Dehydrogenase (GAPDH)

Green fluorescent protein (GFP)

Heat shock protein 70 (HSP70)

Heat shock protein 90 (HSP90)

Heat shock protein beta-1 (HSPB1)

Heat shock proteins (HSPs)

Hemagglutinin (HA)

Inositol-1, 4, 5-trisphosphate ($IP_3$)

Ionized calcium-binding adapter molecule 1 (IBA1)

LAMP-1 (Lysosomal-associated membrane protein 1)

LAPF (lysosome-associated and apoptosis-inducing protein containing PH and FYVE domains)

Late endosomes (LE)

Late endosomes and lysosomes (LE/Lys)

Lethal concentration 50 (LC50)

Low density lipoprotein (LDL)

Lysosomal membrane permeabilization (LMP)

Lysosomes (LY)

Mannose-6-phosphate receptors (MPR)

Mitogen-activated protein kinase-activated protein kinase-2 and 3 (MAPKAPK2/3)

Mitogen-activated protein kinases (MAPK)

Nerve growth factor (NGF)

Niemann-Pick type A (NPA)

Niemann-Pick type B (NPB)

Niemann-Pick type C (NPC)

Niemann-Pick type C1 disease (NPC1 disease)

Non-targeted (NT)

Optimal Cutting Temperature (OCT)

Phosphate-buffered saline (PBS)

Phosphatidylinositol-4,5-bisphosphate 3-kinase (PI3-kinase)

Phosphatidylinositol-specific phospholipase C, X domain containing 2 (PLCXD2)

Phospholipase C (PLC)

Protein kinase C, delta (PKCδ)

Protein kinase D (PKD)

Radioimmunoprecipitation assay buffer (RIPA buffer*)*

Reactive oxygen species (ROS)

Recombinant heat shock protein 70 (rHSP70)

Rough endoplasmic reticulum (RER)

Short hairpin RNA (shRNA)

Significance Analysis of Microarrays (SAM)

Small interfering RNA (siRNA)

Sodium dodecyl sulfate polyacrylamide gel electrophoresis (SDS-PAGE)

Sphingosine 1-phosphate phosphatase 2 (Sgpp2)

Standard deviation (SD)

Standard error of the mean (SEM)

Superoxide dismutase 2 (SOD2)

Trans-Golgi network (TGN)

Tumor necrosis factor (TNF)

Urokinase-type plasminogen activator (uPAR)

Wild type (WT)

## Abstract

Niemann-Pick type C (NPC) disease is a lysosomal storage disorder that causes progressive neurodegeneration and early death, often in children. The two disease-causing proteins, NPC1 and NPC2, are involved in the movement of unesterified cholesterol out of late endosomes and lysosomes (LE/Lys). Loss-of-function mutations in the *NPC1* or *NPC2* genes lead to the accumulation of unesterified cholesterol and glycosphingolipids in LE/Lys. NPC disease is characterized by severe neurological symptoms including ataxia, cognitive decline, seizures, dystonia, and vertical gaze palsy. The mechanism underlying this neurodegeneration has not been identified, and there is no effective treatment for the disease. This dissertation aims to characterize a pathway leading to neuronal death and several modifier genes that promote neuronal survival in NPC disease. This work may provide a foundation for future studies that could lead to the development of novel therapies.

Chapter 1 introduces the genetics and pathology of NPC disease, and reviews lysosomal proteases and heat shock protein beta-1 (HSPB1). After reviewing the known factors involved in NPC disease, chapter 2 presents studies demonstrating that cystatin B (CSTB), an endogenous inhibitor of cathepsins B, H, and L, protects Purkinje cells against cerebellar degeneration in a mouse model of NPC disease. To accomplish this, the effect of CSTB deficiency on cathepsin activity in NPC patient fibroblasts is shown first. Next, the neuropathology is investigated in *Cstb* null mice that are also deficient in *Npc1* globally or specifically within Purkinje cells. These data demonstrate a marked exacerbation of neuron loss in double mutant mice. In addition,

analyses demonstrate that lysosomal membrane permeabilization induces leakage of lysosomal contents, leading to apoptosis in Purkinje cells in the diseased cerebellum.

Chapter 3 presents research that seeks to identify genes that may be neuroprotective or create vulnerability in the NPC brain, using the Allen Brain Atlas. One candidate gene, *HSPB1,* is confirmed to promote neuronal survival in cellular models of NPC disease, and the mechanism by which HSPB1 protects cells from NPC deficiency is shown. Studies also determine the effect of *HSPB1* over-expression on an NPC mouse model by conducting behavioral and histological examinations. In addition, phosphorylation of HSPB1 is found to be tightly associated with Purkinje cell rescue. The modulatory effect of Hspb1 on neurodegeneration *in vivo* is confirmed using *Hspb1* knockdown. Finally, chapter 4 summarizes these findings, discusses relevant questions that remain open, and suggests future directions for work in this area. The work described in this thesis will help us understand the pathways leading to neurodegeneration in NPC disease. It is my hope that this knowledge will enable the identification of targets for the future development of disease modifying therapies.

# Chapter 1

## Introduction

Niemann-Pick disease is a group of inherited lysosomal disorders that is characterized by defects in intracellular lipid trafficking. As a result, patients' lipid metabolism— which encompasses the breakdown, transport, and use of fats and cholesterol in the body—is abnormal. Niemann-Pick disease causes an accumulation of harmful amounts of lipids in the spleen, liver, lungs, bone marrow, and brain. It is divided into three main types: A, B, and C.

Niemann-Pick types A and B (NPA and NPB) are caused by loss of function mutations in the gene encoding acid sphingomyelinase (ASM), the enzyme which converts sphingomyelin into ceramide in lysosomes. A deficiency in ASM causes an accumulation of sphingomyelin in lysosomes, resulting in cell death and the malfunction of major organ systems, eventually leading to early death. Although both NPA and NPB are caused by ASM deficiency, the clinical symptoms in affected patients are remarkably different. NPA patients produce little or no ASM, causing abdominal swelling and severe neurologic disease that leads to death, usually by 2 to 4 years of age. In contrast, NPB patients produce approximately 10% of the normal amount of ASM, which leads to almost no nervous system involvement. They survive into adulthood with health complications, including enlarged livers and spleens and respiratory problems. The

enlargement of organs and repeated respiratory infections can cause cardiovascular stress and lead to heart disease (Schuchman and Wasserstein, 2015).

Niemann-Pick type C (NPC) is caused by loss of function mutations in a pair of proteins called NPC1 (Carstea et al., 1997) and NPC2 (Naureckiene et al., 2000). These proteins appear to be essential for the movement of unesterified cholesterol out of late endosomes and lysosomes (LE/Lys). A deficiency of either of these proteins causes cholesterol and sphingolipid accumulation in LE/Lys. Ninety-five percent of NPC patients have mutations in the gene encoding NPC1 (Patterson et al., 2012). NPC disease is characterized by ataxia, cognitive decline, seizures, dystonia, vertical gaze palsy and early mortality (Pacheco and Lieberman, 2008). A few available drugs provide symptomatic relief but do not alter the course of the disease.

### 1.1 Niemann-Pick type C

NPC disease is an autosomal recessive neurodegenerative disorder with an estimated minimum incidence of 1 per 120 000 live births (Vanier, 2010). Loss of function mutations in *NPC1* or *NPC2* produce a similar biochemical phenotype characterized by the accumulation of unesterified cholesterol in LE/Lys; these lipids are derived from internalized low density lipoprotein (LDL) particles. Under normal conditions, LDL particles are internalized by cell surface receptors and hydrolyzed into unesterified cholesterol in the endocytic compartment. The unesterified cholesterol is then transported to the cell surface or to the endoplasmic reticulum, the site of cholesterol esterification. Both NPC1 and NPC2 are involved in the movement of unesterified cholesterol out of LE/Lys.

### 1.1.1 Genetics

The NPC1 protein is localized to the limiting membranes of LE/Lys and is a large multipass glycoprotein comprising 1278 amino acids. It consists of 13 transmembrane domains, three large lumenal loops (amino acids 25–264, 370–621, and 854–1098), a sterol-sensing domain (amino acids 616–797), and a cytoplasmic C-terminal lysosomal targeting motif (Davies and Ioannou, 2000). The first N-terminal lumenal loop forms a hydrophobic pocket containing a cholesterol binding site (Kwon et al., 2009). The second lumenal loop binds to the NPC2 protein (Deffieu and Pfeffer, 2011), while the third lumenal domain is known as a cysteine-rich loop. Interestingly, approximately one-third of all identified human mutations are located in this loop (Park et al., 2003). The C-terminal tail of NPC1 interacts with the clathrin adaptor AP-1 via a dileucine motif. This interaction appears to be important in the targeting and functioning of LE/Lys (Poirier et al., 2013). The sterol-sensing domain is located between the third and seventh transmembrane domains (Davies and Ioannou, 2000). It must function properly for NPC1 to bind to cholesterol (Ohgami et al., 2004) and for cholesterol homeostasis to occur **(Figure 1.1)** (Millard et al., 2005).

NPC2 is a small soluble glycoprotein comprising 151 amino acids. It is located within lysosomes, binding to cholesterol with high affinity in a 1:1 molar ratio (Xu et al., 2007) and facilitating the rapid transfer of cholesterol—but not glycosphingolipids, oleic or palmitic acids, or cholesterol oleate—between liposomes or membranes in vitro. In an acidic environment, cholesterol is rapidly transferred from NPC2 into membranes containing a bis (monoacylglycero) phosphate (BMP) or an anionic phospholipid (Cheruku et al., 2006). Without NPC2, NPC1 can transfer cholesterol to liposomes bidirectionally but very slowly (Infante et al., 2008; Kwon et al., 2009). Unesterified cholesterol binds to the hydrophobic pocket of NPC2, which is

sandwiched between the two β-sheets of NPC2 (Friedland et al., 2003). The binding of NPC2 to cholesterol reaches NPC1 in the limiting membrane and transfers cholesterol from its 3ß-hydroxyl moiety through a hand-off mechanism. During this process, it is likely that NPC2 binds transiently to NPC1 **(Figure 1.1)** (Deffieu and Pfeffer, 2011).

**Figure 1.1 Model of NPC1/NPC2 function and NPC1 structure**

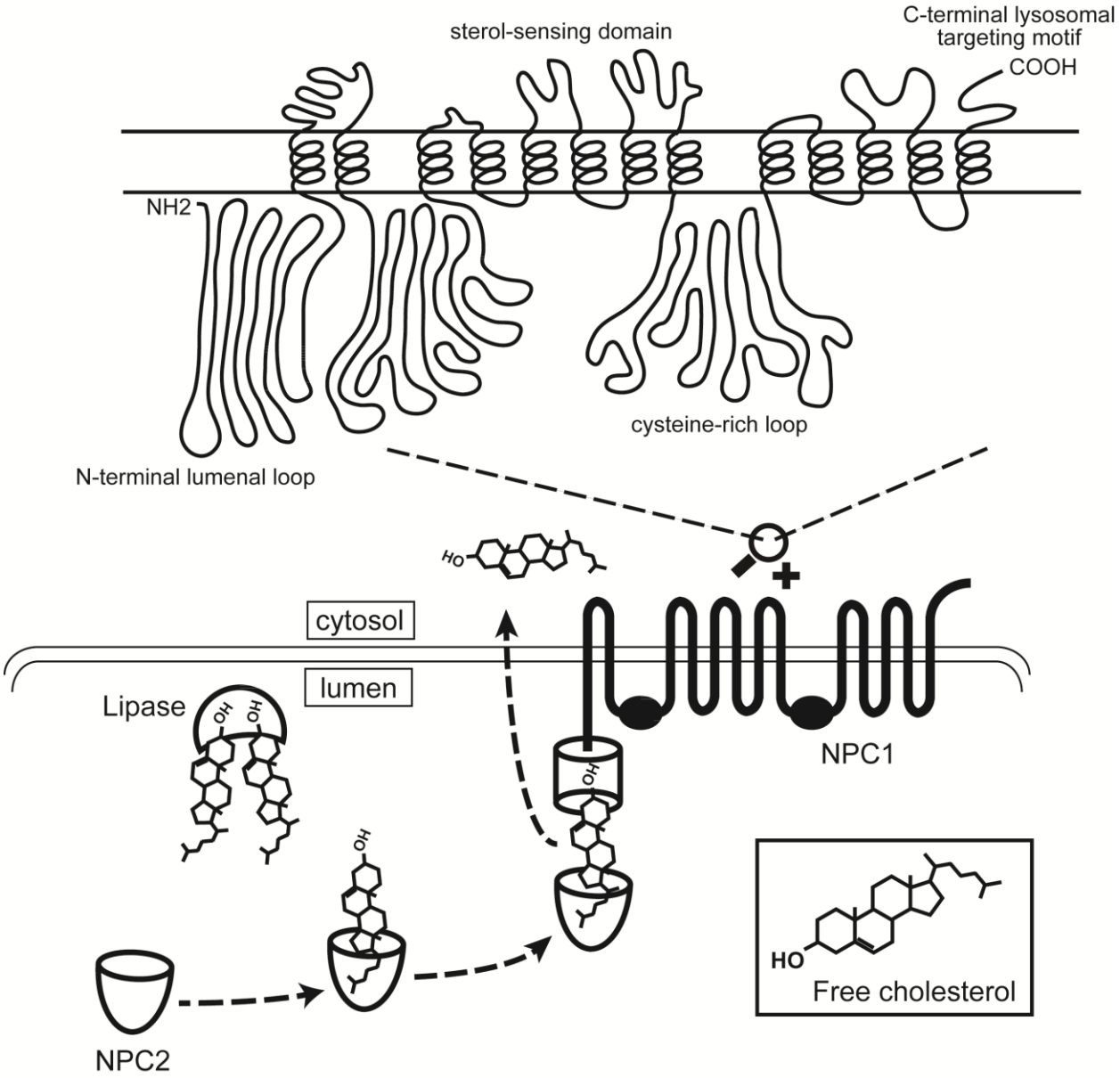

### 1.1.2 Clinical presentation

Because NPC1 and NPC2 are involved in the movement of unesterified cholesterol out of LE/Lys, a defect in either of the two proteins will lead to a progressive accumulation of unesterified cholesterol in the endolysosomal compartment. As noted above, approximately 95 % of NPC patients have NPC1 mutations, and the remaining patients have NPC2 mutations. Although Niemann-Pick type C1 disease (NPC1 disease) and NPC2 disease have different genetic causes, the signs and symptoms are very similar. Disease caused by NPC1 and NPC2 deficiency usually becomes apparent in childhood, although signs and symptoms can develop any time from early infancy to adulthood. Patients usually have difficulty coordinating movements (ataxia), an inability to move their eyes vertically (vertical supranuclear gaze palsy), abnormal muscle tone (dystonia), enlarged spleens and livers, and interstitial lung disease. Patients also have problems with speech and swallowing that worsen over time, eventually interfering with feeding. Affected individuals often experience progressive decline in intellectual function and about one-third have seizures. A child who shows symptoms before age 1 may not live to school age. Those who show symptoms after entering school may live into their mid- to late teens. Some patients may live into their 20s and beyond. Although research has progressed since the gene was discovered in 1997, only one FDA-approved drug (miglustat) exists for the treatment of NPC1 and NPC2. It provides mild symptomatic reduction but does not alter the course of the disease.

## 1.2 Lysosomal proteases (cathepsins)

The lysosome is a critical organelle involved in NPC pathogenesis. It is a bilayer-membrane-limited organelle that contains several hydrolytic enzymes in an acidic lumen

(Settembre et al., 2013). More than 50 diseases related to lysosome dysfunction have been reported since Christian de Duve discovered the lysosome in 1955 (De Duve et al., 1955; Schultz et al., 2011). *Lysosome* means digestive body in Greek, and, as the name implies, lysosomes are the main digestive organelles in eukaryotic cells. Lysosomes degrade intracellular and extracellular macromolecules within their lumina. Intracellular molecules are targeted for lysosomal degradation through autophagy, while extracellular cargo is delivered to the lysosome by endocytosis or phagocytosis (de Duve, 2005). In order to efficiently degrade biological macromolecules, lysosomes contain 50 soluble acidic hydrolases, including proteases, lipases, nucleases, glycosidases, phospholipases, phosphatases, and sulfatases (Bainton, 1981; Journet et al., 2002). Among the lysosomal hydrolases, of particular importance are lysosomal proteases called cathepsins. Cathepsins are classified by their catalytic mechanism: aspartic, serine, threonine, metallo, and cysteine (Pislar and Kos, 2014). Eleven human cysteine cathepsins (B, C, F, H, L, K, O, S, V, W, X/Z) constitute the largest cathepsin family. All cysteine cathepsins were identified in the human genome and characterized by molecular function and structure (Turk et al., 2012).

Among cysteine cathepsins, cathepsin B is the most abundant lysosomal protease. It performs a housekeeping function required for protein turnover, digesting cell proteins, chromatin, complex carbohydrates, and lipids. Cathepsin B is synthesized as a zymogen, which is an inactive enzyme precursor, and is processed to the mature form by autocatalysis or by the action of other proteases. Preprocathepsin B, which consists of 17 amino acids in the pre-part, 62 amino acids in the pro-part, and 252 amino acids in the mature part, is synthesized on the rough endoplasmic reticulum (RER) (Kirschke et al., 1995; Mort and Buttle, 1997). Preprocathepsin B is translocated into the lumen of the RER by the 17 amino acids in the pre-part, which is also

called the signal peptide. Procathepsin B, an inactive 43/46 kDa precursor form, is formed by removal of the signal peptide and is glycosylated at two asparagine residues with high-mannose glycans in the RER lumen. Procathepsin B is then transported to the Golgi apparatus, and processed by modification of mannose residues to mannose-6-phosphate. The phosphorylated protein binds to mannose-6-phosphate receptors (MPR) in the trans-Golgi network (TGN) and is transported to lysosomes via transport vesicles. In an acidic environment, procathepsin B can undergo autocatalytic activation as a result of proteolytic cleavage and dissociation of the propeptide. The removal of the propeptide generates a 31 kDa mature single chain form of cathepsin B. A proteolytic cleavage between residues 47 and 50 and the excision of the dipeptide generates the double chain form, comprising a heavy chain of 25 kDa and a light chain of 5 kDa **(Figure 1.2)** (Frosch et al., 1999; Kirschke et al., 1995; Mort and Buttle, 1997). Alternatively, cathepsin B can be activated by cathepsin D (van der Stappen et al., 1996) and cathepsin G, urokinase-type plasminogen activator (uPAR), tissue-type plasminogen activator, and elastase (Dalet-Fumeron et al., 1996; Dalet-Fumeron et al., 1993). Structurally, cathepsin B is a bilobal protein, generating the active site of the enzyme at the interface between the two lobes (Musil et al., 1991). Cathepsin B can function as an endopeptidase and an exopeptidase (Keppler and Sloane, 1996; Musil et al., 1991). This dual activity is caused by an occluding loop that disturbs the access of substrates to the active site (Illy et al., 1997). In the acidic environment of lysosomes, the occluding loop partially blocks and prevents large substrates from gaining access to the active site but allows access of synthetic substrates or the C-terminus of proteins. Thus, cathepsin B has carboxydipeptidase activity in an acidic environment. At neutral pH, the occluding loop of cathepsin B is moved from active site, which allows large substrates to bind to

the active site. This model explains how cathepsin B can function as an endopeptidase as well as an exopeptidase (Illy et al., 1997; Quraishi et al., 1999).

**Figure 1.2 Cathepsin B maturation**

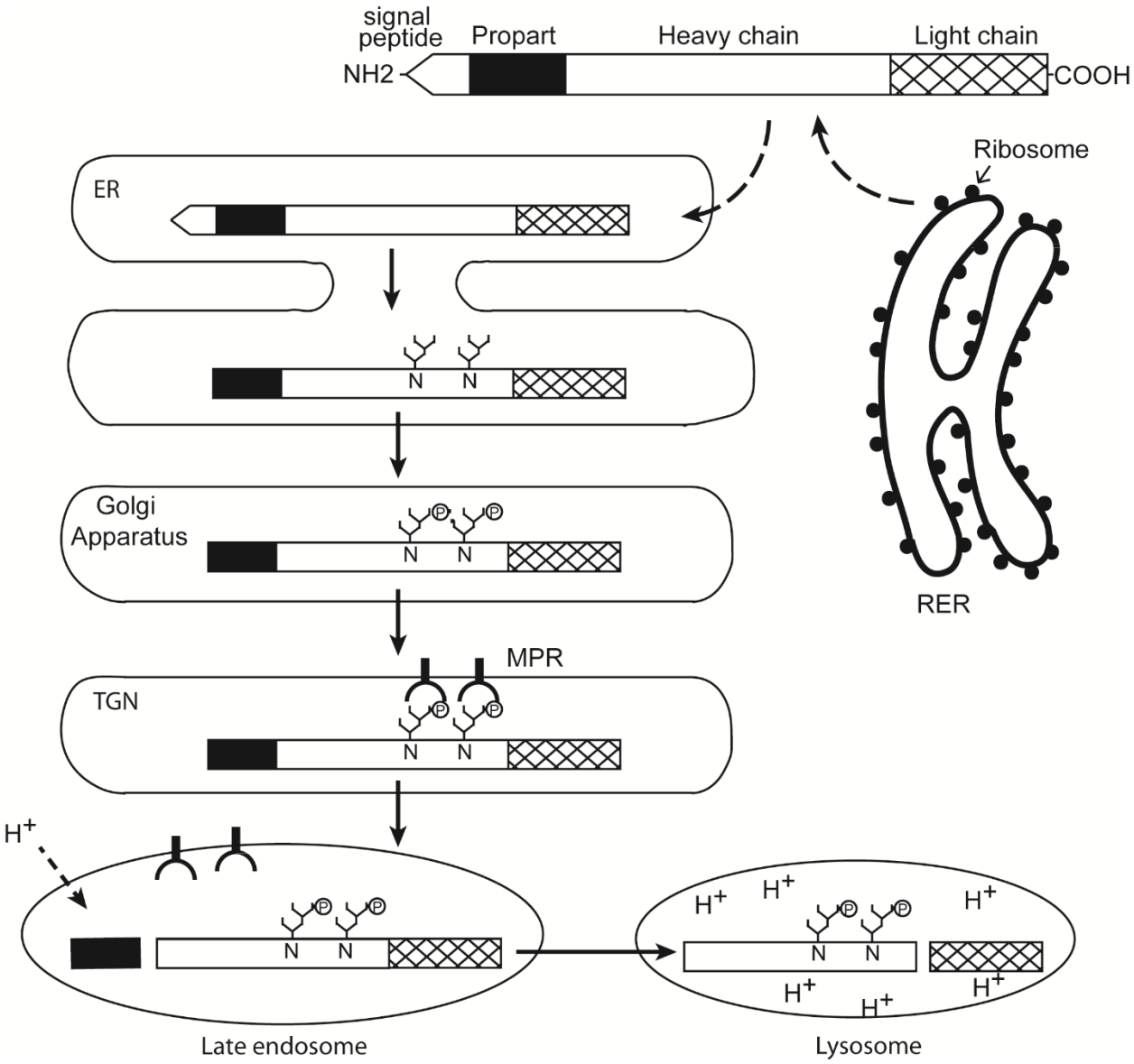

### 1.3 Lysosomal cell death

Christian de Duve used the term “recycling bin” to describe the function of lysosomes. Also, because of the acid hydrolases in lysosomes, he defined them as “suicide bags” (de Duve, 1983). Three major pathways regulate cell death: necrotic, autophagic, and apoptotic (Galluzzi et al., 2007). The results of many studies have shown that lysosomes can be involved in each of these cell death pathways.

Necrosis is largely triggered when cell damage is too severe and catastrophic to control. Because lysosomes contain catabolic enzymes, their rupture can be potentially harmful to the cell. The release of lysosomal contents can trigger a cascade of hydrolysis in the cytoplasm and generalize cytoplasmic acidification with potentially lethal consequences for the cell. However, increasing evidence suggests that even the necrotic process may be tightly regulated. Cytosolic calcium concentration in neurons was demonstrated to increase during necrosis, leading to an imbalance of proteolysis and, in particular, activation of calpains and aspartic cathepsins due to lysosomal membrane permeabilization (LMP) (Syntichaki et al., 2002). Moreover, later studies reported that calpain-mediated LMP was essential in hypotonic shock, heat shock, oxidative stress, hypoxia, and cation channel hyperactivity, with cysteine cathepsins found to be the major downstream regulators (Luke et al., 2007). While a few key components of the necrotic cell death pathway have been identified, the molecular mechanisms of necrosis are much less clear than those of apoptosis and autophagy. It is likely that necrosis results from the interplay of several signaling pathways, such as mitochondrial dysfunction, reactive oxygen species (ROS), ATP depletion, calpain- and cathepsin-mediated proteolysis, and early plasma membrane rupture (Golstein and Kroemer, 2007).

A second cell death pathway is autophagic cell death, also called type II programmed cell death. It is characterized by the large-scale accumulation of autophagosomes (Levine and Kroemer, 2008). Autophagy is the main process for degrading and recycling cellular components (Kobayashi, 2015). During autophagy, double membrane autophagosomes are packed with cargo that is delivered to lysosomes. Autolysosomes, which are the fusion products of autophagosomes and lysosomes, break down this cargo using lysosomal hydrolases. This pathway helps maintain the cellular energy level during starvation. Similarly, the removal of damaged organelles provides nutrients to the cell and promotes survival. Through this mechanism, autophagy protects the organism from various stressors and pathologies and is essential for maintaining homeostasis (Levine and Kroemer, 2008; Mizushima et al., 2008). However, under certain conditions, autophagy is detrimental to the cell. For example, at the end of *Drosophila* larval development, larval midgut and salivary gland cells display apoptotic phenotypes including DNA fragmentation and increased proapoptotic genes. In addition, these cells show numerous autophagosomes and increased expression of autophagic genes, as assessed by elevated levels of *Atg* mRNAs (Denton et al., 2009; Jiang et al., 1997; Lee et al., 2002; Li and White, 2003). This cell death is delayed by autophagy blockage (Berry and Baehrecke, 2007; Denton et al., 2009). Also, in a mammalian cell line, autophagic genes are required for cell death that occurs in a caspase-independent manner (Shimizu et al., 2004; Yu et al., 2004). Cells undergoing autophagic cell death initially show degradation of cytoplasmic components by the autophagic process, and this precedes nuclear collapse (Bursch, 2001). Notably, however; no study has shown this pathway to trigger cell death in a mammalian animal model. Therefore, the importance of autophagic cell death in mammalian systems is open to debate. It is conceivable that constitutive

autophagy could eventually destroy a cell, and that some proteins that are essential for autophagy could participate in signaling pathways that lead to cell death (Tsujimoto and Shimizu, 2005).

A third cell death pathway is apoptosis. This pathway is characterized morphologically by the production of apoptotic bodies. These remnants of dead cells are engulfed and removed by phagocytic cells before they induce damage to surrounding cells. Apoptosis plays an especially important role in development and homeostasis. A molecularly critical step in apoptosis is caspase activation, which can be initiated in several ways: by death receptors, apoptosomes, and granzymes. A number of apoptotic proteins target mitochondria, which are the central organelles in this cell death pathway (Danial and Korsmeyer, 2004; Krenn et al., 2015). These proteins cause the formation of membrane pores or increase the membrane permeability of mitochondria, leading to the leakage of apoptotic effectors. It has also been suggested that lysosomes and lysosomal cathepsins play a role in apoptosis, including in neurodegeneration and aging, mediated primarily by oxidative stress (Kurz et al., 2008b; Leist and Jaattela, 2001; Turk et al., 2002; Wei et al., 2008). Lysosomes can be damaged by free radicals. Following treatment with hydrogen peroxide, which easily crosses membranes and catalyzes Fenton reactions with lysosomal iron, free radicals destabilize the lysosomal membrane and induce LMP-dependent cell death. The iron chelator, deferoxamine, inhibits oxidant-induced lysosomal damage. Studies on this topic strongly support the role of Fenton chemistry in oxidant-induced LMP (Krenn et al., 2015; Terman et al., 2006; Zhao et al., 2003). In addition to direct effects of lysosomal ROS in LMP, cathepsin B released into cytosol can enhance ROS formation in mitochondria and activate phospholipase A2, which is capable of inducing LMP, thereby creating a positive feedback loop (Zhao et al., 2003). Also, LMP has been shown to trigger a cascade of regulated cell demise mediated by the release of lysosomal enzymes into the cytosol, which induces cell death.

### 1.3.1 LMP-dependent apoptosis

Accumulating evidence suggests that the release of cathepsins into the cytoplasm triggers lysosomal cell death in either a mitochondrion-independent manner or a mitochodrion-dependent manner (Groth-Pedersen and Jaattela, 2013). Because caspases are activated in the cytosol during apoptosis, it is logical that lysosomal proteases would redistribute to the cytosol during LMP-dependent apoptosis. However, massive rupture of lysosomes has been show to lead to necrosis **(Figure 1.3)** (Bursch, 2001). To induce apoptosis without necrosis, small-scale lysosomal leakage and relocation of lysosomal proteases to the cytosol are thought to be required. It was reported that active lysosomal proteases and their precursor forms traffic within different organelles and across lysosomal membranes spontaneously (Berg et al., 1995; Claus et al., 1998). Also, cathepsins are synthesized as inactive precursors and activated by cleavage in the acidic environment of the lysosome (Katunuma, 2010). Therefore, in the past, it was assumed that lysosomal cysteine proteases were extremely unstable and rapidly inactivated at neutral pH. However, a number of studies have reported that cysteine cathepsins are stable, maintaining activity at neutral pH such as that which is found in the cytoplasm (Turk et al., 1995; Turk et al., 1993; Turk et al., 1994). In vitro experiments performed at neutral pH showed that the cathepsins B, H, L, S, and K cleave Bid predominantly at Arg residues 65 or 71 and trigger the release of cytochrome c from isolated mitochondria (Cirman et al., 2004). Released cytochrome c builds apoptosomes with apoptotic protease-activating factor (Apaf-1) and activates capase-9. Activated caspase-9 induces the activation of caspase-3, 6, and -7, leading to cell death **(Figure 1.3)** (Taylor et al., 2008). In addition, cathepsin B, under certain conditions, has been shown to increase caspase-3 activity in brain cells (Yakovlev et al., 2008).

Many studies have reported that tumor necrosis factor (TNF) induces LMP. This has been demonstrated by staining lysosomal components or by tracking a loaded dextran into lysosomes through endocytosis (Gyrd-Hansen et al., 2006; Li et al., 2007; Werneburg et al., 2004; Werneburg et al., 2002). In a mouse model, caspase-9, which is essential for TNF-induced cell death, was cleaved and activated directly by caspase-8, allowing for mitochondrion-independent LMP induction (Varfolomeev et al., 1998). In human cancer cells, TNF-induced LMP depends on mitochondrial outer membrane permeabilization, cytochrome c release, and apoptosome-mediated activation of caspase-9 rather than caspase-8 **(Figure 1.3)** (Foghsgaard et al., 2001; Gyrd-Hansen et al., 2006). These studies suggest that caspase-9 may function as a more general link between the intrinsic apoptosis pathway and LMP. Also, TNF can induce an increase in ROS, leading to caspase-independent cell death (Jaattela and Tschopp, 2003). Other LMP inducers—bortezomib, omeprazole, norfloxacin, and siramesine—promote the production of ROS as well (Boya et al., 2003; De Milito et al., 2007; Ostenfeld et al., 2005; Yeung et al., 2006). It is also known that ROS or photo-oxidation triggers LMP (Caruso et al., 2004; Ollinger and Brunk, 1995) and that ROS initiates cell death in many pathways (Orrenius, 2007; Raj et al., 2011; Valencia and Moran, 2004). In chapter 2, I will test whether LMP and cathepsin leakage contribute to the neurodegeneration of Purkinje cells in the Niemann-Pick C brain.

**Figure 1.3 LMP-dependent apoptosis**

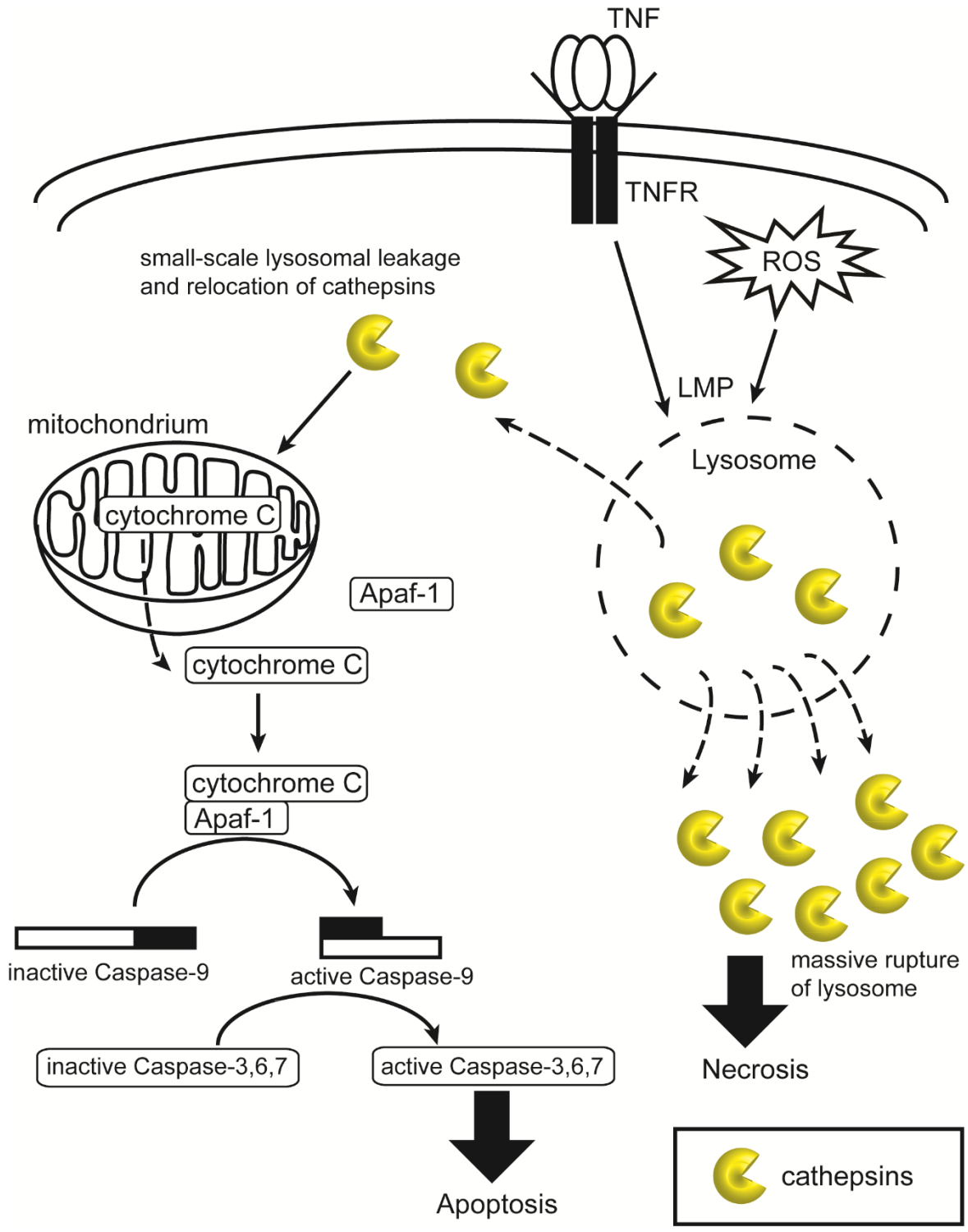

### 1.4 Selective neuronal survival

Many inherited neurodegenerative diseases affect only select populations of neurons, despite the fact that the mutant or aggregated protein is widely present throughout the nervous system (Double et al., 2010). For example, Parkinson's disease shows severe loss of pigmented neurons in the pars compacta of the substantia nigra although alpha-synuclein is expressed in most brain regions (Sulzer and Surmeier, 2013). Similarly, selective neuronal vulnerability characterizes many of the age-dependent protein aggregation disorders, including Alzheimer's disease (Mann, 1996), amyotrophic lateral sclerosis and the polyglutamine expansion disorders (Byers et al., 1973). It remains unclear why specific brain regions are vulnerable in different neurodegenerative diseases, and how some neurons in the regions of vulnerability survive despite progressive neurodegeneration.

We study Purkinje cells as one example of selective neuronal vulnerability in the NPC brain. Correlated with loss of Purkinje cells are behavioral deficits, including ataxia and abnormalities of posture and gait (Mullen et al., 1976). Although Purkinje cells are uniform morphologically and electrophysiologically, and similarly express the NPC1 and NPC2 proteins, the extent of Purkinje cell loss occurs in a nonuniform manner across the cerebellum of NPC1 and NPC2 deficient mice (Elrick et al., 2010; German et al., 2001; Marschalek et al., 2014). In the cerebellar midline, Purkinje neurons in lobule X are strongly resistant to loss of NPC1 or NPC2. In contrast, neurons in the anterior zone (lobules II-V) show severe degeneration, while neurons in the intermediate (lobules VI-VII) and posterior zones (lobule VIII and rostral aspect of lobule IX) are moderately susceptible to degeneration (Elrick et al., 2010; German et al., 2001; Marschalek et al., 2014). Interestingly, a similar distinct spatiotemporal pattern of loss is reproducible across many unrelated diseases and injuries (Clark et al., 1997; Sarna et al., 2001;

Sleat et al., 2004; Takahashi et al., 1998; Tavani et al., 2003; Yoneshige et al., 2010). As a similar pattern of Purkinje cell death results from a variety of genetic and environmental injuries, we hypothesize that the selective vulnerability of Purkinje cell subpopulations arises not from the initiating event of the disease process, but rather from the differential activation of cell death pathways in response to the disease. To test this hypothesis, in chapter 3, I will identify and test genes that protect Purkinje neurons from the toxicity of NPC disease using a bioinformatics approach. Among the potential genetic regulators of Purkinje cell vulnerability that I identify is a small heat shock protein known as heat shock protein beta-1 (HSPB1).

### 1.5 Heat shock protein beta-1 (HSPB1)

It was reported in 1974 that a few proteins are synthesized after subjecting *Drosophila* salivary glands to heat shock (Tissieres et al., 1974). This study initiated the discovery of a universal protective mechanism to preserve cellular function and homeostasis from not only hyperthermia but also from different types of environmental stress such as toxins, ROS, starvation, and viral infection (Lindquist, 1986; Santoro, 2000). This mechanism involves the rapid induction of a specific set of genes encoding cytoprotective proteins: heat shock proteins (HSPs) (Lindquist and Craig, 1988; Morimoto and Santoro, 1998). Despite the name, HSPs can be activated under non-stressful conditions such as those that occur during progression through the cell cycle, development, and differentiation. (Hang et al., 1995; Jerome et al., 1993; Milarski and Morimoto, 1986; Sistonen et al., 1992; Yang et al., 2006). HSPs are divided into different families, based on molecular size: hsp100, hsp90, hsp70, hsp60, hsp40, and small HSPs. In mammalian cells, several HSPs function as molecular chaperones, enabling proteins to attain a native confirmation, promoting the clearance of terminally misfolded proteins, and assembling or

disassembling macromolecular structures. Under conditions of stress, protein aggregation is increased, eventually leading to cell and tissue death. One function of HSPs is to hold misfolded proteins in an intermediate folded state before the protein enters into a competent refolded state. During the intermediate state, HSPs function as kinetic traps to prevent formation of aggregates (Morimoto and Santoro, 1998). Another function of HSPs under stress is to increase cellular viability in various ways, such as lysosomal membrane stabilization, survival gene induction, and apoptotic gene inhibition (Enomoto et al., 2013; Nylandsted et al., 2000; Nylandsted et al., 2004).

HSPB1 is one of the small heat shock proteins. It is also called HSP27 in humans and HSP25 in mice. HSPB1 functions as a chaperone, and acts to prevent the formation of aggregates of polypeptides or misfolded or unfolded proteins. HSPB1 has been shown to act in multiple cellular pathways, including the stabilization of the cytoskeleton and as an anti-apoptotic and anti-oxidant protein, similar to other HSPs that act in response to stress or in non-stress conditions (Arrigo, 2007).

HSPB1 resides mainly in the cytosol and acts as an ATP-independent chaperone (Lianos et al., 2015). The chaperone function of HPSB1 was first shown in a study in which murine Hspb1 and human HSPB1 prevented the aggregation of citrate synthase and α-glucosidase (Jakob et al., 1993). Many studies have revealed that phosphorylation of HSPB1 mediates its oligomerization state. HSPB1 forms homo-ologomers, ranging from dimers and tetramers (favored by phosphorylation) to multimers of up to 800 kDa (favored by dephosphorylation) (Arrigo and Gibert, 2012). Dephosphorylated large complexes of HSPB1 have chaperone functions (Ehrnsperger et al., 2000; Jakob et al., 1993). In contrast, phosphorylated HSPB1 stabilizes the actin cytoskeleton (Huot et al., 1996; Lavoie et al., 1995).

HSPB1 also has potent anti-apoptotic properties and has been implicated in a number of additional disease pathways, having both protective and counter-protective capacities (Khalil et al., 2011). In an environment of chemical stress, HSPB1 performs anti-apoptotic functions by interacting with caspase-dependent and independent apoptosis steps. In the caspase-independent apoptosis pathway, HSPB1 binds to Daxx (death domain-associated protein 6) and prevents its interaction with Ask1 (apoptosis signal regulated kinase 1) and Fas (a cell death receptor), leading to inhibition of their proapoptotic activities (Charette and Landry, 2000). Additionally, HSPB1 inhibits Bax-mediated mitochondrial apoptosis by promoting Akt activation via a PI3-kinase-dependent mechanism (Havasi et al., 2008). It has also been reported that HSPB1 provides protection against programmed cell death by inhibiting caspase-dependent apoptosis at multiple levels, through the binding and sequestration of cytochrome c (Bruey et al., 2000) and caspase-3 (Pandey et al., 2000). Whether the phosphorylation state is required for most anti-apoptotic activities is unknown. However, a clue can be found in one study, which demonstrated that phosphorylated HSPB1 is required to inhibit DAXX (Charette and Landry, 2000). Recently, phosphomimetic HSPB1 was shown to protect against apoptosis inducers such as Fas agonist antibodies, staurosporine, and cytochalasin D, while non-phosphorylatable HSPB1 gave no protection or only mild protection against apoptosis inducers. These data suggest that the anti-apoptotic activities of HSPB1 are primarily attributable to the phosphorylated species (Paul et al., 2010). In contrast, large complexes of dephosphorylated HSPB1 have been shown to prevent oxidative damage (Preville et al., 1999). HSPB1 can also act to reduce the concentration of ROS by increasing intracellular glutathione levels and lowering intracellular iron concentration through downregulation of transferrin receptor 1-mediated iron uptake (Arrigo et al., 2005; Chen et al., 2006).

### 1.5.1 HSPB1 function in the brain

Mutations or modifications in HSPB1 can lead to adverse pathological conditions due to (1) toxicity from misfolded or aggregated proteins whose clearance is impaired by diminished HSPB1 function, or (2) an inability to cope with stress as a result of loss of HSPB1 function. That the chaperone activity of HSPB1 can limit toxicity of misfolded or aggregated proteins is supported by data showing that overexpression of HSPB1 ameliorates neurodegeneration in models of Alzheimer disease (Shimura et al., 2004; Toth et al., 2013), Parkinson disease (Lee et al., 2012; Renkawek et al., 1999), and amyotrophic lateral sclerosis (Vleminckx et al., 2002). Moreover, a mutation in HSPB1 diminishes axonal transport in the peripheral nervous system (Almeida-Souza et al., 2011) and impairs neurofilament assembly (Ackerley et al., 2006). In addition, the HSPB1 mutant reduces acetylated α-tubulin in dorsal root ganglion cells, leading to reduced mitochondrial movement and dysfunction of the axon cytoskeleton and axonal transport (Irobi et al., 2004).

HSPB1 also functions in the brain to provide neuroprotection against a variety of cellular stressors. Overexpression of HSPB1 protects dorsal root ganglia neurons from apoptosis induced by nerve growth factor withdrawal or exposure to retinoic acid (Wagstaff et al., 1999). Similarly, induced HSPB1 protects PC12 cells from MPP+ toxicity, leading to a decrease in caspase activity (Quigney et al., 2003). In vivo, HSPB1 transgenic mice showed reduced apoptosis induced by kainic acid injection into the hippocampus (Akbar et al., 2003). In addition, it was demonstrated that phosphorylation of HSPB1 reduced infarct size by diminishing neuronal cell death in HSPB1 transgenic mice (Stetler et al., 2012; van der Weerd et al., 2010).

The expression of HSPB1 in the mouse cerebellum characterizes a subset of Purkinje neurons. This heterogeneity of Purkinje neurons reflects the organization of the cerebellar cortex, which is divided into a series of transverse zones, with each zone subdivided into parasagittal stripes. The expression pattern of many molecules defines the parasagittal stripes and the transverse zones in greater detail. For example, the expression of zebrin II reveals an array of transverse zones in the vermis and in both hemispheres (Marzban and Hawkes, 2011).

An additional marker of Purkinje cell heterogeneity is HSPB1 (Kalesnykas et al., 2007; Plumier et al., 1997; Wilkinson and Pollard, 1993). A number of studies have shown that specific populations of Purkinje cells express HSPB1 in the transverse zones, and that these cells appear to be more resistant to neurodegeneration in a variety of model systems, including shaker rats (Tolbert et al., 1995), toppler mice (Duchala et al., 2004), and PrP null mice (Rossi et al., 2001). Interestingly, studies have demonstrated that various mouse models of Niemann-Pick disease, with loss of function mutations in the genes encoding acid sphingomyelinase, Npc1 or Npc2, display a similar pattern of Purkinje cell degeneration and resistance (Sarna et al., 2001; Sarna et al., 2003). In all of these mice, the surviving Purkinje cells are in the same transverse zone as HSPB1. These cells are also aligned in parasagittal stripes in the central zone and the nodular zone, and along the border of the posterolateral crescent in the paraflocculus/flocculus, directly corresponding to the expression pattern that occurs using HSPB1 immunohistochemistry (Armstrong et al., 2000). In chapter 3, I will provide evidence that HSPB1 is neuroprotective against NPC1 deficiency both in vitro and in vivo.

### 1.6 Research objectives

Although many research teams have been studying the removal of accumulated cholesterol as a therapy for NPC patients, these studies are not focused on the mechanisms underlying neurodegeneration. It is our expectation that detailed analysis of the pathways leading to neuronal dysfunction and death will identify currently unknown therapeutic targets. The work presented in this dissertation pursues mechanisms that protect against neurodegeneration and may serve as potential targets for future therapy development. The first objective is to explore the genetic interaction of NPC1 deficiency with deletion of cystatin B, an endogenous inhibitor of lysosomal cathepsins. In chapter 2, I will provide data implicating a cascade of LMP and cathepsin leakage as contributing to neurodegeneration due to NPC1 deficiency. I show that genetic or small molecule approaches to modulate cathepsin activity in mice and in cellular models of NPC disease alter cell viability and neurodegeneration. The second objective of this dissertation is to identify genes that protect neurons from the toxicity of NPC1 deficiency. In chapter 3, I explore genes that potentially modify neuronal survival and death in the NPC brain. To identify these genes, we analyze gene expression patterns in the cerebellum using bioinformatics tools to identify several candidate modifier genes. I confirm that one potential neuroprotective gene, *HSPB1*, promotes survival in cellular models of NPC disease through a mechanism involving the inhibition of apoptosis. Moreover, I confirm HSPB1 neuroprotective activity in an NPC mouse model using both overexpression and knock-down approaches. In conclusion, it is my underlying hope that uncovering pathways that lead to neurodegeneration in NPC1 deficiency will contribute to the identification of novel therapeutic targets.

# Chapter 2

# Cystatin B, an endogenous inhibitor of lysosomal cathepsins, protects against Niemann-Pick C cerebellar degeneration

## 2.1 Abstract

Niemann-Pick C1 (NPC) disease, an autosomal recessive lipid trafficking disorder caused by loss-of-function mutations in the *NPC1* gene, is characterized by progressive neurodegeneration resulting in cognitive impairment, ataxia and early death. Little is known about the cellular pathways leading to neuron loss, yet impairments of lysosomal protein quality control and decreased cathepsin activity have been documented in mutant cells. Here, we studied the effects of diminishing expression of cystatin B, an endogenous inhibitor of cathepsins B, H and L, on the development of neuropathology. We show that decreased expression of cystatin B in patient fibroblasts enhances cathepsin activity. Deletion of the encoding *Cstb* gene in Npc1 deficient mice resulted in unexpected and deleterious effects, particularly within the cerebellum where diffuse loss of Purkinje cells was observed in young mice. This severe pathology occurred through cell autonomous mechanisms that triggered Purkinje cell death. Moreover, our analyses demonstrated the mislocalization of lysosomal cathepsins within the cytosol of Npc1 deficient Purkinje cells. We provide evidence that this may be a consequence of damage to lysosomal membranes by reactive oxygen species, leading to the leakage of lysosomal contents that

culminates in apoptotic cell death. The observation that *Npc1* and *Cstb* deletion genetically interact to potently enhance the degenerative phenotype of the NPC cerebellum provides strong support for the notion that the lysosomal cell death pathway contributes to cerebellar degeneration in Niemann-Pick C disease.

## 2.2 Introduction

Lysosomes are critical components of the cellular degradation machinery and important nodes in the homeostatic response to metabolic demands (Settembre et al., 2013). These vesicles degrade macromolecules delivered to them through endocytosis or autophagy by the action of a family of acidic hydrolases including proteases, lipases, nucleases, glycosidases, phospholipases, phosphatases, and sulfatases (de Duve, 2005). More than 50 diseases related to lysosomal dysfunction, many caused by enzyme deficiencies, have been identified since Christian De Duve discovered this organelle in the mid-twentieth century (Schultz et al., 2011).

Lysosomal proteases, or cathepsins, are required for the housekeeping function of these organelles in protein turnover. These cathepsins have been implicated in a variety of human diseases, including neurodegenerative disorders (Elrick et al., 2012; Nakanishi, 2003; Yamashima, 2000). Cathepsins are classified by their catalytic mechanism into aspartic, serine, threonine, metallo, or cysteine proteases (Pislar and Kos, 2014). Cysteine cathepsins, the largest family of lysosomal proteases, are synthesized as inactive precursors and are activated by cleavage in the acidic environment of the lysosome (Katunuma, 2010). While it was initially thought that lysosomal cysteine proteases are unstable and rapidly inactivated outside the lysosome, a number of studies have established that cysteine cathepsins are stable and partially active at neutral pH, such as within the cytoplasm (Turk et al., 1995; Turk et al., 1993; Turk et

al., 1994). Indeed, accumulating evidence suggests that the release of cathepsins into the cytosol triggers apoptotic cell death (Groth-Pedersen and Jaattela, 2013). A first line of self-defense in preventing apoptosis initiated through this mechanism is provided by intracellular inhibitors of cysteine proteases, the cystatins. Cystatin B, which inhibits cathepsins B, H and L, is a reversible and competitive inhibitor of these proteases (Turk and Bode, 1991). As such, cystatin B is poised to play an important role in limiting the activation of apoptosis in situations where cells are exposed to a variety of toxic challenges that impact lysosomal membrane integrity.

Here we tested the extent to which cystatin B regulates neurodegeneration in Niemann-Pick type C (NPC) disease, an autosomal recessive disorder characterized by progressive cognitive decline, seizures, dystonia, abnormal eye movements and early death (Vanier, 2013). The cause of NPC disease is loss-of-function mutations in the *NPC1* or *NPC2* genes (Carstea et al., 1997; Naureckiene et al., 2000) whose protein products act cooperatively in the efflux of cholesterol from late endosomes and lysosomes (Infante et al., 2008; Kwon et al., 2009). In NPC disease, the accumulation of unesterified cholesterol and glycosphingolipids in late endosomes and lysosomes is associated with impairments of cellular proteostasis, including abnormalities in autophagy (Elrick and Lieberman, 2013; Lieberman et al., 2012; Pacheco et al., 2007; Sarkar et al., 2013), accumulation of ubiquitinated proteins (Higashi et al., 1993; Liao et al., 2007; Ordonez et al., 2012) and impairment of lysosomal cathepsin activity (Elrick et al., 2012). These abnormalities correlate with the occurrence of severe neurodegeneration that is characterized, in part, by the loss of cerebellar Purkinje neurons. However, little is known about the cellular pathways leading to neurodegeneration in this disorder.

In this study, we present evidence that cystatin B is a potent modifier of cerebellar degeneration in NPC mice. We show that knockdown of cystatin B markedly increases cathepsin

activity in NPC1 deficient fibroblasts, and that deletion of the encoding *Cstb* gene enhances cerebellar degeneration in *Npc1-/-* mice. This accentuation of NPC neuropathology is shown to be neuron autonomous and due to enhanced apoptotic death of Purkinje cells. Our findings uncover an important pathway that regulates neuron loss in the NPC brain, and suggest that damage to organelle membranes by reactive oxygen species may be a significant contributor to disease.

## 2.3 Results

### 2.3.1 Cystatin B deficiency increases cathepsin activity in NPC1 patient fibroblasts.

Previous studies demonstrated that deficiency of NPC1 results in impaired lysosomal cathepsin B activity, a defect that is driven by lysosomal lipid storage (Elrick et al., 2012). Here, we sought to reverse this defect by relieving the activity of cystatin B, an endogenous inhibitor of cathepsins B, H and L that has been shown to regulate enzymatic activity in models of cancer and neurodegenerative disease (Butinar et al., 2014; Chang et al., 2009; Yang et al., 2011). To accomplish this, we diminished expression of cystatin B (CSTB) in NPC1 patient fibroblasts by transfecting CSTB targeted siRNA. Cathepsin B activity in live cells was monitored using Magic Red, a fluorophore covalently bound to a di-arginine peptide motif. Prior to cleavage, Magic Red is cell permeable and non-fluorescent. After it is cleaved by cathepsin B in lysosomes, the dye fluoresces red. The rate of fluorescence accumulation was quantified and used to estimate cathepsin B activity *in situ*. In accordance with prior studies (Elrick et al., 2012), we found that cathepsin B activity in primary fibroblasts from NPC1 patients was reduced to approximately half of controls **(Figure 2.1A)**. Cystatin B knockdown in NPC1 deficient cells increased cathepsin B activity to the level of unaffected controls **(Figure 2.1A)**. This enhancement of

enzymatic B activity was associated with diminished cystatin B expression **(Figure 2.1B)**. In contrast, we observed no change in the expression or maturation of cathepsin B. In addition, we observed no change in NPC1 protein expression **(Figure 2.1B)** or in the accumulation of filipin-positive unesterified cholesterol **(Figure 2.1C)**. We conclude that diminishing cystatin B expression in NPC1 deficient cells rescued defects in lysosomal cathepsin activity without altering lipid storage.

**Figure 2.1 Cystatin B knockdown increases cathepsin B activity in NPC1 patient fibroblasts.** Control fibroblasts and NPC1 deficient fibroblasts treated with non-targeted siRNA (NT siRNA) or cystatin B siRNA (CSTB siRNA) for 48 hrs were analyzed. **(A)** Relative cathepsin B activity. Data are mean ± SD, *n* = 3 independent experiments, *P < 0.05, **P<0.01. **(B)** *Left panel*, western blot analysis of the expression of NPC1, cathepsin B, cystatin B and GAPDH. *Right panel*, NPC1 and cathepsin B intensity relative to GAPDH (mean ± SD, *n* = 3, *P < 0.05). **(C)** Unesterified cholesterol was stained by filipin and quantified across three independent experiments. Data are mean ± SD, *n* = 40-50 fields of cells per group in total, ****P<0.0001.

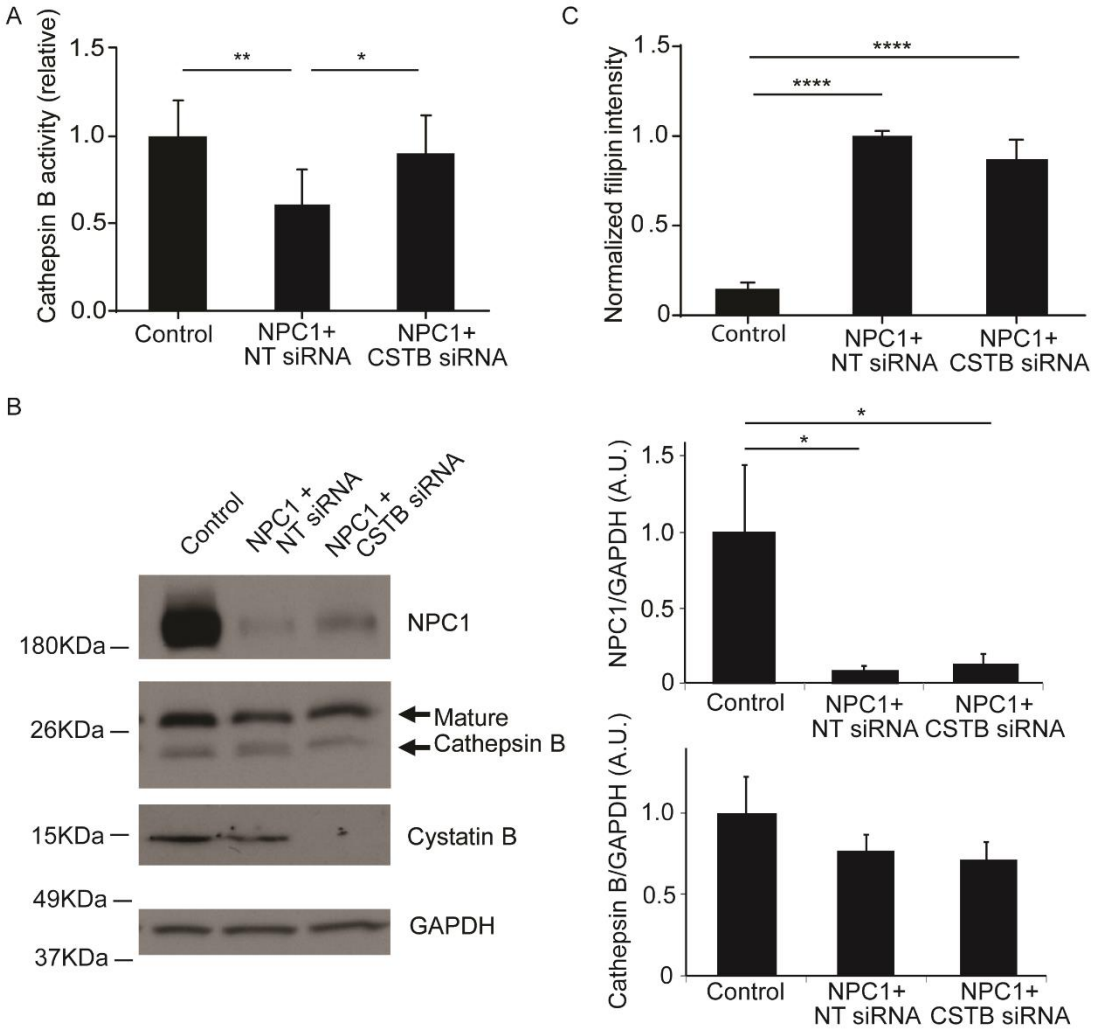


### 2.3.2 Cystatin B protects against Niemann-Pick C cerebellar degeneration.

Niemann-Pick C disease is characterized by impaired proteostasis, as reflected by defects in macroautophagy (Elrick et al., 2012; Sarkar et al., 2013) and by the accumulation of

ubiquitinated proteins in the CNS (Elrick et al., 2012; Higashi et al., 1993; Liao et al., 2007; Love et al., 1995; Walkley and Suzuki, 2004). We therefore sought to determine whether enhanced lysosomal cathepsin activity would modify the disease phenotype in mouse models. To accomplish this, we generated *Npc1* null mice that were deficient in cystatin B. Mice with a cystatin B null allele were previously generated to model progressive myoclonic epilepsy of the Unverricht-Lundborg type. These mice begin to develop disease around 6 months of age that includes loss of cerebellar granule neurons, but not Purkinje cells. At earlier time points, between 1 - 3 months, mutants are normal in body size, weight, behavior and histopathology compared to wild type littermates (Pennacchio et al., 1998). We therefore generated *Npc1* and *Cstb* double null mice and focused our analysis on young animals. Unexpectedly, these double null mutants were generated at a very low frequency. Of the 101 *Cstb -/-* pups generated from multiple matings of *Npc1* +/-, *Cstb* +/- adults, only 4% were homozygous for the *Npc1* null allele. By chi-squared analysis, only double null mutants (*Npc1 -/-*, *Cstb -/-*) were derived from these matings at a frequency that was significantly lower than expected ($P < 0.001$; see Table 2.1).

**Table 2.1** Expected and observed genotype ratios for pups

| | | *Cstb* +/+ background *N* = 130 | *Cstb* -/- background *N* = 101 |
|---|---|---|---|
| *Npc1* genotype | Expected ratio | Obeserved | Obeserved |
| *Npc1* +/+ | 1 | 31 | 18 |
| *Npc1* +/- | 2 | 72 | 79 |
| *Npc1* -/- | 1 | 27 | 4 |
| Chi square | | 1.75 | 36.05* |

* Statistically significant. Chi-square for 2 degrees of freedom for a *P* value of 0.05 is 5.99.

We observed a significant and unanticipated enhancement of the NPC phenotype in mice that were deficient in cystatin B. As early as 4 weeks of age, double null mutants showed marked deficits in body and liver weight compared to *Npc1* nulls that were haploinsufficient or wild type for cystatin B **(Figure 2.2A)**. We were unable to train these young double null mutants to cross a balance beam (data not shown), a motor task that is sensitive to Purkinje cell loss in Npc1 deficient animals (Elrick et al., 2010). This severe, early onset behavioral impairment prompted us to perform histologic examination of the brains of these mice and littermate controls at 4 weeks of age. Remarkably, the double null mutants contained virtually no cerebellar Purkinje cells, except for only rare neurons in lobule X **(Figure 2.2B)**. At this age, there was no detectable Purkinje cell loss in either anterior or posterior cerebellar lobules of *Npc1* or *Cstb* single null mutants. The loss of Purkinje cells in lobule X is particularly noteworthy since these neurons are typically resistant to toxic effects of *Npc1* deficiency, even in animals aged to 6 months (Elrick et al., 2010). The paucity of calbindin-positive Purkinje cells in anterior and posterior cerebellar lobules of double null mutants was associated with marked astrocytic and microglial reaction **(Figure 2.2C, D)**. In contrast, cystatin B deficiency did not exacerbate accumulation of the ganglioside GM2 or unesterified cholesterol in the brains of Npc1 deficient mice **(Figure 2.2E, F)**, suggesting that mechanisms other than enhanced lipid storage led to the worsened phenotype. These analyses indicated that there was a genetic interaction between *Npc1* and *Cstb* deficiency that markedly increased the severity of neuropathology.

While our initial studies focused on cerebellar Purkinje cells, they left unanswered whether other brain regions in *Npc1* deficient mice showed enhanced pathology in the setting of *Cstb* deletion. To begin to address this question, we stained midline sagittal brain sections for GFAP since reactive astrocytes are sensitive indicators of damage in the CNS. We observed

marked gliosis that was largely restricted to the cerebellum and was only seen in double null mutants at 4 weeks of age **(Figure 2.3A-D)**. This gliosis was associated with significant cerebellar atrophy **(Figure 2.3E)**, which reflected the extensive loss of Purkinje neurons, the main output neurons of the cerebellum. Our findings indicate that cystatin B normally functions to protect the NPC cerebellum, and that deletion of the *Cstb* gene resulted in marked cerebellar atrophy and gliosis in young *Npc1* deficient mice.

**Figure 2.2 Phenotype of *Npc1, Cstb* null mice. (A)** Body weight, at *left*, and liver weight, at *right*, of mice at 4 weeks of age (mean ± SD, *n* = 3-6 mice/genotype, *P<0.05, **P<0.01, ***P<0.001). **(B)** Purkinje cell density in midline cerebellar sections at 4 weeks of age (mean ± SD, *n* = 3 mice/genotype, ****P<0.0001). **(C, D)** Immunofluorescent staining (red) for Purkinje cells (calbindin), astrocytes (GFAP), and microglia (Iba1) in cerebellar lobule III (C) and lobule X (D). Nuclei are stained with DAPI. Scale bar = 50 μm. **(E)** Immunohistochemical staining of cerebral cortex for GM2 at 4 weeks of age. Scale bar = 200 μm. **(F)** Filipin staining of cerebral cortex at 4 weeks of age. Scale bar = 100 μm.

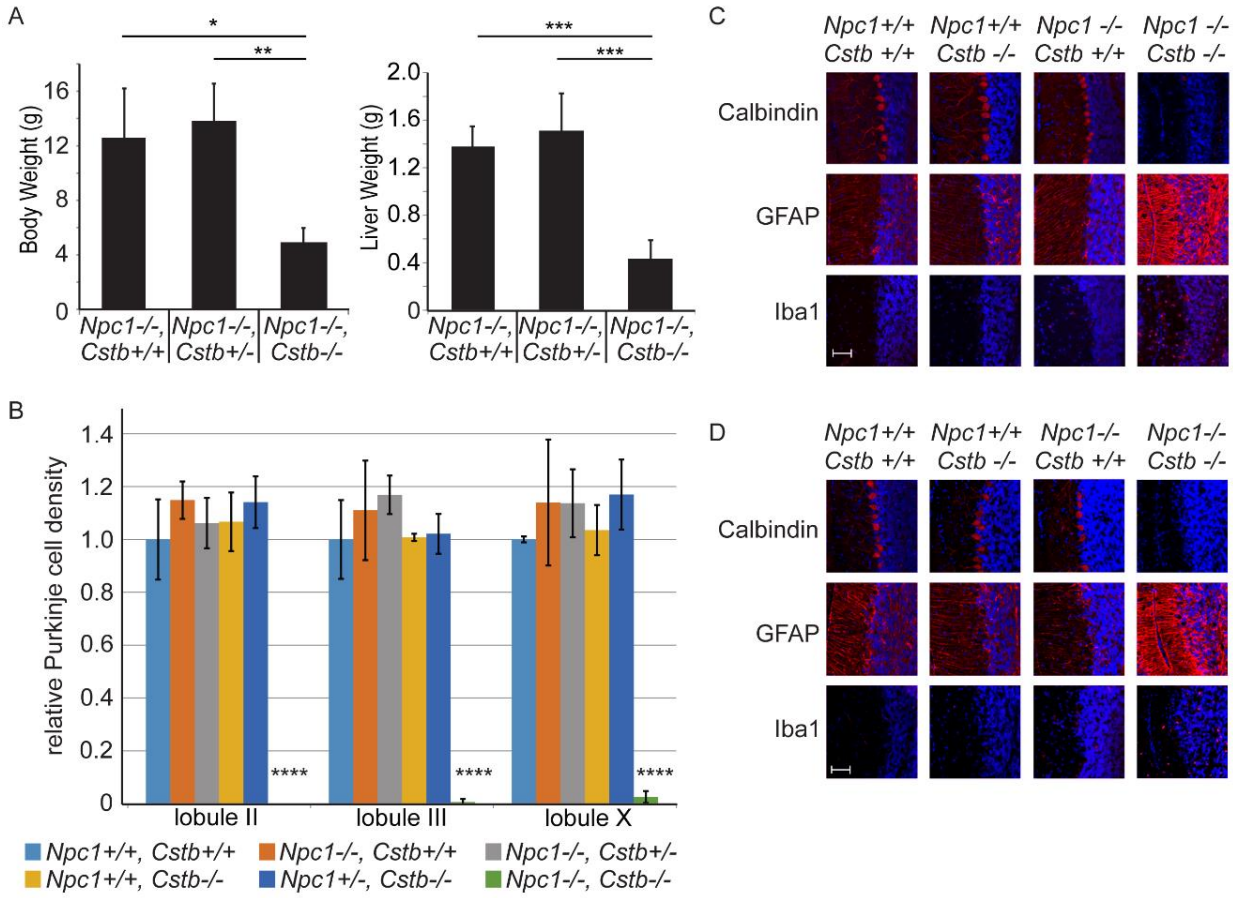

**Figure 2.3 The cerebellum of *Npc1, Cstb* null mice is markedly gliotic and atrophic.** Midline brain sections of mice at 4 weeks of age were stained by immunofluorescence for GFAP. **(A)** *Npc1*+/+, *Cstb*+/+, **(B)** *Npc1*-/-, *Cstb*+/+, **(C)** *Npc1*+/+, *Cstb*-/-, **(D)** *Npc1*-/-, *Cstb*-/-. Cb = cerebellum, Mb = midbrain, P = pons, C = cerebral cortex, Cc = corpus callosum, H = hippocampus, Th = thalamus, Ht = hypothalamus. Scale bar = 500 μm. **(E)** Quantification of cerebellar area in midline sections (mean ± SD, *n* = 3/genotype, *P<0.05, **P<0.01).

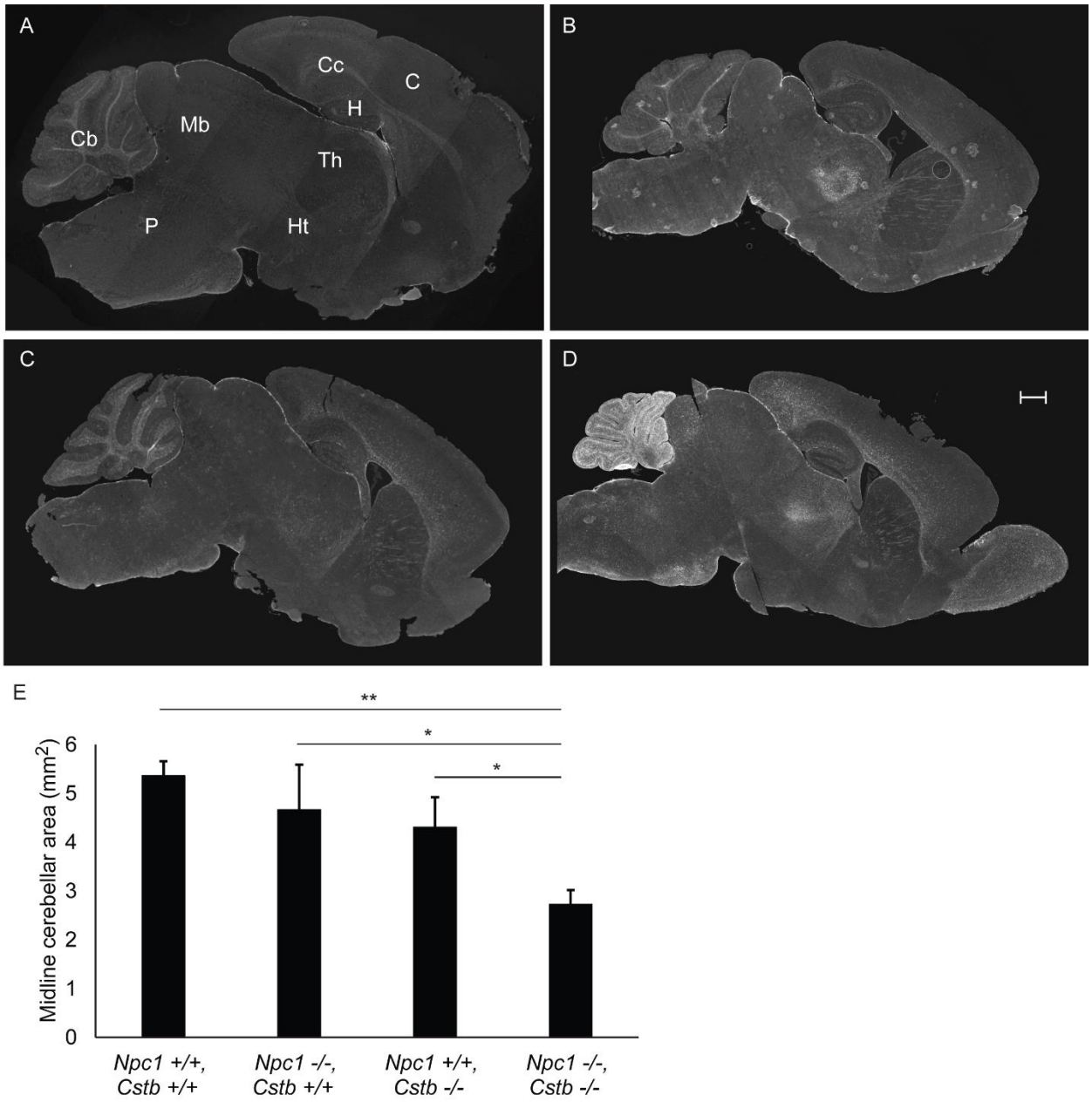

### 2.3.3 Cystatin B deficiency triggers enhanced, cell autonomous Purkinje cell degeneration.

We next sought to determine whether cystatin B deficiency exacerbated cerebellar degeneration in a cell autonomous manner. To accomplish this, we generated *Cstb-/-* mice that were deficient in *Npc1* only in Purkinje cells by using a previously characterized conditional null allele (Elrick et al., 2010). Cre recombinase driven by the *Pcp2* promoter resulted in transgene expression in Purkinje cells that initiated around postnatal day 6 and was present in all Purkinje cells by postnatal days 14 - 21 (Barski et al., 2000). Therefore, this strategy enabled post-developmental and cell-type restricted deletion of *Npc1*.

At 8 weeks of age, partial Purkinje cell loss restricted to anterior cerebellar lobules was detected in *Npc1 Flox/-, Pcp2-Cre, Cstb +/+* mice, as previously reported (Elrick et al., 2010). In contrast, strikingly few Purkinje cells were observed in anterior and posterior cerebellar lobules of *Npc1 Flox/-, Pcp2-Cre* mice that were deficient in cystatin B **(Figure 2.4A, B)**. Quantification confirmed that cystatin B deficiency significantly diminished soma size of Purkinje cells remaining in lobule X **(Figure 2.4C)** and enhanced neuron loss in anterior and posterior cerebellar lobules **(Figure 2.4D)**. This exacerbation of Purkinje cell loss in *Npc1 Flox/-, Pcp2-Cre, Cstb-/-* mice impacted the disease phenotype as it led to impaired motor function as measured by balance beam performance **(Figure 2.4E)**.

The paucity of Purkinje cells in adult double null mutant mice could reflect either a neurodevelopmental impairment or neurodegeneration. To distinguish between these possibilities, we examined Purkinje cell density in 3 week old *Npc1 Flox/-, Pcp2-Cre, Cstb -/-* mice **(Figure 2.5A)**. These young mutants showed Purkinje neurons in all cerebellar lobules, although at a density that was lower than *Npc1 Flox/-, Pcp2-Cre, Cstb +/+* controls. A comparison of Purkinje cell density jn *Npc1 Flox/-, Pcp2-Cre, Cstb -/-* mice at 3 and 8 weeks of

age revealed an age-dependent loss of neurons **(Figure 2.5B)**. This was associated with the occurrence of Purkinje cells that stained for activated caspase-3 in the cerebellum of 3 week old *Npc1 Flox/-, Pcp2-Cre, Cstb -/-* mice **(Figure 2.5C)**. We conclude that cystatin B deficiency triggered apoptotic death of Purkinje neurons in young Npc1 deficient mice.

**Figure 2.4 Enhanced Purkinje cell loss following cystatin B deficiency is cell autonomous.** **(A)** Immunofluorescent staining for Purkinje cells (calbindin antibody) at 8 weeks of age in the cerebellar midline. *Left panel, Npc1 F/-, Pcp2-Cre, Cstb+/+*; *right panel, Npc1 F/-, Pcp2-Cre, Cstb-/-*. Scale bar = 200 μm. **(B)** Immunofluorescent staining for calbindin (red) in cerebellar lobules II, III, and X; nuclei were stained by DAPI. Scale bar = 50 μm. **(C)** Quantification of Purkinje cell soma area (mean ± SD, $n \geq 45$ cells/genotype, *P<0.05). **(D)** Purkinje cell density in lobules II, III and X was quantified in the cerebellar midline (mean ± SD, $n = 4$ mice/genotype, *P<0.05, **P<0.01, ***P<0.001). **(E)** Balance beam performance at 8 weeks of age (mean ± SD, $n \geq 3$ mice/genotype, **P<0.01).

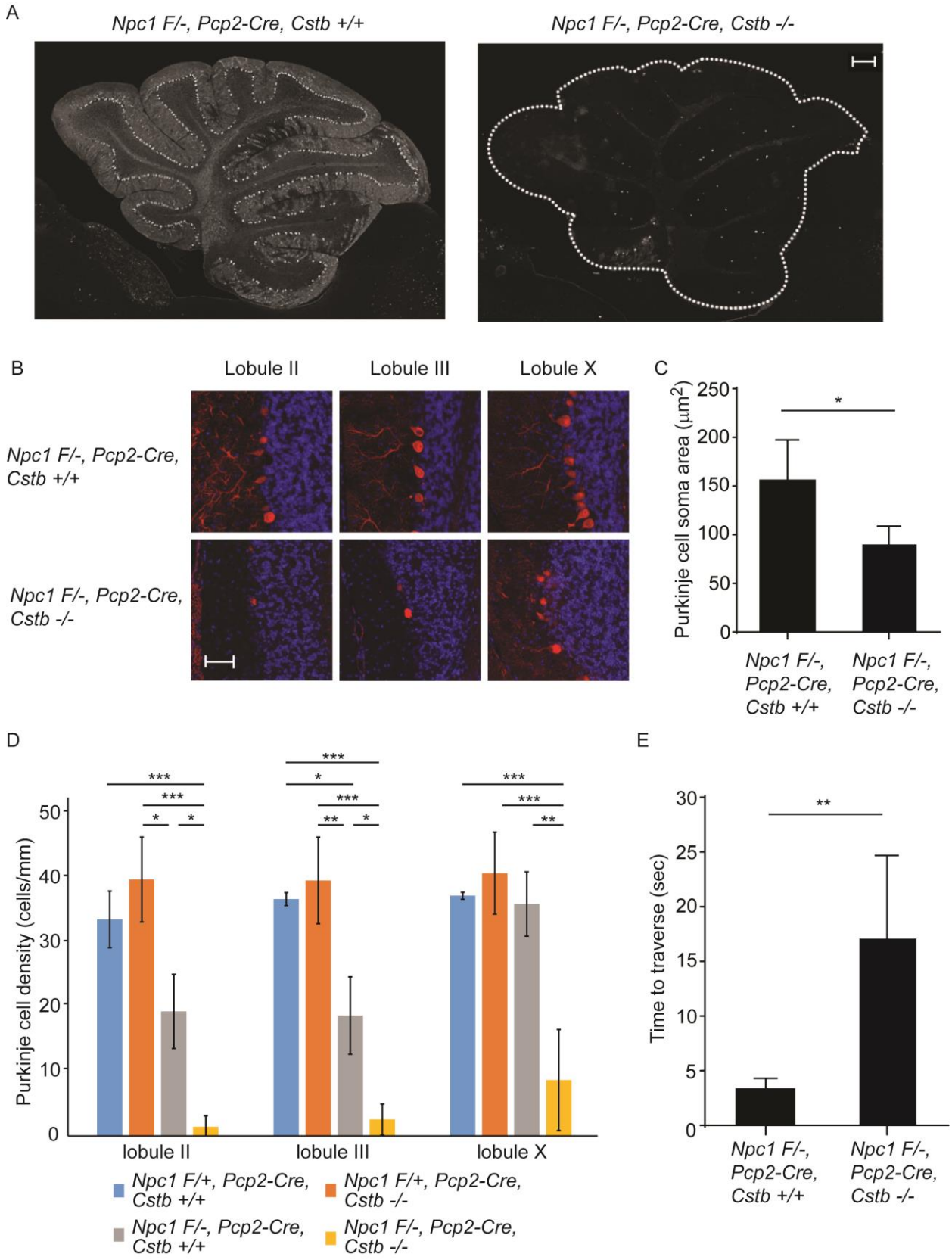
A
Npc1 F/-, Pcp2-Cre, Cstb +/+
Npc1 F/-, Pcp2-Cre, Cstb -/-
B
Lobule II
Lobule III
Lobule X
Npc1 F/-, Pcp2-Cre, Cstb +/+
Npc1 F/-, Pcp2-Cre, Cstb -/-
C
Purkinje cell soma area (μm2)
250
200
150
100
50
0
*
Npc1 F/-, Pcp2-Cre, Cstb +/+
Npc1 F/-, Pcp2-Cre, Cstb -/-
D
Purkinje cell density (cells/mm)
50
40
30
20
10
0
lobule II
lobule III
lobule X
Npc1 F/+, Pcp2-Cre, Cstb +/+
Npc1 F/+, Pcp2-Cre, Cstb -/-
Npc1 F/-, Pcp2-Cre, Cstb +/+
Npc1 F/-, Pcp2-Cre, Cstb -/-
E
Time to traverse (sec)
30
25
20
15
10
5
0
**
Npc1 F/-, Pcp2-Cre, Cstb +/+
Npc1 F/-, Pcp2-Cre, Cstb -/-

**Figure 2.5 Purkinje cell loss following cystatin B deficiency is due to neurodegeneration and not a neurodevelopmental deficiency. (A)** Immunofluorescent staining of Purkinje cells (calbindin antibody) at 3 weeks of age in the cerebellar midline. *Left panel*, *Npc1 F/-, Pcp2-Cre, Cstb+/+*; *right panel*, *Npc1 F/-, Pcp2-Cre, Cstb-/-*. Scale bar = 200 μm. **(B)** Purkinje cell density in lobules II, III and X was quantified in the cerebellar midline of 3-week-old *Npc1 F/-, Pcp2-Cre, Cstb-/-* mice; data from 8-week-old *Npc1 F/-, Pcp2-Cre, Cstb-/-* mice (from Figure 2.4C) is shown for comparison (mean ± SD, $n = 4$, *P<0.05, **P<0.01). **(C)** Detection of apoptotic Purkinje cells by co-immunofluorescent staining for calbindin (red) and activated caspase-3 (green) at 3 weeks of age in the cerebellar midline; nuclei were stained by DAPI. *Top panel*, *Npc1 F/-, Pcp2-Cre, Cstb+/+*; *bottom panel*, *Npc1 F/-, Pcp2-Cre, Cstb-/-*. Scale bar = 50 μm.

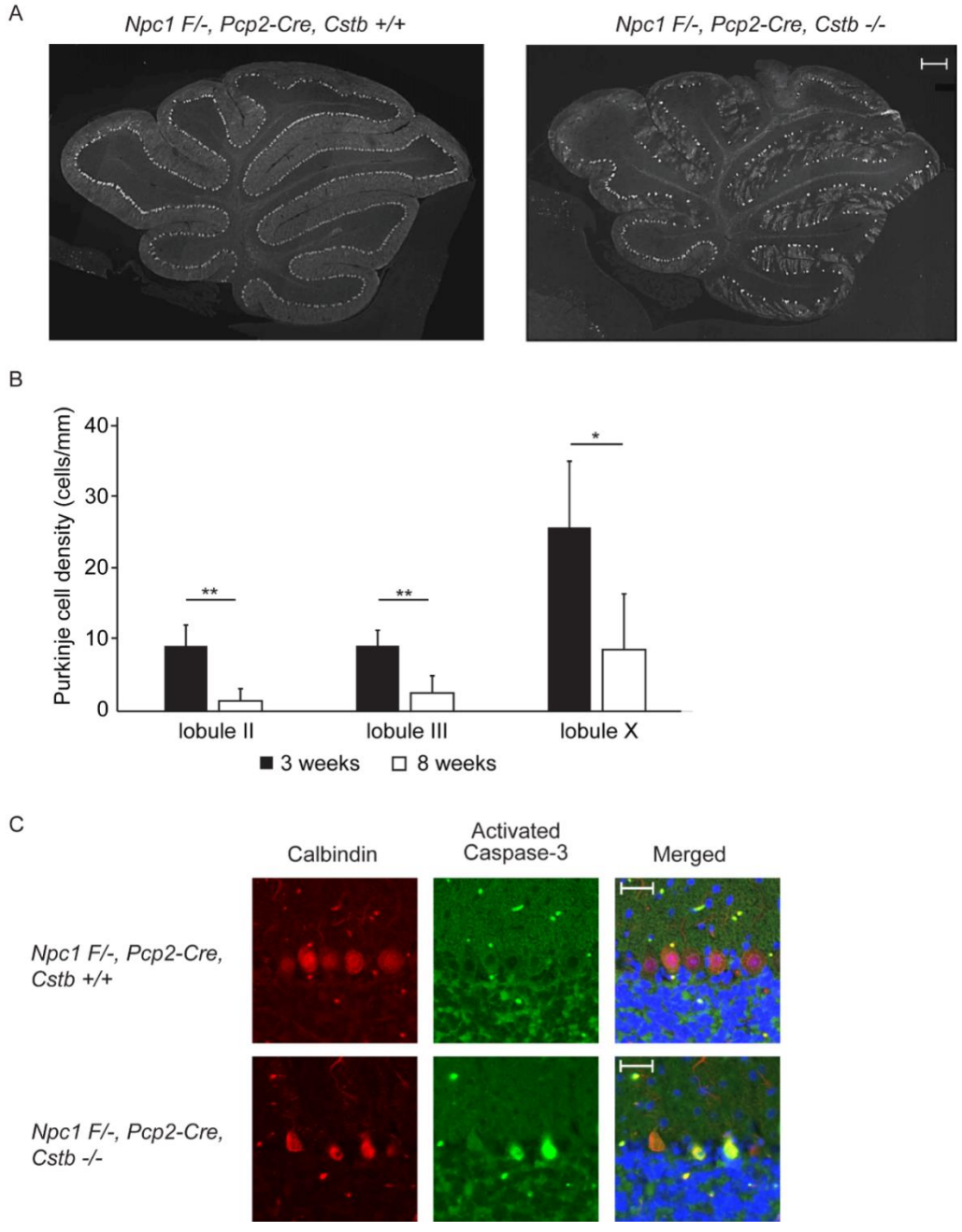

### 2.3.4 Npc1 deficiency disrupts cathepsin localization in cerebellar Purkinje cells.

To explore the mechanism by which cystatin B deficiency enhanced cerebellar degeneration in NPC mice, we considered the possibility that cathepsins were partially mislocalized outside lysosomes in the diseased brain, rendering Purkinje cells sensitive to cystatin B deletion and leading to apoptosis. This notion was based on prior work showing that cathepsin B is markedly increased in cytosolic fractions of cerebellar lysates from Npc1 deficient mice compared to controls (Amritraj et al., 2009). Furthermore, the release of cathepsins into the cytosol has been shown to trigger cell death (Groth-Pedersen and Jaattela, 2013). To determine cathepsin localization in Npc1 deficient Purkinje cells, we performed immunofluorescence staining for cathepsins B or L and LAMP-1, a marker of late endosomes and lysosomes **(Figure 2.6)**. Confocal microscopy demonstrated that the majority of the cathepsin signal in the cytosol of Purkinje cells co-localized with Lamp1 in *Npc1 Flox/+, Pcp2-Cre* mice, irrespective of the *Cstb* genotype. In contrast, co-localization of cathepsins with Lamp1 was significantly diminished in *Npc1-/-* Purkinje cells. These data indicated that disease was associated with an increased fraction of cathepsins outside Lamp1-positive vesicles, consistent with previous observations (Amritraj et al., 2009). Similar findings have been reported in a mouse model of Niemann-Pick type A (NPA) disease, a related neurodegenerative disorder caused by deficiency of acid sphingomyelinase (Gabande-Rodriguez et al., 2014). Notably, the mislocalization of cathepsins in *Npc1-/-* Purkinje cells was not influenced by *Cstb* genotype, suggesting that cystatin B deficiency exerted affects on disease phenotype by modulating cathepsin activity rather than localization.

Enhanced cytoplasmic localization of cathepsins could reflect leakage of lysosomal contents due to organelle membrane damage. Indeed, prior studies have indicated that lysosomal

membrane permeabilization triggers cell death, and that this can occur after damage by reactive oxygen species (ROS) (Boya et al., 2003; Brunk et al., 1997; Cirman et al., 2004; Kagedal et al., 2001). Analysis of the *Npc1-/-* mouse brain has demonstrated the occurrence of oxidative damage (Kennedy et al., 2013; Vazquez et al., 2012), and lipid oxidation products have emerged as a sensitive biomarker of NPC disease (Porter et al., 2010). Consistent with these observations, we found that cerebellar Purkinje cells deficient in Npc1 exhibited substantially more staining for superoxide dismutase 2 (SOD2) than controls, irrespective of *Cstb* genotype **(Figure 2.7A)**. These observations prompted us to study the sensitivity of control and NPC1 patient fibroblasts to cytotoxicity induced by ROS. This approach is based on published studies demonstrating that ROS can trigger cell death by promoting lysosomal membrane permeabilization (Boya et al., 2003; Brunk et al., 1997; Cirman et al., 2004; Kagedal et al., 2001). We used hydrogen peroxide as an oxidative stressor since it easily crosses membranes and induces formation of reactive hydroxyl radicals and iron-centered radicals (Terman et al., 2006). These free radicals destabilize the lysosomal membrane and induce lysosomal membrane permeabilization-dependent cell death (Krenn et al., 2015; Terman et al., 2006; Zhao et al., 2003). As shown in Figure 2.7B, NPC1 deficient fibroblasts are significantly more sensitive to cytotoxicity induced by hydrogen peroxide than control fibroblasts, with mean lethal concentration 50 ($LC_{50}$) values in NPC1 deficient and control cells of 337.9 μM (95% confidence intervals range 316.0 to 361.3) and 486.8 μM (95% confidence intervals range 465.4 to 509.1). To determine the extent to which cathepsins contributed to the cytotoxicity of NPC1 deficient cells exposed to hydrogen peroxide, we used genetic and pharmacological approaches to diminish cathepsin activity. Cystatin B overexpression rendered NPC1 deficient cells significantly more resistant to hydrogen peroxide-induced cell death **(Figure 2.7C)**. Similarly, treatment with CA-074 methyl ester (CA-074ME),

which is a selective, irreversible and membrane-permeable cathepsin B inhibitor (Buttle et al., 1992; Towatari et al., 1991; Yamamoto et al., 1992), significantly increased cell viability following exposure to hydrogen peroxide **(Figure 2.7D)**. Taken together, these data indicate that cathepsin activity contributes to the susceptibility of NPC1 deficient cells to ROS-induced cytotoxicity, and support a model in which lysosomal membrane permeabilization is a component of the cascade leading to neuron loss in the NPC brain.

**Figure 2.6 Cathepsin mislocalization in *Npc1* deficient Purkinje cells.** Co-localization of cathepsin B or L with LAMP1 was examined in midline cerebellar sections of mice at 8 weeks of age. Immunofluorescent staining for LAMP1 (red) and cathepsin B (green, **panel A**) or cathepsin L (green, **panel C**) is shown; nuclei were stained by DAPI. Scale bar = 10 μm. Co-localization of cathepsin B and LAMP1 (**panel B**) or cytosolic cathepsin L and LAMP1 (**panel D**) was quantified (mean ± SD, n=10 cells, pooled from three independent experiments, **P<0.01, ***P<0.001, ****P<0.0001).

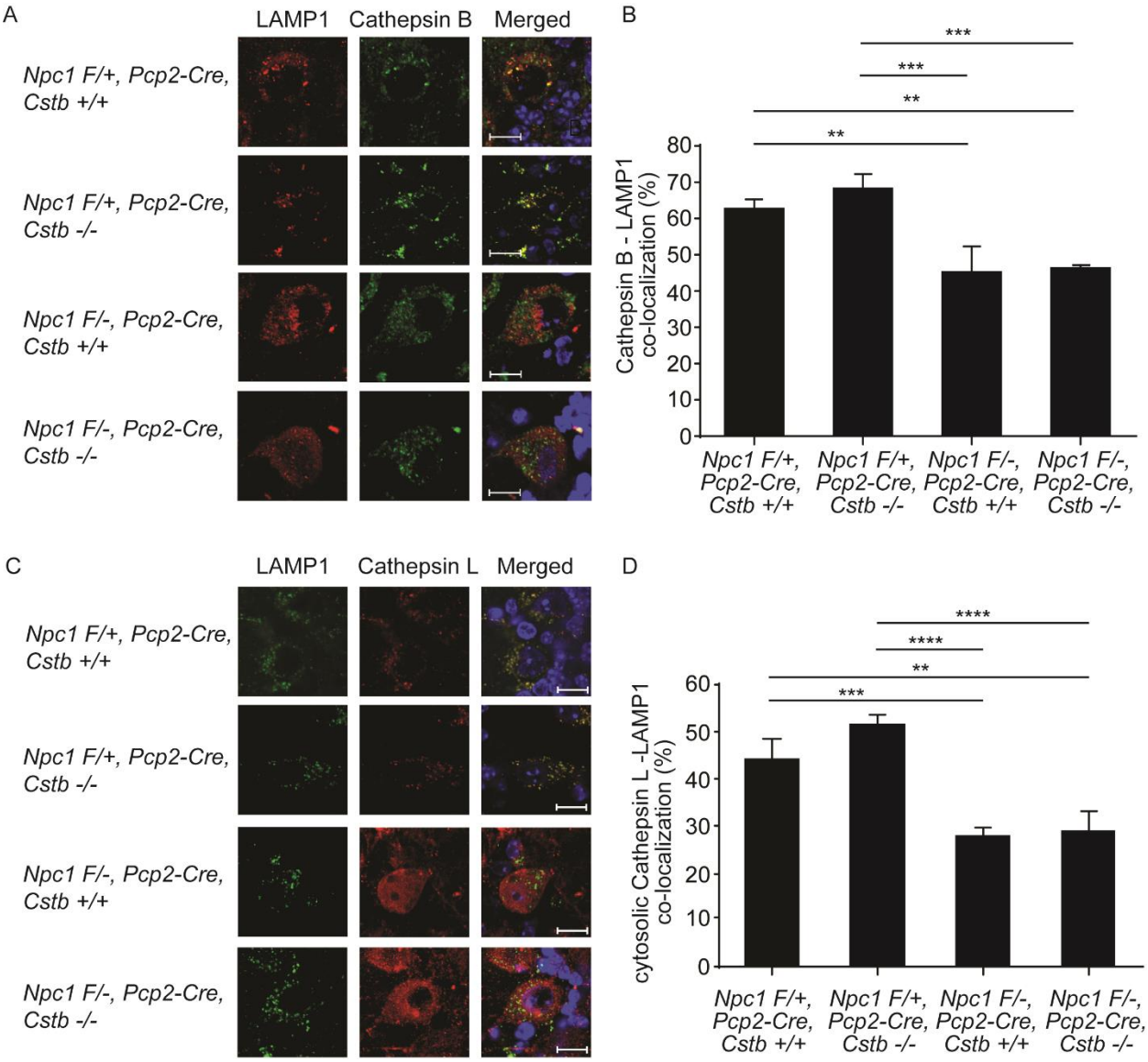

**Figure 2.7 NPC1 deficient cells are more sensitive to oxidative damage and rescued by cathepsin B inhibition. (A)** Immunofluorescence staining for SOD2 (green) and calbindin (red) at 3 weeks of age in the cerebellar midline; nuclei were stained by DAPI. Scale bar = 10 μm. **(B - D)** Viability of primary fibroblasts was determined by XTT assay. Data are mean ± SD, *n* = 3 independent experiments, normalized to untreated control cells. **P<0.01, ***P<0.001 **(B)** Control and NPC1 deficient fibroblasts were treated with increasing concentrations (0 - 2000 μM) of $H_2O_2$ for 24 hrs. **(C)** NPC1 deficient fibroblasts were transfected to express CSTB or vector control. After 48hr, cells were treated with increasing concentrations of $H_2O_2$ for 24 hrs. **(D)** NPC1 deficient fibroblasts were treated concurrently with 0 or 500 μM $H_2O_2$, and with vehicle (DMSO) or 1μM CA-074ME for 24 hrs.

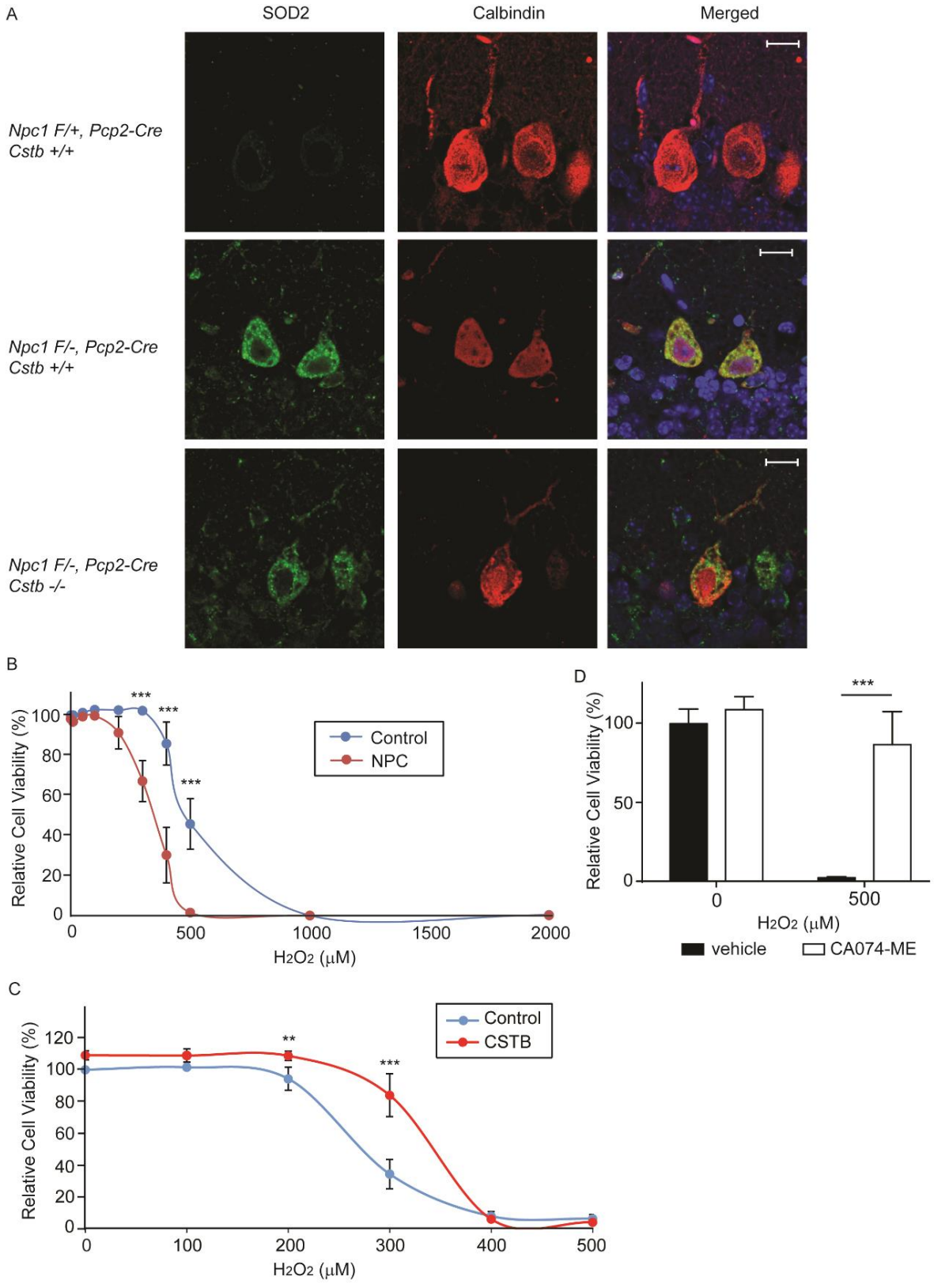
A
SOD2
Calbindin
Merged
Npc1 F/+, Pcp2-Cre
Cstb +/+
Npc1 F/-, Pcp2-Cre
Cstb +/+
Npc1 F/-, Pcp2-Cre
Cstb -/-
B
Relative Cell Viability (%)
Control
NPC
H2O2 (μM)
C
Relative Cell Viability (%)
Control
CSTB
H2O2 (μM)
D
Relative Cell Viability (%)
H2O2 (μM)
vehicle
CA074-ME

## 2.4 Discussion

Recent biochemical and structural studies have provided important insights into the mechanisms by which the NPC1 and NPC2 proteins regulate intracellular lipid transport (Infante et al., 2008; Kwon et al., 2009). Nonetheless, pathways leading to the severe neurodegeneration that underlies the clinical phenotype of NPC disease have remained elusive. Here, we demonstrate that cystatin B, an endogenous inhibitor of lysosomal cathepsins B, H and L, plays a critical role in regulating Purkinje cell degeneration in NPC mice. We show that decreased expression of cystatin B in patient fibroblasts enhances cathepsin activity. Deletion of the encoding *Cstb* gene in Npc1 deficient mice results in unexpected and deleterious effects, particularly within the cerebellum where diffuse loss of Purkinje cells is observed. This severe pathology is shown to occur through cell autonomous mechanisms that trigger apoptotic Purkinje cell death. Moreover, our analyses corroborate data in the literature showing that lysosomal cathepsins are mislocalized within the cytosol of Npc1 deficient Purkinje cells (Amritraj et al., 2009; Gabande-Rodriguez et al., 2014). We provide evidence that this may be a consequence of damage to lysosomal membranes by reactive oxygen species, leading to the leakage of lysosomal contents that culminates in neurodegeneration **(Figure 2.8)**. The observation that *Npc1* and *Cstb* deletion genetically interact to potently enhance the degenerative phenotype of the NPC cerebellum provides strong support for this proposed pathogenic mechanism.

This model of disease takes into account the observation that Npc1 deficiency does not alter cathepsin maturation, a process that is dependent upon normal trafficking to lysosomes. Moreover, our data are consistent with reports from NPC and NPA mouse models in which enhanced cytosolic localization of cathepsins (Amritraj et al., 2009; Gabande-Rodriguez et al., 2014) and the occurrence of oxidative damage within the CNS (Kennedy et al., 2013; Vazquez et

al., 2012) have been documented. Notably, a number of studies have demonstrated that cathepsins retain some activity at neutral pH (Turk et al., 1995; Turk et al., 1993; Turk et al., 1994). Furthermore, *in vitro* experiments performed at neutral pH demonstrate that cathepsins B, H, L, S and K cleave Bid and induce release of cytochrome c from isolated mitochondria, leading to the activation of caspases (Cirman et al., 2004; Taylor et al., 2008). Prior studies have also shown that cystatin B deficiency sensitizes neurons or tumor cells to oxidative stress (Butinar et al., 2014; Lehtinen et al., 2009), observations that are consistent with our model. We note that cystatin B may exert additional protective effects on the survival of Purkinje cells through alternative mechanisms. For example, cystatin B has been shown to protect mitochondrial integrity following exposure to reactive oxygen species, independent of its action on lysosomal cathepsins (Maher et al., 2014). Accordingly, we can infer that cystatin B may exert beneficial effects on Purkinje cells by acting upon several distinct targets.

The exquisite sensitivity of Npc1 deficient Purkinje neurons to the effects of cystatin B deletion is noteworthy. To glean insights into this observation, we queried the Allen Brain Atlas, an on-line database that contains quantitative three-dimensional expression data derived from *in situ* hybridizations performed on the adult mouse brain. In this database cystatin B expression is observed in the cerebellum, medulla and pons, while cathepsin B expression occurs widely throughout the central nervous system. Thus, cystatin B may function as a vital inhibitor of cathepsins in cerebellar Purkinje cells, while other mechanisms predominate in many other brain regions. Additional factors may also contribute to Purkinje cell degeneration in double null mutant mice, such as increased sensitivity to reactive oxygen species that leads to enhanced lysosomal membrane damage. Our studies offer insights into mechanisms underlying neuron loss in NPC disease and suggest potential strategies to ameliorate this process. Indeed, a cathepsin

inhibitor has been shown to abrogate death of cortical neurons *in vitro* following treatment with U18666A, a small molecule that mimics the NPC phenotype (Amritraj et al., 2009). These findings suggest that targeting the lysosomal cell death pathway may be beneficial in preventing neurodegeneration in NPC disease. Our data provide critical support that this pathogenic cascade underlies neuronal loss in NPC disease, an insight that provides a foundation for the future development of therapeutic strategies.

**Figure 2.8 Model of cerebellar neurodegeneration in NPC1 disease.** NPC1 deficiency results in increased production of reactive oxygen species, which damage lysosomal membranes, promote leakage of cathepsins into the cytosol, and lead to apoptotic death of Purkinje cells. Cystatin B functions to block this cascade by inhibiting cytosolic cathepsins.

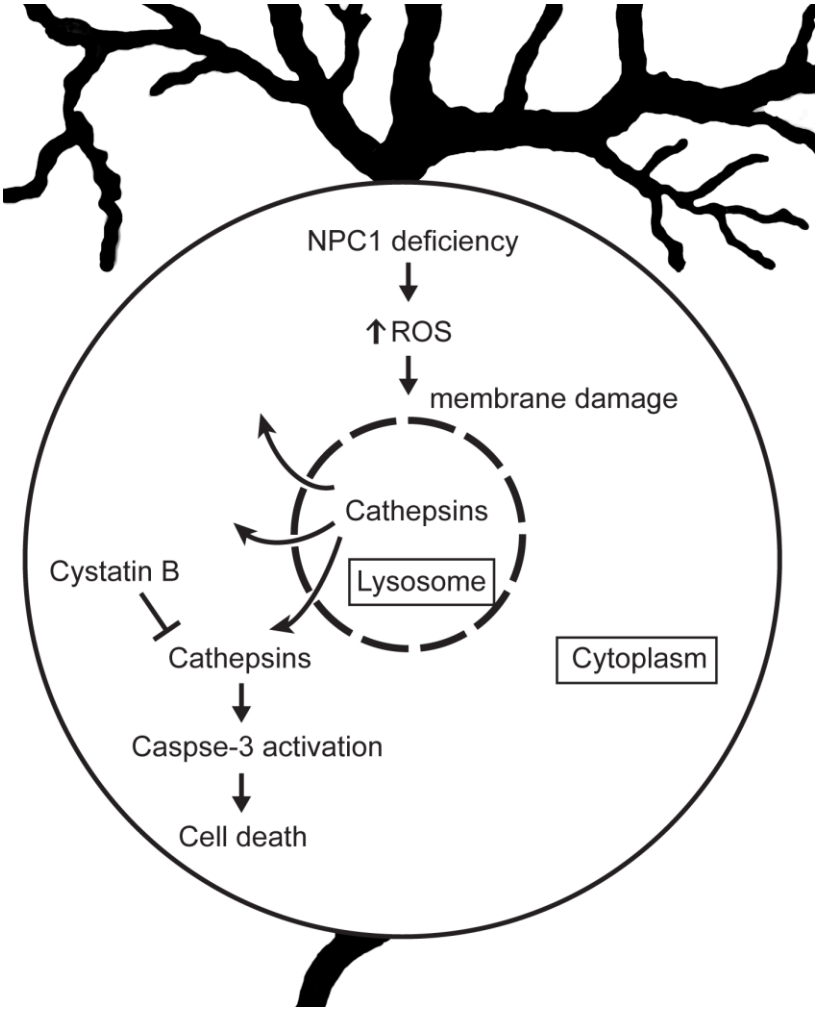

## 2.5 Materials and Methods

### 2.5.1 Reagents

Magic Red cathepsin B assay kit (cat. 938) was from Immunochemistry Technologies. Fluorescent dextran (D3305) and BODIPY 493/503 (D3922) was from Life Technologies. Filipin (F9765) and all other chemicals were from Sigma-Aldrich. Antibodies used in this study were anti-NPC1 (Abcam, ab36983), anti-GAPDH (Santa Cruz, sc-25578), anti-glial fibrillary acidic protein (GFAP) (Dako, Z0334), anti-Iba1 (Wako, 019-19741), anti-calbindin (Sigma-Aldrich, c2724), anti-cathepsin B (Abcam, ab33538), anti-cathepsin L (Athens Research and Technology, 01-12-030112), anti-cystatin B (Sigma-Aldrich, C5243), anti-SOD-2 (Novus Biologicals, NB100-1992) and anti-caspase-3 (cell signaling, 9664). Anti-GM2 antibody was a gift from Dr. Kostantin Dobrenis (Albert Einstein College of Medicine).

### 2.5.2 Mice

Mice containing the flox and null *Npc1* alleles and the *Pcp2-Cre* transgene were generated and genotyped as described previously (Elrick et al., 2010). Mice with a cystatin B null allele were initially from Dr. Richard Myers (Pennacchio et al., 1998). All lines were backcrossed to C57BL6/J for ≥10 generations. All animal procedures were approved by the University of Michigan Committee on the Use and Care of Animals.

### 2.5.3 Behavioral testing

Motor function was measured by balance beam test. Mice at 7 weeks of age were trained on three consecutive days to cross a 6 mm wide beam suspended at 50 cm. Mice were then tested in triplicate at 8 weeks of age. Data are reported as average time to traverse the beam, allowing a maximum of 25 sec and scoring falls as 25 sec.

### 2.5.4 Filipin staining

Human fibroblasts (Coriell Cell Repositories, control, GM08399; NPC1 P237S/ I1061T, GM03123) were grown in chamber slides (Lab-Tek, 154526), rinsed with PBS, and fixed with 4% paraformaldehyde for 30 min. After washing with PBS, cells were incubated with 1.5 mg/ml glycine for 10 min, washed with PBS and stained with 0.05 mg/ml filipin, 0.02 mg/ml BODIPY and 10% FBS in PBS for 2 hrs at room temperature. Stained cells were imaged by focusing on the BODIPY channel. Filipin images were captured with the UV filter set on a Zeiss AxioImager Z1 microscope. Quantitative analysis of filipin images from more than 5 fields/experiment was performed by NIH ImageJ software as described previously (Yu et al., 2012). Data reported are from three independent experiments. For mouse brain staining, tissue embedded in Optimal Cutting Temperature (OCT) compound (Tissue-Tek) was sectioned at 10 μm and stained as described above. Representative images are from one of three mice per genotype.

### 2.5.5 Immunofluorescence staining

5 μm sections from brains embedded in paraffin were deparaffinized with xylenes and ethanol. Sections were boiled in 10 mM sodium citrate, pH 6, for 10 min for antigen retrieval. After washing with water, sections were blocked with 5% goat serum and 1% BSA in PBS for 1 hr and then incubated in primary antibody (calbindin 1:500, LAMP1 1:10, cathepsin B 1:50, cathepsin L 1:100, GFAP 1:1000, Iba1 1:1000, caspase-3 1:200, SOD-2 1:200) diluted in 1.5% blocking solution overnight at $4^{o}$ C. Sections were subsequently incubated in secondary antibodies conjugated to Alexa Fluor 594 or 488 for 2 hrs and mounted with mounting medium

including DAPI (Vector Lab**,** H-1200). Images were captured on an Olympus FluoView 500 Confocal microscope. Co-localization was quantified using Zeiss MetaMorph imaging software.

### 2.5.6 Gene knockdown

ON-TARGET plus SMART pool cystatin B siRNA (Dharmacon, L-017240-00-0005) and ON-TARGET plus non-targeting pool (Dharmacon, D-001810-10-05) were used to modulate gene expression. Cells were transfected with 10 μl of 10 μM siRNA using the Nucleofector II (Lonza, program U-23) following the manufacturer's instructions.

### 2.5.7 Cathepsin B assay

Control or NPC1 deficient fibroblasts were transfected with siRNA as indicated in the figure legend, cultured in a chamber slide (Lab-Tek, 1554096), and analyzed for cathepsin B activity after 48 hrs, as described previously (Elrick et al., 2012). Briefly, the cells were incubated with a 1:3000 dilution of cathepsin B-specific Magic Red reagent and imaged using a Deltavision-RT Live Cell Imaging System. Images were captured at 1 min intervals for 20 min. Fluorescence at 554/25 nm excitation and 609/25 nm emission was quantified using NIH ImageJ. Total fluorescence intensity above threshold was plotted as a function of time, and the slope of the line was used to determine cathepsin B activity.

### 2.5.8 Immunohistochemical staining

10 μm sections from brains embedded in OCT were boiled in 10 mM sodium citrate, pH 6, for 10 min. After washing with PBS, tissue sections were treated with 3% hydrogen peroxide for 10 min to quench endogenous peroxidase activity. Sections were blocked with 5% goat serum, 1% BSA, 0.02% saponin in PBS for 1 hr and then stained overnight at 4$^{o}$C with a GM2

antibody (1:15) diluted in 1.5% blocking solution. Sections were subsequently incubated with a biotinylated anti-mouse antibody (1:400) for 2 hrs at room temperature. Vectastain Avidin-Biotin Complex (ABC) reagent (Vector lab, PK4001) and a peroxidase substrate (DAB) reagent (Vector lab, SK4100) were used to detect the biotinylated secondary antibody. Representative images in the figure are from one of three mice per genotype.

### 2.5.9 Morphological analysis

Purkinje cell density and cerebellar area were quantified in midline sagittal sections stained with hematoxylin and eosin. For cell density, Purkinje cells were recognized as large cells with amphophilic cytoplasm, large nuclei with open chromatin and prominent nucleoli that were located between the molecular and granular layers. The number of cells was normalized to the length of the Purkinje layer, as measured by NIH ImageJ software. For cerebellar area, the cerebellum was selected and measured by NIH ImageJ, and pixel size was converted to $mm^2$ using the scale bar as a calibration standard. For analysis of Purkinje cell soma size, calbindin staining was used to define the cell soma. The area was measured as described above for analysis of cerebellar area.

### 2.5.10 Western blotting

Cells were lysed in RIPA buffer (Thermo Scientific) containing Complete protease inhibitor (Roche) and Halt phosphatase inhibitor (Thermo Scientific). Protein concentrations were measured by the Bio-Rad DC protein assay kit (Bio-Rad) and normalized. Proteins were separated by 4 - 20% gradient sodium dodecyl sulfate polyacrylamide gel electrophoresis (SDS-PAGE) and transferred to nitrocellulose membranes using a semidry electrophoretic transfer apparatus (BioRad). Immunoreactivity was detected by TMA-6 (Lumigen) or ECL (Thermo

Scientific). Antibodies used were anti-cathepsin B (1:500), anti-cystatin B (1:10000), anti-GAPDH (1:5000) and anti-NPC1 (1:1000). Each protein band was selected and quantified by ImageJ software after subtracting the background signal. Specific band intensity was normalized to GAPDH.

### 2.5.11 Cell viability assay

Control or NPC1 deficient fibroblasts were treated with the indicated doses of $H_2O_2$ for 24 hrs. Cells viability was determined by XTT assay (ATCC, 30-1011K) following the manufacturer's instructions. In brief, 50µl XTT was added in 100µl cell culture medium and cells were incubated for 4 hrs in a $CO_2$ incubator at 37$^o$ C. The plates were assessed spectrophotometrically at 490 nm for specific absorbance and at 650 nm for non-specific absorbance using a microplate reader. For cystatin B overexpression, Nucleofector II (Lonza, program U-23) was used to transfect cells with the indicated plasmids. After 48 hrs, cells were treated with $H_2O_2$ for 24 hrs and tested for viability. To inhibit cathepsin B activity, 1µM CA-074ME was used.

### 2.5.12 Statistics

Statistical significance was assessed by unpaired Student's *t* test (for comparison of two means) or ANOVA (for comparison of more than two means). Statistics were performed using the Prism 6.02 software (GraphPad). P values less than 0.05 were considered significant.

## 2.6 Acknowledgements

We thank Drs. Richard Myers and Ralph Nixon for *Cstb* null mice, Dr. Kostantin Dobrenis for anti-GM2 antibody and Dr. Marialuisa Melli for Cystatin B plasmid. This work was supported by the National Institutes of Health [R01 NS063967 to A.P.L.].

# Chapter 3

# Heat shock protein beta-1 modifies anterior to posterior Purkinje cell vulnerability in a mouse model of Niemann-Pick type C disease

## 3.1 Abstract

Selective neuronal vulnerability is characteristic of most degenerative disorders of the CNS, yet mechanisms underlying this phenomenon remain poorly characterized. Many forms of cerebellar degeneration exhibit an anterior-to-posterior gradient of Purkinje cell loss including Niemann-Pick type C1 (NPC) disease, a lysosomal storage disorder characterized by progressive neurological deficits that often begin in childhood. Here, we describe an approach to identify candidate genes underlying vulnerability of Purkinje cells in anterior cerebellar lobules using data freely available in the Allen Brain Atlas. This approach led to the identification of 16 candidate neuroprotective or susceptibility genes. We demonstrate that one candidate gene, heat shock protein beta-1 (*HSPB1*), promoted neuronal survival in cellular models of NPC disease through a mechanism that involved inhibition of apoptosis. Additionally, we show that *HSPB1* over-expression in NPC mice slowed the progression of motor impairment and diminished cerebellar Purkinje cell loss. We confirmed the modulatory effect of Hspb1 on Purkinje cell degeneration *in vivo*, as knockdown by *Hspb1* shRNA significantly enhanced neuron loss. These results suggest that strategies to promote HSPB1 activity may slow the rate of cerebellar

degeneration in NPC disease, and highlight the use of bioinformatics tools to uncover pathways leading to neuronal protection in neurodegenerative disorders.

### 3.2 Introduction

Selective vulnerability of specific neuronal populations is a well characterized, though often perplexing feature of many neurodegenerative diseases (Double et al., 2010). Most commonly, these disorders are initiated by a uniform stress to the entire CNS, such as a genetic mutation, toxic insult, or aging. However, only a subset of neurons respond to these stressors by degenerating, while others remain resistant and apparently maintain their normal function (Schultz et al., 2011). Although this phenomenon is widely observed, the underlying mechanisms remain poorly understood. Notably, the factors regulating neuronal vulnerability represent attractive therapeutic targets, with the potential to convert susceptible neuronal populations into ones that are disease resistant.

One particularly striking example of selective vulnerability is the degeneration of cerebellar Purkinje cells (Sarna and Hawkes, 2003). Purkinje cells represent the sole output of the cerebellar cortex. Loss of Purkinje cells, therefore, leads to significant deficits of motor coordination, including ataxia and tremors. Despite the apparent similarity of Purkinje cells in their morphology, connectivity, and electrophysiological properties, many cerebellar disorders affect Purkinje cells in a non-uniform way, leading to a distinct spatiotemporal pattern of loss that is reproducible not only between cases of a single disease, but across many otherwise unrelated diseases and injuries. One common pattern reveals a strong resistance of Purkinje cells in lobule X to degeneration, contrasted with the exquisite sensitivity of the anterior zone (lobules

II-V), and moderate susceptibility of the intermediate (lobules VI-VII) and posterior zones (lobule VIII and rostral aspect of lobule IX). Superimposed onto this anterior-to-posterior gradient is often a pattern of parasagittal stripes in which differential vulnerability is also observed (Sarna and Hawkes, 2003). Diseases displaying the classic anterior-to-posterior gradient may arise from genetic mutations, including spinocerebellar ataxias type 1 (Clark et al., 1997) and 6 (Takahashi et al., 1998), late infantile neuronal ceroid lipofuscinosis (Sleat et al., 2004), saposin C deficiency, a rare cause of Gaucher Disease (Yoneshige et al., 2010), ataxia telangiectasia (Tavani et al., 2003), and Niemann-Pick disease types A/B (Sarna et al., 2001) and C (Sarna et al., 2003); sporadic disorders, including multiple system atrophy (Kume et al., 1991) and chronic epilepsy (Crooks et al., 2000); toxins, including alcohol (Torvik and Torp, 1986), cytosine arabinoside (Winkelman and Hines, 1983), methotrexate (Ciesielski et al., 1994); hypoxia/ischemia (Biran et al., 2011; Welsh et al., 2002); paraneoplastic syndromes (Mizutani et al., 1988); and even normal aging (Andersen et al., 2003). This pattern is also seen in many spontaneous mouse mutants, including *pcd* (Wang and Morgan, 2007), *leaner* (Heckroth and Abbott, 1994), *toppler* (Duchala et al., 2004), *robotic* (Isaacs et al., 2003), *shaker* (Tolbert et al., 1995), and *lurcher* (Armstrong et al., 2010); or targeted mutants, such as *saposin D* knockout (Matsuda et al., 2004), prion protein knockout (Rossi et al., 2001), and overexpression of the prion protein related gene *doppel* (Anderson et al., 2004). The fact that such a diverse array of insults leads to the same pattern of Purkinje cell death suggests that selective vulnerability of Purkinje cell subpopulations arises not from the initiating event of the disease process, but instead from differential regulation of cellular survival or death pathways in response to these injuries. We hypothesize that the identification of pathways responsible for this phenomenon will yield therapeutic targets broadly applicable to this large class of cerebellar disorders.

As a model for patterned Purkinje cell loss, we have studied murine Niemann-Pick type C1 disease (NPC). NPC is caused by mutations in the genes encoding NPC1 or NPC2 proteins, which are thought to act cooperatively in the efflux of cholesterol from late endosomes (LE) and lysosomes (LY) (Carstea et al., 1997; Kwon et al., 2009; Naureckiene et al., 2000). The consequence of these mutations is the accumulation of cholesterol and glycosphingolipids in the LE/LY compartment, leading to neurodegeneration by mechanisms that are not yet understood (Vanier and Millat, 2003). We recently demonstrated that conditional deletion of *Npc1* in Purkinje cells leads to a purely cell autonomous degeneration that recapitulates the spatiotemporal pattern of cell loss observed in mice with germline *Npc1* deletion (Elrick et al., 2010). Further, because Purkinje cell death does not cause early mortality in these mice, we were able to follow Purkinje cell survival beyond the typical lifespan of NPC mice. During this period, the population of surviving Purkinje cells in lobule X remained stable, while neurodegeneration continued to progress in lobules II-IX, thus highlighting the strong resistance of these cells to degeneration. Given the cell autonomous nature of Purkinje cell loss in NPC, we hypothesized that this selective vulnerability arises from intrinsic biological differences that are driven by differential gene expression. To test this notion, here we used a bioinformatics approach to identify genes that are differentially expressed between disease-resistant and vulnerable Purkinje cell populations. To test the biological function of these differentially expressed genes, we used *in vitro* and *in vivo* model of NPC and characterized the ability of one of these candidate genes to protect neurons from degeneration.

## 3.3 Results

### 3.3.1 Identification of candidate genes underlying selective vulnerability of Purkinje cells

Using mice containing a conditional null allele of the *Npc1* gene, we found that gene deletion in Purkinje cells recapitulates the spatiotemporal pattern of neuron loss observed in mice with global germline deletion of *Npc1* **(Figure 3.1A)** (Elrick et al., 2010; Sarna et al., 2003). The population of surviving Purkinje cells is located within posterior lobules of the cerebellar midline, while age-dependent progressive Purkinje cell loss is observed anterior lobules **(Figure 3.1B)** (Elrick et al., 2010). We hypothesized that differential gene expression underlies this selective neuronal vulnerability. To search for genes differentially expressed between Purkinje cell subpopulations, we utilized the Allen Brain Atlas **(Figure 3.1C)**. This resource contains quantitative three-dimensional expression data derived from *in situ* hybridizations for greater than 20,000 genes in the adult C57BL6/J mouse brain (Lein et al., 2007). The complete gene expression dataset was downloaded and used to construct a single expression matrix with spatial coordinates and gene identifiers arrayed on separate axes. This strategy allowed us to treat the data for each location in the brain analogously to a single microarray experiment. The coordinates corresponding to cerebellar lobule X, the location of the most resistant Purkinje cells, and lobules II and III, the most highly vulnerable, were defined as regions of interest **(Figure 3.1B)**. For analysis, all coordinates falling within one region of interest were treated as replicate microarray experiments. This approach allowed us to use bioinformatics tools developed for microarray analysis to query the Allen Brain Atlas dataset. Differential gene expression between lobules was determined by *t*-test and Significance Analysis of Microarrays (SAM) (Tusher et al., 2001), followed by manual curation of *in situ* hybridization images. Manual curation was required to remove false positives created by expression in non-Purkinje cell types and technical artifacts in the archived images.

Initial analysis revealed 234 differentially expressed genes, of which 185 were more highly expressed in lobules II and III and 49 were more highly expressed in lobule X. We next sought to prioritize this list to identify testable candidates with putative roles in promoting or preventing neurodegeneration. The Allen Brain Atlas data, being derived from *in situ* hybridizations, presented a challenge in this regard, as expression levels were regarded as semi-quantitative. Further, because expression data within each *z* plane came from the same hybridization experiment, they were not considered statistically independent samples. For these reasons, we were unable to rank the gene list by either the magnitude of differential expression or the degree of significance. Instead, we prioritized genes whose expression differences were absolute and tightly correlated with Purkinje cell survival in midline cerebellar sections. To accomplish this, we only included genes whose expression was undetectable in one region of interest, and whose expression matched or was the inverse of the survival pattern in 20 week old *Npc1 flox/-;Pcp2-Cre* mice: strong in lobule X, patchy throughout the intermediate and posterior zones, with additional sparing in the caudal aspect of lobule IX and a region spanning the caudal aspect of lobule VI and rostral lobule VII **(Figure 3.1A)**. This yielded sixteen candidate neuroprotective or susceptibility genes **(Figure 3.3A, Table 3.1)**; *in situ* hybridization images from the Allen Brain Atlas for the candidate genes highly expressed in regions of cell survival are shown in Figure 3.2.

**Figure 3.1 Schematic of gene expression analysis. (A)** Calbindin staining of cerebellum from 20-week old *Npc1 flox/-*, *Pcp2-Cre* mouse, demonstrating survival pattern of Purkinje cells in midline. Scale bar = 500 μm. **(B)** Schematic of differential vulnerability of Purkinje cell subpopulations. Regions of interest (ROI) were selected to include the population that experiences the most rapid neurodegeneration (lobules II and III, ROI #1) or the population that does not degenerate (lobule X, ROI #2). **(C)** Approach to gene expression analysis. Allen Brain Atlas data was downloaded and consolidated into a single gene expression matrix. Each row

represents gene expression data from a single series of *in situ* hybridization data, while each column represents a single voxel within the mouse brain. The data set was then narrowed to include only voxels lying within the defined regions of interest. To identify genes differentially expressed between regions of interest, expression data was treated analogously to replicate microarrays and subjected to standard statistical tests (*t*-test and Significance Analysis for Microarrays). The top 1000 most significant genes were accepted for manual curation to verify expression in Purkinje cells. The gene list was further narrowed to include only genes with absolute expression differences between regions of interest, and expression matching the pattern of Purkinje cell survival or death throughout the entire cerebellum.

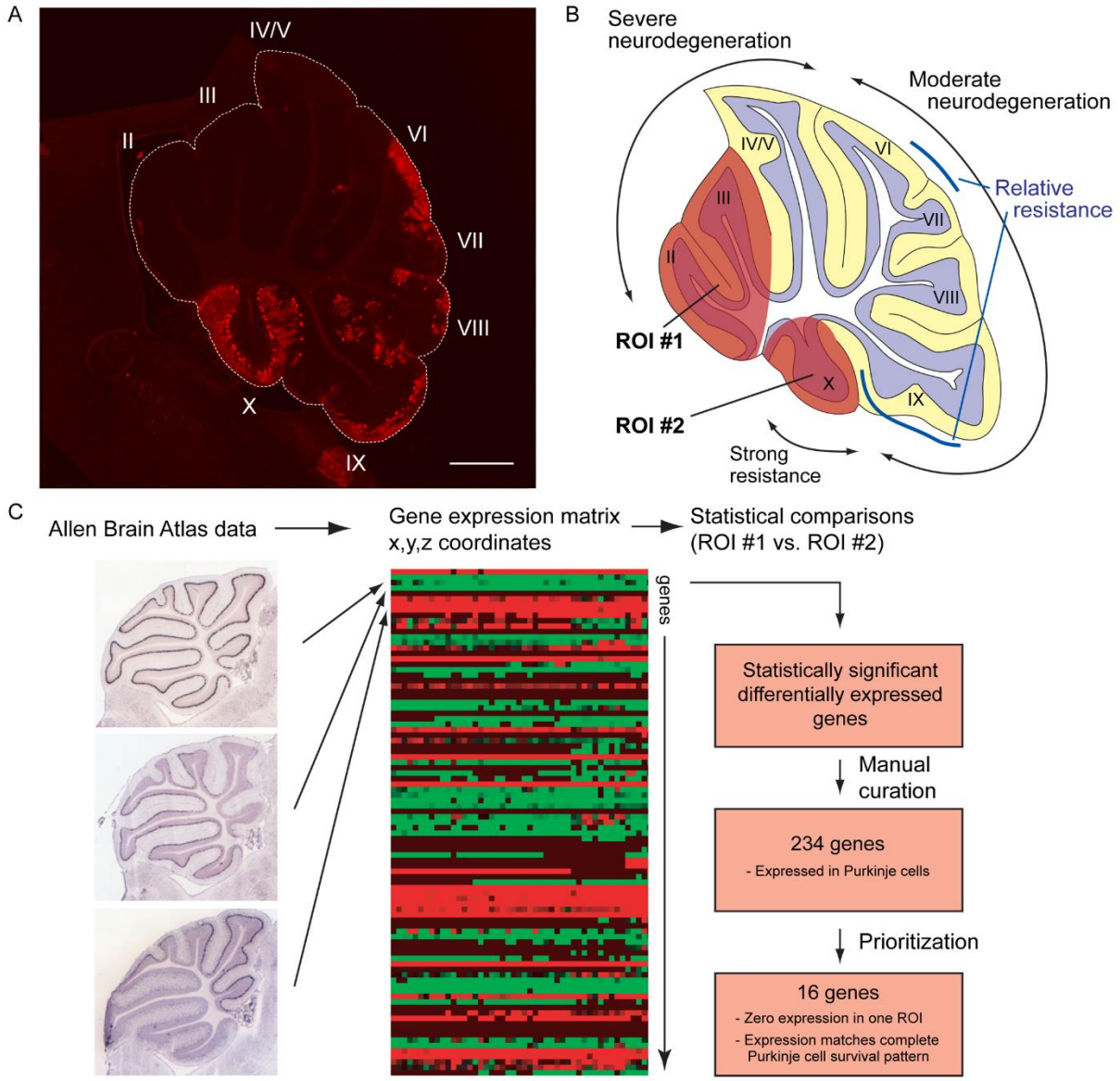

**Table 3.1 Genes differentially expressed in Purkinje cells in anterior or posterior lobules**

| Gene symbol | Gene name | Gene ID | Region of expression |
|---|---|---|---|
| B3galt5 | UDP-Gal:betaGlcNAc beta 1,3-galactosyltransferase, polypeptide 5 | 93961 | posterior |
| Hspb1 | heat shock protein beta-1 | 15507 | posterior |
| Pde1b | phosphodiesterase 1B, Ca2+-calmodulin dependent | 18574 | posterior |
| Plcxd2 | phosphatidylinositol-specific phospholipase C, X domain containing 2 | 433022 | posterior |
| Prkcd | protein kinase C, delta | 18753 | posterior |
| Th | tyrosine hydroxylase | 21823 | posterior |
| Alpk2 | alpha-kinase 2 | 225638 | anterior |
| Bace1 | beta-site APP cleaving enzyme 1 | 23821 | anterior |
| Chml | choroideremia-like | 12663 | anterior |
| Chst8 | carbohydrate (N-acetylgalactosamine 4-0) sulfotransferase 8 | 68947 | anterior |
| Dbc1 | deleted in bladder cancer 1 | 56710 | anterior |
| Kcnh7 | potassium voltage-gated channel, subfamily H (eag-related), member 7 | 170738 | anterior |
| Lgr5 | leucine rich repeat containing G protein coupled receptor 5 | 14160 | anterior |
| Opn3 | opsin (encephalopsin) | 13603 | anterior |
| Prkca | protein kinase C, alpha | 18750 | anterior |
| Sgpp2 | sphingosine-1-phosphate phosphotase 2 | 433323 | anterior |

**Figure 3.2 Genes selectively expressed in posterior lobules of the cerebellar midline.** *In situ* hybridization images from the Allen Brain Atlas.

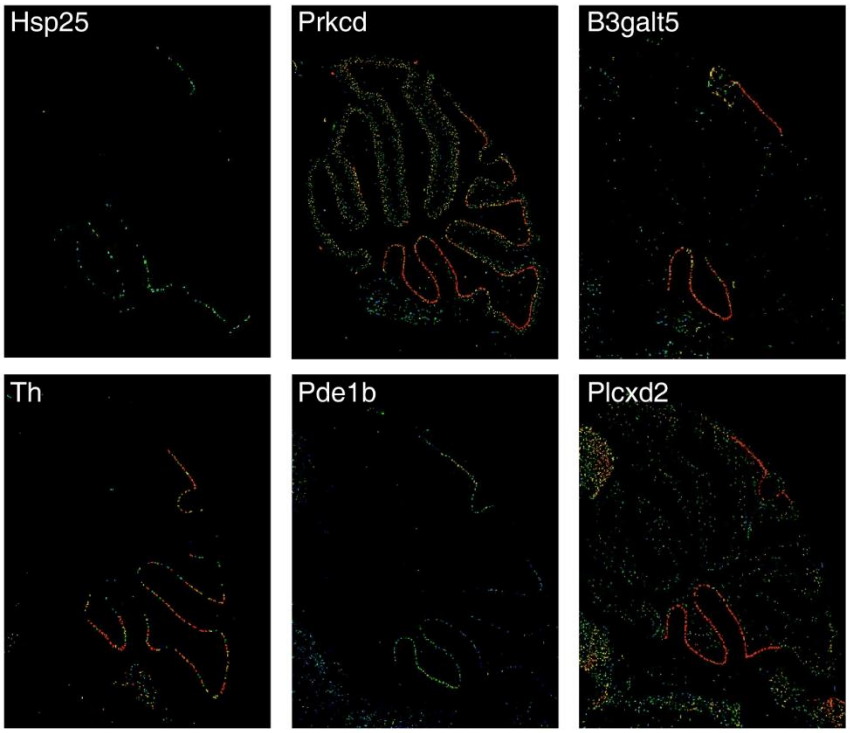


We analyzed the functions of these candidate genes and their human orthologs by querying their gene ontology (GO) annotations using AmiGO (Carbon et al., 2009). The GO Term Enrichment tool revealed significant over-representation ($p<0.01$) for GO terms containing *Prkca, Prkcd,* and *Plcxd2*, members of the phospholipase C – protein kinase C signal transduction cascade, suggesting that this pathway is differentially regulated between regions of interest. AmiGO was also used to query the complete list of GO Biological Process terms associated with candidate genes. In support of our hypothesis that the differentially expressed genes would include regulators of cellular survival and death decisions, 5 genes were associated with cell death related annotations, including "cell death" (GO:0008219, *Dbc1* and *Hspb1*), "apoptosis" (GO:0006915, *Pde1b* and *Prkcd*), "negative regulation of apoptosis" (GO:0043066, *Hspb1*), and "induction of apoptosis by intracellular signals" (GO:0008629, *Prkca*).

Furthermore, the gene product of *Sgpp2*, sphingosine 1-phosphate phosphatase 2, is likely involved in the regulation of apoptosis as well due to its hydrolysis of sphingosine 1-phosphate (Ogawa et al., 2003), a lipid second messenger that is a negative regulator of apoptosis (Spiegel and Milstien, 2003). Finally, we performed an analysis of Cellular Component annotations to determine the subcellular localization of the protein products of candidate genes **(Figure 3.3B)**. The vast majority of gene products are localized outside of the endosome-lysosome system, further suggesting that selective vulnerability of Purkinje cell populations arises not from the primary site of pathogenesis in NPC disease, but from responses to cellular stress that take place elsewhere.

**Figure 3.3 Candidate neuroprotective or pro-degenerative genes. (A)** Hierarchical clustering of candidate genes, demonstrating strong differential expression between regions of interest. Rows, genes; columns, individual voxels within the regions of interest. Red designates higher and green designates lower expression. **(B)** Subcellular localization of candidate genes, based on GO terms and review of supporting literature.

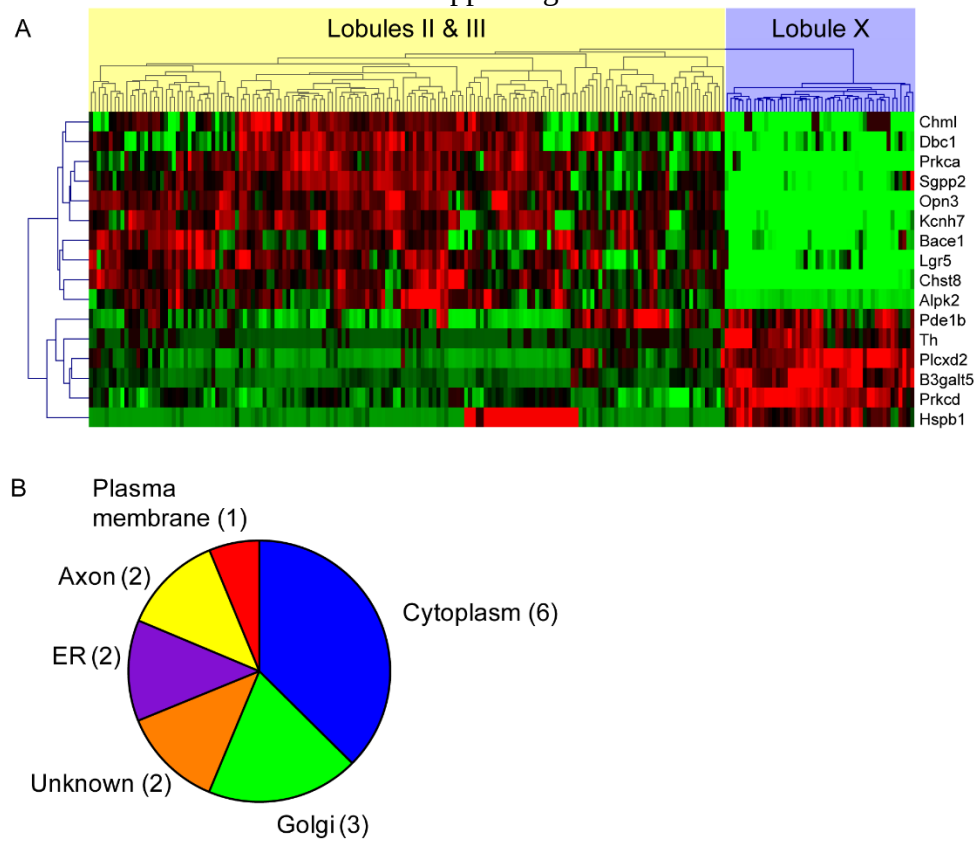

### 3.3.2 *HSPB1* promotes survival of *in vitro* models of NPC disease

We next sought to directly test the extent to which candidate genes influence cell survival in models of NPC disease. For this initial analysis, we chose to study one gene that was over-expressed by lobule X Purkinje cells, heat shock protein beta 1 (*Hspb1*). This gene has been linked previously to neurodegeneration, as mutations in human *HSPB1* cause some cases of Charcot-Marie-Tooth disease and distal hereditary motor neuropathy (Evgrafov et al., 2004). Additionally, HSPB1 regulates multiple events that influence neuronal viability, including stability of the actin cytoskeleton, protein folding, reactive oxygen species (ROS), and apoptosis (Arrigo, 2007), and its robust expression has been documented in surviving Purkinje cells from *Npc1-/-* mice (Sarna et al., 2003).

We initially sought to confirm that Hspb1 expression in mutant mice with active disease matched the pattern predicted by the Allen Brain Atlas. Strong expression of *Hspb1* was detected in lobule X Purkinje cells of *Npc1 flox/-;Pcp2-Cre* mice at 7 weeks of age, prior to the significant Purkinje cell degeneration **(Figure 3.4A)**. In contrast, Hspb1 was undetectable in the more susceptible Purkinje cells of lobules II and III. To determine whether HSPB1 functions as an inhibitor of cell death pathways in NPC cell models, we knocked down its expression using siRNA. We initially treated HeLa cells with U18666A, a small molecule which induces lipid trafficking defects identical to those seen in NPC disease (Liscum et al., 1989). Knockdown of *HSPB1* in U18666A-treated cells, but not in vehicle controls, led to a significant increase of caspase activity **(Figure 3.4B)**. Likewise, *HSPB1* knockdown in NPC patient fibroblasts significantly increased the percentage of cells with chromatin condensation, while *HSPB1* knockdown had no effect on control fibroblasts **(Figure 3.4C)**. These results are consistent with

a model in which HSPB1 prevents the induction of cell death in response to the intracellular lipid trafficking defects caused by NPC1 deficiency.

To initially test the role of HSPB1 in the survival of neurons, the cell type critical for NPC disease neuropathology (Elrick et al., 2010; Ko et al., 2005; Yu et al., 2011), we utilized a neuronal culture model. Primary cortical neurons treated with U18666A develop filipin-positive lipid inclusions and progressive degeneration, and have been used previously to model NPC disease (Amritraj et al., 2009; Cheung et al., 2004). Neurons treated with U18666A demonstrated progressive degeneration, and exogenous over-expression of *HSPB1* almost completely prevented this death **(Figure 3.4D)**. To probe the mechanism of this effect, we took advantage of the fact that serine phosphorylation is critical for HSPB1-mediated protection against neuronal damage *in vitro* and *in vivo* (Stetler et al., 2012) . Mutation of these residues to alanine (non-phosphorylatable) or aspartate/glutamate (phosphomimetic) has been widely used to study phosphorylation state-dependent properties of HSPB1 (Arrigo, 2007). Transduction of U18666A-treated neurons with the phosphomimetic *HSPB1*-3E recapitulated the neuroprotective effects of wild-type *HSPB1*, while non-phosphorylatable *HSPB1*-3A was inactive **(Figure 3.4D**). We conclude that the neuroprotective effects of HSPB1 in NPC cell models are mediated by the phosphorylated species.

**Figure 3.4 HSPB1 promotes survival in cellular models of NPC1 disease. (A)** Expression of Hspb1 *(left panel)* and calbindin *(right panel*, Purkinje cells) in cerebellar midline of *Npc1 flox/-*, *Pcp2-Cre* mice 7 weeks. Scale bar = 200 μm. **(B)** (*Upper panel*) HeLa cells were transfected with non-targeted (lanes 1 and 3) or *HSPB1* siRNA (lanes 2 and 4), then treated with vehicle (lanes 1-2) or 1 μg/ml U18666A (lanes 3-4) for 24 hr. HSPB1 expression was determined by western blot. GAPDH controls for loading. (*Lower panel*) Caspase-3 in HeLa cell lysates. Data are mean ± SEM. **p*<0.05. **(C)** NPC1 patient fibroblasts were transfected with non-targeted or *HSPB1* siRNA. Cells were stained with Hoechst, and the percentage of cells with condensed chromatin was scored. Data are mean ± SEM. ***p*<0.01. **(D)** Primary mouse cortical neurons were transduced with wild type *HSPB1*, *HSPB1*$^{3A}$, *HSPB1*$^{3E}$, or empty vector, and then treated with 2.5 μg/ml U18666. XTT assay was performed 72 hrs post U18666A. Neuron survival is reported relative to vehicle treated cells. Data are mean ± SEM. ****p*<0.001.

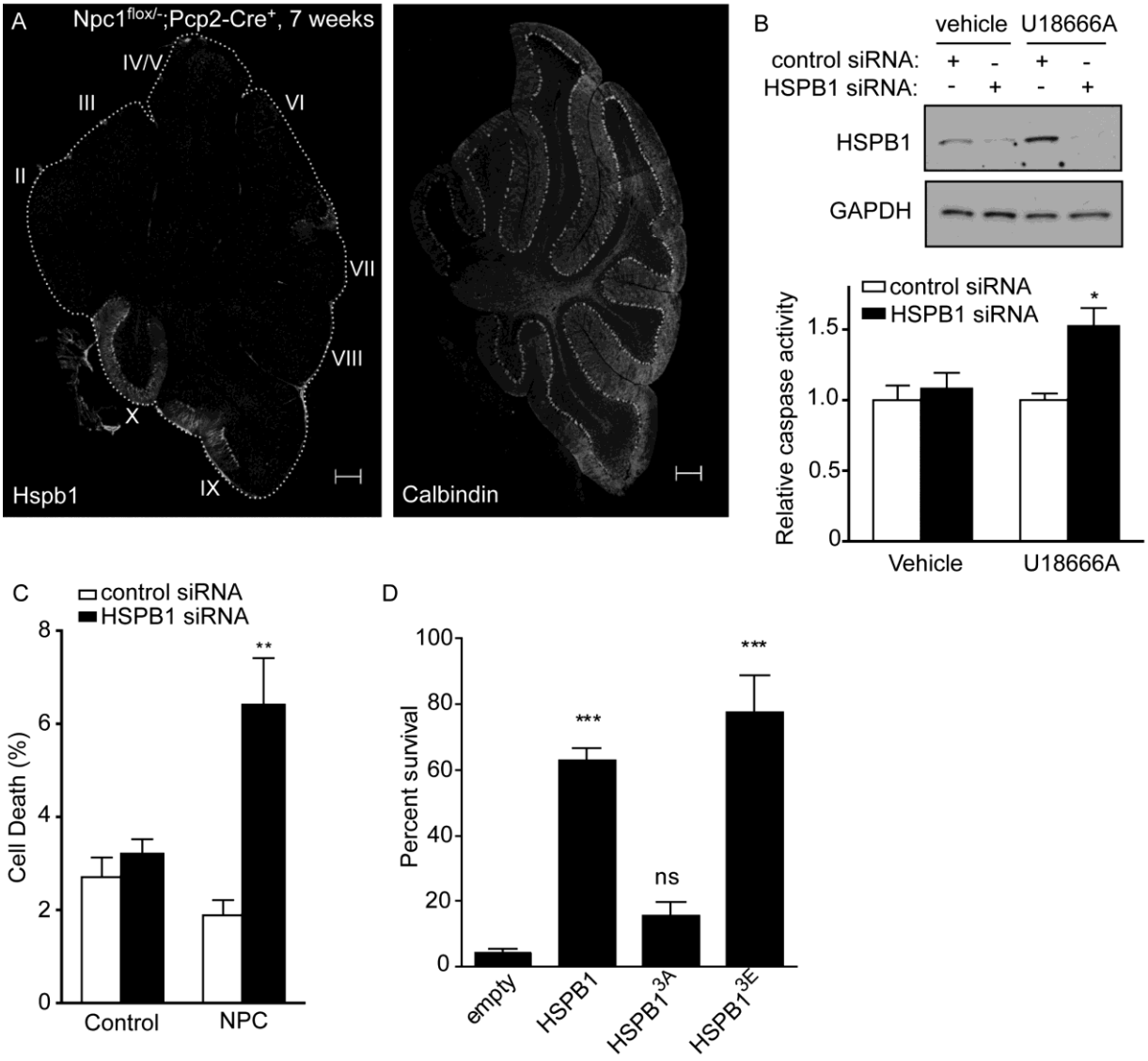

### 3.3.3 *HSPB1* over-expression diminishes motor impairment and Purkinje cell loss

We next sought to determine whether HSPB1 over-expression impacts Purkinje cell survival and motor impairment in NPC mice. To accomplish this, we generated mice deficient in *Npc1* only in Purkinje cells by using a previously characterized conditional null allele (Elrick et al., 2010). Cre recombinase expression driven by the *Pcp2* promoter initiated around postnatal day 6 and was present in all Purkinje cells by postnatal days 14 - 21 (Barski et al., 2000). Therefore, this strategy enabled post-developmental as well as cell-type restricted deletion of *Npc1*. Expression of the hemagglutinin (HA)-tagged human *HSPB1* cDNA transgene was driven by the chicken β-actin promoter and cytomegalovirus enhancer. These transgenic mice express exogenous HSPB1 in brain, spinal cord, heart, muscle, liver, kidney, lung, and pancreas, and exhibit normal reproductive patterns, longevity and behavior (Akbar et al., 2003) . We determined the behavioral effect of HSPB1 over-expression on Npc1 deficiency by measuring the time to traverse a balance beam. Purkinje cell specific null mutants (*Npc1 flox/-;Pcp2-Cre*), but not littermate controls (*Npc1 flox/+;Pcp2-Cre*), displayed a progressive, age-dependent behavioral impairment beginning at 10 weeks **(Figure 3.5A)**, consistent with our previous study (Elrick et al., 2010). HSPB1 over-expression significantly rescued motor performance in mice at 10 and 15 weeks of age **(Figure 3.5A)**. Previous work has demonstrated that this motor task is a sensitive measure of Purkinje cell loss in Npc1 deficient mice (Elrick et al., 2010). To determine the extent to which HSPB1 over-expression improved neuron survival, we examined the density of Purkinje cells in the cerebellar midline of mice at 11 weeks. This analysis revealed that HSPB1 over-expression significantly rescued Purkinje cell density in posterior (lobules VIII-X) but not anterior cerebellar lobules **(Figure 3.5B, C-J)**. Purkinje cell rescue in posterior lobules was confirmed by immunofluorescence staining for calbindin, a marker of Purkinje cells **(Figure**

**3.5G versus I)**. This rescue was associated with the expression of HA-tagged HSPB1 transgene **(Figure 3.5H versus J)**. Transgene expression was also noted in anterior lobules, suggesting that HSPB1 over-expression alone was insufficient to account for effects on neuron survival. The HSPB1 transgene did not alter the accumulation of ubiquitinated proteins or filipin-positive unesterified cholesterol in Purkinje cells of posterior lobules **(Figure 3.6)**. We conclude that exogenous HSPB1 protects Purkinje cells in posterior lobules and delays the onset of behavioral impairment, without altering the aberrant accumulation of proteins or cholesterol.

**Figure 3.5 HSPB1 over-expression rescues motor impairment and Purkinje cell loss. (A)** Age-dependent performance on balance beam indicates that transgenic *HSPB1* over-expression delays motor impairment in *Npc1 flox/-*, *Pcp2-Cre* mice. Data are mean ± SD, $n \geq 7$ mice/genotype. ***$p<0.001$. **(B)** Purkinje cell density in indicated lobules of the cerebellar midline of 11-week-old mice. Data are mean ± SD, $n = 3$ mice/genotype. *$p<0.05$. **(C - J)** Purkinje cells (calbindin, *in red*) and transgenic HSPB1 (HA, *in green*) in anterior and posterior lobules of the cerebellar midline of 11-week-old mice. *Top row*, lobule II; *bottom row*, lobule IX. Scale bar = 50 μm.

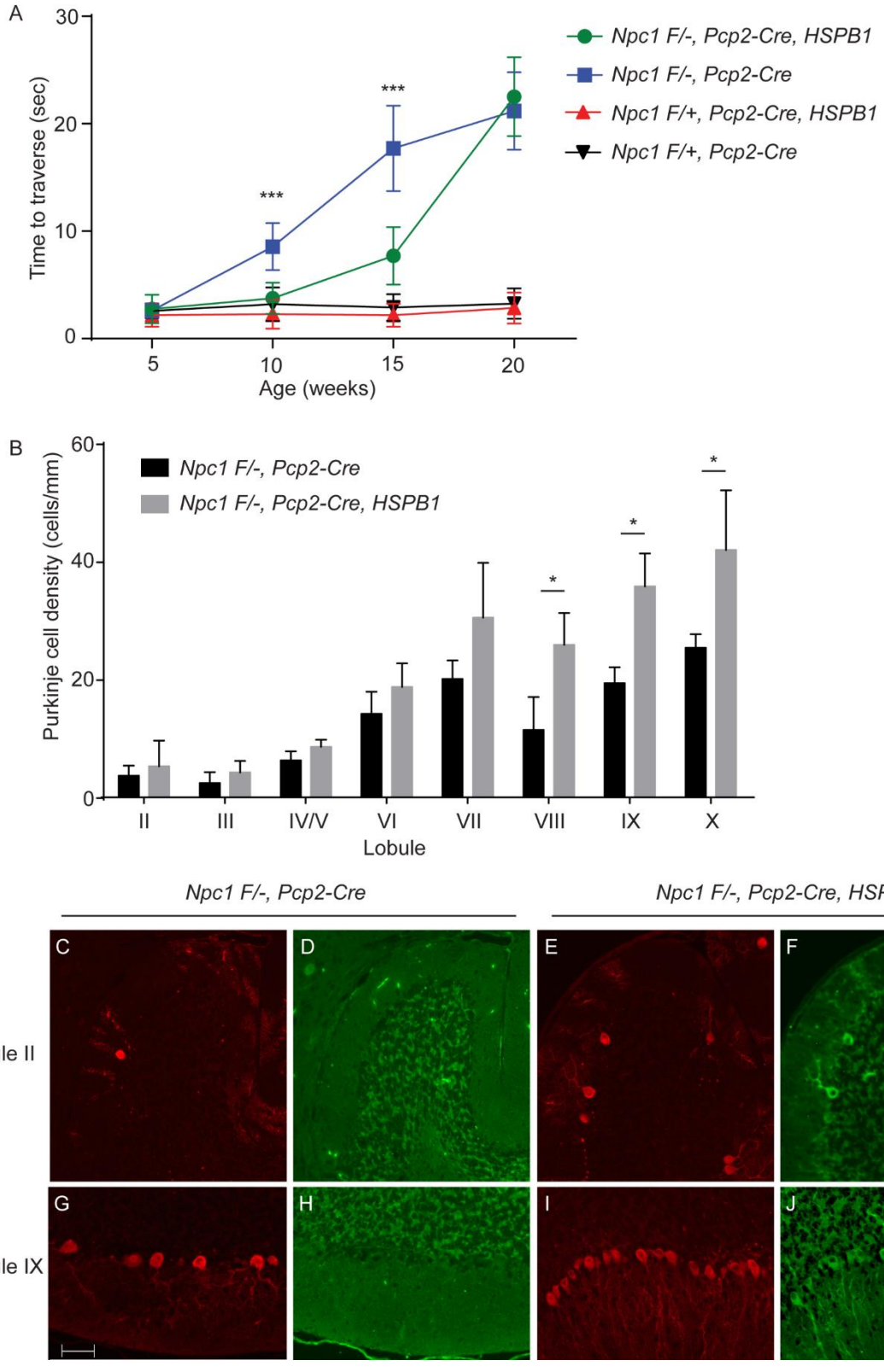
A
Time to traverse (sec)
Age (weeks)
Npc1 F/-, Pcp2-Cre, HSPB1
Npc1 F/-, Pcp2-Cre
Npc1 F/+, Pcp2-Cre, HSPB1
Npc1 F/+, Pcp2-Cre
***
***
B
Purkinje cell density (cells/mm)
Lobule
II
III
IV/V
VI
VII
VIII
IX
X
Npc1 F/-, Pcp2-Cre
Npc1 F/-, Pcp2-Cre, HSPB1
Lobule II
Lobule IX
C
D
E
F
G
H
I
J

**Figure 3.6 HSPB1 over-expression does not rescue accumulation of ubiquitinated proteins or unesterified cholesterol.**
Sections of the cerebellar midline were examined from mice at 11 weeks of age. **(A)** Immunofluorescent staining for calbindin (green) and ubiquitin (red); nuclei were stained by DAPI. **(B)** Immunofluorescent staining for calbindin (red) and filipin (blue). Scale bar = 20 μm.

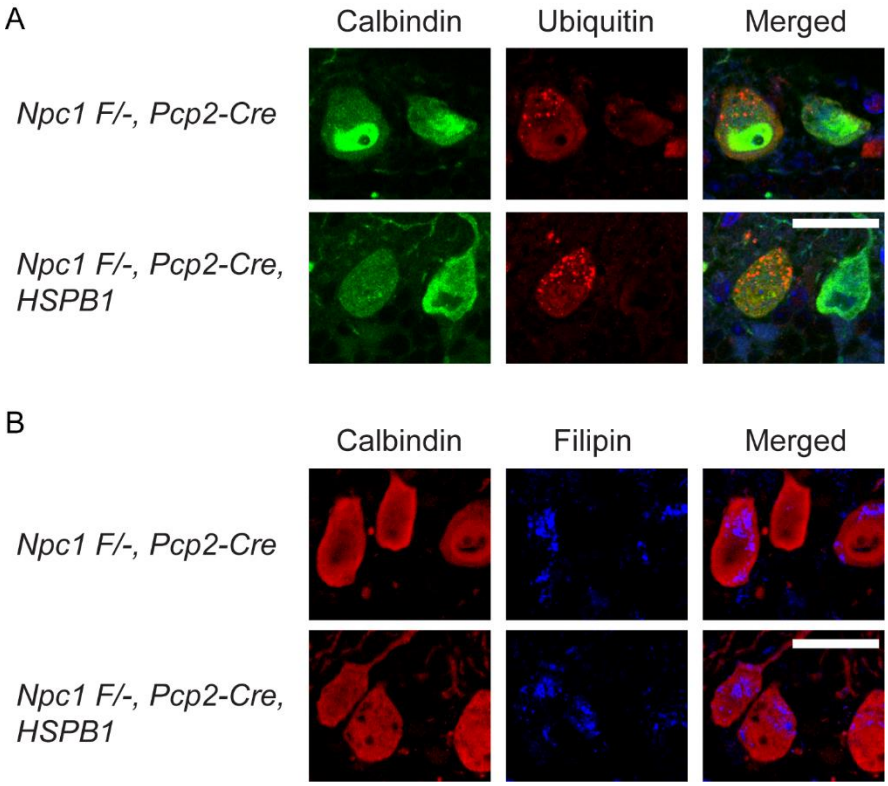


To further explore the basis of the beneficial effects of HSPB1 on select Purkinje cell subpopulations, we first evaluated whether the transgene was uniformly expressed. HA staining of the cerebellar midline confirmed diffuse reactivity of Purkinje cells in 7 week old *Npc1 flox/-;Pcp2-Cre, HSPB1* mice **(Figure 3.7A)**. We next considered the possibility that HSPB1 was differentially activated in cerebellar lobules. Because phosphorylation of HSPB1 influences its ability to promote neuronal survival in vitro **(Figure 3.4D)**, we examined HSPB1 phosphorylation state in Purkinje cells using phospho-HSPB1 [pS15] immunofluorescence.

Strikingly, only Purkinje cells in posterior lobules were positive for phospho-HSPB1 **(Figure 3.7B)** despite the fact that the transgene was diffusely expressed **(Figure 3.7A)**. Intriguingly, our expression analysis identified restricted expression of the HSPB1 kinase PKCδ (Gaestel et al., 1991; Lee et al., 2005; Maizels et al., 1998) to Purkinje cells in the posterior lobules **(Figure 3.2, Table 3.1)**, a finding that was confirmed by immunofluorescence staining **(Figure 3.7C)**. Taken together, these data indicated that phosphorylation of HSPB1 was tightly associated with Purkinje cell rescue in animals expressing the transgene.

**Figure 3.7 PKCδ and phosphorylated HSPB1 are co-expressed in Purkinje cells in posterior lobules. (A)** Transgenic HSPB1 (HA) in the cerebellar midline of 7-week-old *Npc1 flox/–, Pcp2-Cre, HSPB1* mice. Scale bar = 200 μm. **(B, C)** Expression of phospho-HSPB1 (serine 15, *in green, panel B*) and PKCδ (*in green, panel C*) were examined in Purkinje cells (calbindin, *in red*) in the cerebellar midline of *Npc1 flox/–, Pcp2-Cre, HSPB1* mice at 7 weeks of age. Nuclei were stained by DAPI. *Top row*, lobule II; *bottom row,* lobule IX. Scale bar = 20 μm.

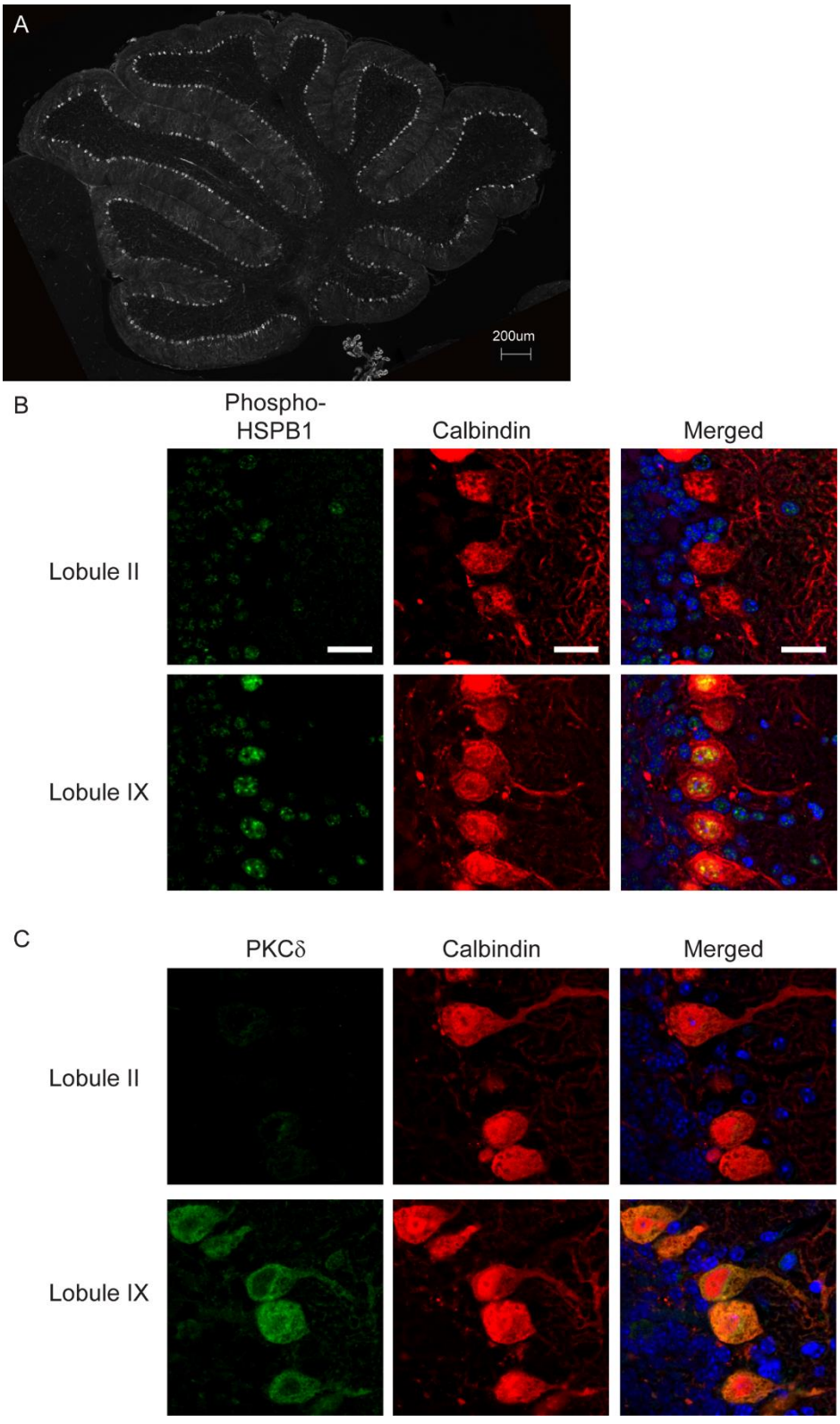
A
200um
B
Phospho-
HSPB1
Calbindin
Merged
Lobule II
Lobule IX
C
PKCδ
Calbindin
Merged
Lobule II
Lobule IX

### 3.3.4 Hspb1 knockdown exacerbates Purkinje cell loss

Our over-expression studies demonstrated that HSPB1 delays motor impairment and Purkinje cell loss in posterior cerebellar lobules. We next sought to determine the effects of Hspb1 knockdown in the NPC mouse cerebellum. The feasibility of this approach was supported by prior work demonstrating that *Hspb1* null mice are viable and fertile, without obvious morphological abnormalities (Huang et al., 2007). To accomplish gene knockdown, we used an adeno-associated virus serotype 2 (AAV2) vector to produce a short hairpin RNA (shRNA) driven by the U6 promoter. *Hspb1* shRNA was cloned into an AAV2 shuttle plasmid (pFBAAV/mU6mcsCMVeGFP). To initially confirm knockdown efficiency, NIH3T3 cells were transfected to express non-targeted (NT) or *Hspb1* shRNA, heat shocked, and analyzed by western blot **(Figure 3.8A)**. These targeted and control shRNA clones were then used for virus generation, and injected into the deep cerebellar nuclei of *Npc1 flox/-;Pcp2-Cre* mice at 7 weeks. Animals were examined six weeks post-infection. At this time point, calbindin staining for Purkinje cells was markedly diminished in the posterior cerebellar lobules of mice receiving *Hspb1* shRNA **(Figure 3.8B)**. We confirmed viral transduction of remaining Purkinje neurons by GFP staining and assessed knockdown efficiency by Hspb1 staining. We observed diffuse GFP reactivity of Purkinje cells in mice expressing NT and *Hspb1* shRNA, whereas Hspb1 staining was specifically diminished by *Hspb1* shRNA **(Figure 3.8C)**. Quantification of Purkinje cell density confirmed a significant exacerbation of neuron loss in posterior cerebellar lobules (lobules VII-IX) of mice expressing *Hspb1* shRNA **(Figure 3.8D)**. Furthermore, although Purkinje cell density was not altered in lobule X, Hspb1 knockdown significantly diminished soma size **(Figure 3.8E)**. These data indicate that Hspb1 knockdown exacerbates Purkinje cell degeneration due to NPC1 deficiency.

**Figure 3.8 *Hspb1* knockdown exacerbates Purkinje cell loss. (A)** NIH3T3 cells were transfected with NT shRNA or *Hspb1* shRNA. After 24 hrs, cells were heat shocked (43º C for 90 min) and protein lysates were collected after 24 hrs. Hspb1 expression was determined by western blot. Hsp90 controls for loading. **(B - D)** 7-week-old *Npc1 flox/-, Pcp2-Cre* mice were injected with AAV2 expressing non-targeted shRNA (NT shRNA) or *Hspb1* shRNA, and then examined at 13 weeks of age. **(B)** Immunofluorescent staining of Purkinje cells (calbindin) in the cerebellar midline. *Left panel*, NT shRNA; *right panel*, *Hspb1* shRNA. Roman numerals identify lobules. Scale bar = 500 μm. **(C)** Expression of AAV2-encoded GFP (green) and endogenous Hspb1 (red). *Top row*, NT shRNA; *middle and bottom rows*, *Hspb1* shRNA. Nuclei were stained by DAPI. Scale bar = 20 μm. **(D)** Quantification of Purkinje cell density by lobule. Data are mean ± SD, $n = 3$ mice/genotype. *$p<0.05$, ***$p<0.001$. **(E)** Quantification of Purkinje cell soma area in lobule X. Data are mean ± SD, $n \geq 91$ cells/genotype. **$p<0.01$.

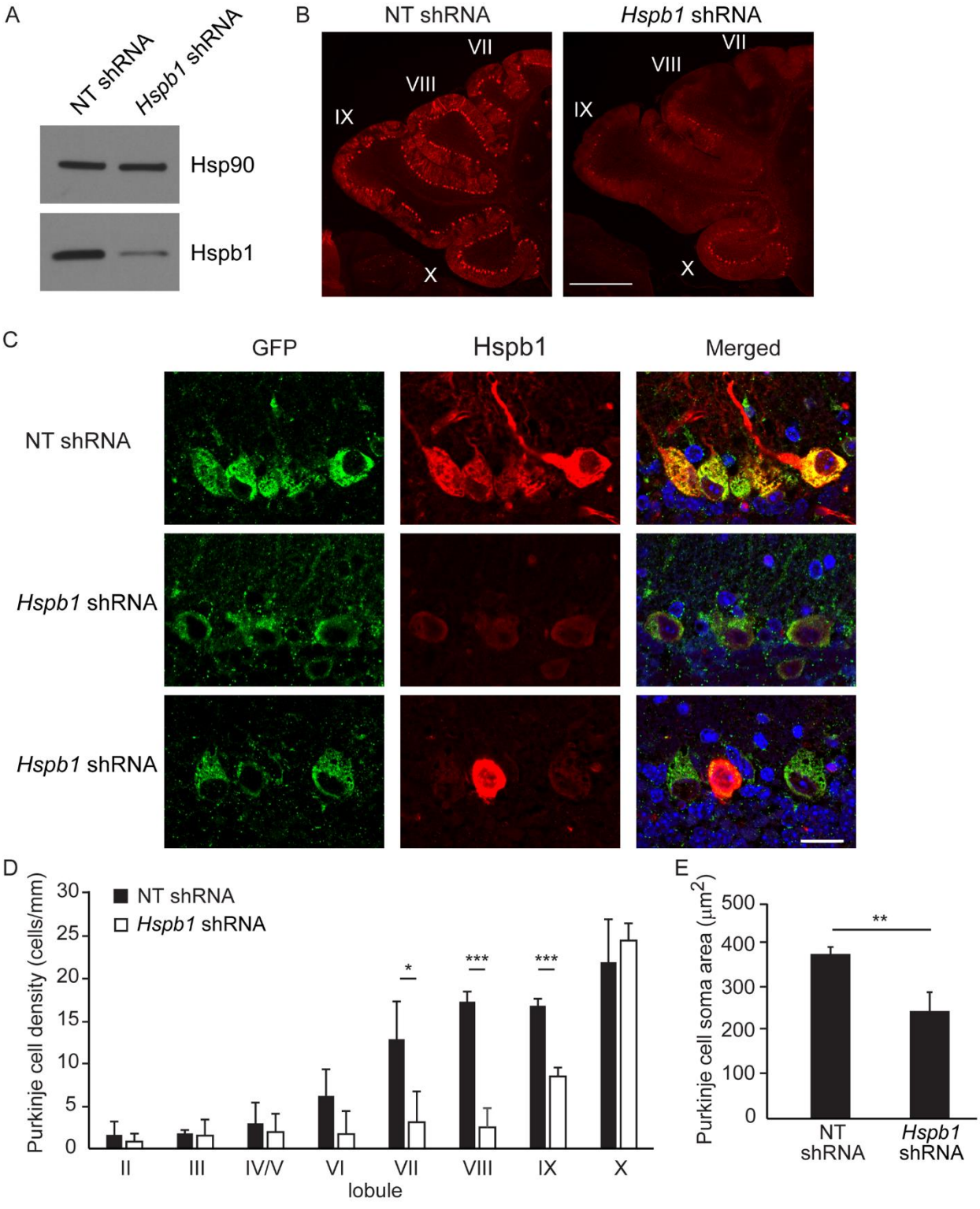
A
NT shRNA
Hspb1 shRNA
Hsp90
Hspb1
B
NT shRNA
Hspb1 shRNA
VII
VIII
IX
X
C
GFP
Hspb1
Merged
NT shRNA
Hspb1 shRNA
Hspb1 shRNA
D
NT shRNA
Hspb1 shRNA
Purkinje cell density (cells/mm)
30
25
20
15
10
5
0
*
***
***
II
III
IV/V
VI
VII
VIII
IX
X
lobule
E
Purkinje cell soma area (μm2)
500
400
300
200
100
0
**
NT shRNA
Hspb1 shRNA

### 3.4 Discussion

Many progressive neurological diseases are characterized by the selective vulnerability of neuronal populations, yet mechanisms underlying this phenomenon remain poorly characterized. Here, we report a bioinformatics approach to the identification of potential modifier genes that influence the susceptibility of neurons to disease. Using NPC disease as a model for the study of selective neuronal vulnerability, we demonstrate that one of the candidate genes we identified, HSPB1, promotes neuronal survival in cellular model systems through a mechanism that likely involves phosphorylation-dependent inhibition of apoptosis. Additionally, we show that HSPB1 over-expression *in vivo* slows the progression of motor impairment and diminishes cerebellar Purkinje cell loss. The neuroprotection from Npc1 deficiency afforded by HSPB1 over-expression in mice was associated with HSPB1 phosphorylation and expression of the kinase PKCδ. We confirmed the modulatory effect of Hspb1 on Purkinje cell degeneration *in vivo*, as knockdown by *Hspb1* shRNA significantly enhanced neuron loss. This effect of *Hspb1* gene knockdown was particularly robust, resulting in Purkinje cell degeneration in posterior lobules (VII-IX) that approached the severity observed in anterior cerebellar lobules. Although diminished Hspb1 expression did not trigger Purkinje neuron loss in lobule X, we observed a significant decrease in soma size, a compensatory change reported in other degenerative ataxias to regulate membrane excitability (Dell'Orco et al., 2015). These results highlight the novel use of bioinformatics tools to uncover pathways leading to neuronal protection in neurodegenerative disorders.

HSPB1 is a multifunctional protein with documented roles in actin stability, protein folding, oxidative damage, and apoptosis (Arrigo, 2007). Interestingly, HSPB1 is a direct inhibitor of apoptosis at multiple levels, through binding and sequestration of cytochrome c

(Bruey et al., 2000) and caspase-3 (Pandey et al., 2000), and inhibition of Bax activation (Havasi et al., 2008) and DAXX signaling (Charette and Landry, 2000). The phosphorylation state required for most of these activities is unknown, with the exception of DAXX inhibition, which requires phosphorylated HSPB1 (Charette and Landry, 2000). Recently, phosphomimetic mutants of HSPB1 were shown to protect against a broad array of apoptosis-inducing stimuli, while non-phosphorylatable mutants showed no protection against some stimuli and only mild protection against others, suggesting that anti-apoptotic activities of HSPB1 are primarily attributable to the phosphorylated species (Paul et al., 2010). Although both phosphorylated and dephosphorylated HSPB1 have chaperone activity (Ehrnsperger et al., 2000; Jakob et al., 1993) and prevent oxidative damage (Preville et al., 1999), it is unlikely that these functions play a primary role in exerting beneficial effects in NPC models. This conclusion is based on the tight association that we observed between HSPB1 phosphorylation and neuroprotection, and the finding that neuronal rescue is not associated with diminished accumulation of ubiquitinated proteins. Instead, we favor a model in which HSPB1 acts through a direct anti-apoptotic mechanism. Interestingly, our bioinformatics screen also identified the expression of PKCδ in disease-resistant Purkinje cells. This kinase has been shown to phosphorylate Hspb1 at Ser-15 and Ser-86 to reduce apoptosis (Gaestel et al., 1991; Lee et al., 2005; Maizels et al., 1998), suggesting that these two proteins may act together to promote Purkinje cell survival. We note the possibility that other kinases also contribute to the regulation of Hspb1 activity in the cerebellum. Nonetheless, our findings suggest that strategies that promote HSPB1 expression or phosphorylation may diminish the rate of cerebellar degeneration in NPC disease.

Our identification of candidate disease modifying genes relied on quantitative *in situ* hybridization data available in the Allen Brain Atlas. Methods had not been developed

previously to use this resource for unbiased studies of differential gene expression. For guidance in designing our approach, we looked to tools developed for the analysis of microarray data, where studies of differential gene expression are commonplace. Several caveats exist when applying our strategy to Allen Brain Atlas data. First, this method is heavily dependent upon manual curation as standard statistical tests yielded high false positive rates. These were variably due to signals generated by other cell types that fell within or adjacent to the region of interest, or artifacts and noise on the *in situ* hybridization images. Second, while the majority of differentially expressed genes were identified by both *t*-test and SAM, others were found only by one method. Therefore, it was necessary to combine the use of both approaches, and it remains possible that some differentially expressed genes were not discovered by either. To streamline future studies, a more robust method for working with Allen Brain Atlas data may need to be developed. Despite these technical limitations, our study provides proof of concept for the use of Allen Brain Atlas data to identify therapeutic targets in neurodegenerative disease. This method is readily applicable to any brain region, and could be used to discover novel therapeutic targets in other neurodegenerative diseases.

## 3.5 Materials and Methods

### 3.5.1 Antibodies

Antibodies used in this study were anti-GAPDH (Santa Cruz, sc-25578), anti-calbindin (Sigma-Aldrich, c2724), anti-HSPB1 (abcam, ab5579), anti-Hspb1 (Enzo Life Sciences, SPA-801), anti-HSPB1 phospho-Ser 15 (Novus, NBP1-60864), anti-PKCδ (Fisher, BDB610397), anti-hemagglutinin (HA) (Covance, 16B12), anti-GFP (Novus, NB 100-1770), anti-Hsp90 (Santa Cruz, sc-7947) and anti-ubiquitin (Dako, Z0458).

### 3.5.2 Mice

Mice containing the *Npc1* floxed (exon 9) (Elrick et al., 2010) and null alleles (Loftus et al., 1997), and transgenic mice expressing the *Cre* transgene driven by the *Pcp2* promoter (Zhang et al., 2004) were generated and genotyped as described previously. Transgenic mice over-expressing hemagglutinin tagged human HSPB1 were from Dr. Jacqueline de Belleroche (Imperial College, London, UK) (Akbar et al., 2003). All lines were backcrossed to C57BL6/J for ≥10 generations. All animal procedures were approved by the University of Michigan Committee on the Use and Care of Animals.

### 3.5.3 Cell culture

All cell lines were cultured at 37℃ with 5% $CO_2$. HeLa cells were maintained in DMEM (Gibco, 11965-092) supplemented with 10% FBS, 1X penicillin, streptomycin, and glutamine (Gibco, 10378-016). Human skin fibroblasts GM03123 from an NPC patient and GM08399 from an age and sex matched control (Coriell Cell Repositories) were maintained in MEM (Gibco, 10370-021) supplemented with 15% FBS, 1X penicillin, streptomycin, and glutamine (Gibco). To manipulate HSPB1 expression, cells were transfected with ON-TARGET*plus* SMART pool human HSPB1 or non-targeting control (Dharmacon). HeLa cells were transfected using the DharmaFECT reagent (Dharmacon), according to the manufacturer's instructions. Fibroblasts were transfected by electroporation with the Lonza Nucleofector normal human dermal fibroblast kit.

### 3.5.4 Genome-wide expression profiling

The Expression Energy Volume for each gene in the Allen Mouse Brain Atlas was downloaded via the Allen Brain Atlas API (Lein et al., 2007). These data were then reorganized into a single expression matrix and filtered to include locations corresponding to the regions of interest, cerebellar lobules X and II/III, and extending laterally 1400 microns from the midline. This data matrix was then loaded into TM4 MultiExperiment Viewer software (Saeed et al., 2003), in which differential expression between regions of interest was determined by Student's *t*-test and Significance Analysis of Microarrays (SAM) (Tusher et al., 2001). The top 1000 genes returned by each method were manually verified by direct inspection of *in situ* hybridization data on the Allen Brain Atlas website in midline and several adjacent sagittal sections. Criteria for validation were (1) expression present in the Purkinje cell layer in at least one region of interest, and (2) differential expression between regions of interest.

### 3.5.5 Western blotting

Cells were lysed in RIPA buffer (Thermo Scientific) containing Complete protease inhibitor (Roche) and Halt phosphatase inhibitor (Thermo Scientific). Samples were electrophoresed through a 10% SDS-PAGE gel, and then transferred to nitrocellulose membranes (BioRad) using a semidry transfer apparatus. Primary antibodies were anti-HSPB1 (1:1000), anti-Hsp90 (add dilution) and anti-GAPDH (1:5000). HRP-conjugated secondary antibodies were from BioRad. Blots were developed using ECL (Thermo Scientific) or TMA-6 (Lumigen) chemilluminescent reagents, following manufacturers' protocols.

### 3.5.6 Apoptosis assays

Caspase-3 activity in HeLa cells was determined by assaying DEVDase activity in cell lysates using the ApoTarget caspase 3 / CPP32 fluorimetric protease assay kit (Biosource) according to the manufacturer's instructions. Fluorescence was measured using a SpectraMax Gemini EM plate reader (Molecular Devices). NPC fibroblasts were stained with Hoechst (Immunocytochemistry Technologies). Cells were counted in five randomly selected fields per transfection at 200x magnification and scored for chromatin condensation.

### 3.5.7 Primary cortical neuron culture and viability assay

Cortices from P0 C57BL6/J mouse pups were dissected free of meninges, minced, and then dissociated and cultured as described previously (Jakawich et al., 2010). Neurons were plated in poly-D-lysine (Millipore) treated 96-well plates at a density of $6x10^4$ cells per well. Cytosine arabinoside (Sigma) was added to the culture media the following day at a final concentration of 5 µM to prevent glial growth. U18666A was added at 2.5 µg/ml at 7 div to induce lipid storage. Neuronal viability was determined by XTT assay (Cell Proliferation Kit II, Roche) following the manufacturer's instructions.

### 3.5.8 Viral vectors

A lentiviral expression clone of human *HSPB1* with a C-terminal FLAG tag was obtained from Genecopoeia. Serine-to-alanine and serine-to-glutamate mutations were introduced at serines 15, 78, and 82 using the QuikChange Lightning Multi Site-Directed Mutagenesis kit (Stratagene). Wild type *HSPB1*, *HSPB1*-3A, *HSPB1*-3E, and empty vector plasmids were packaged into feline immunodeficiency virus (FIV) vectors by the Iowa Vector Core. Viral

infection of cultured primary neurons was performed at 10 MOI, followed by a 75% media change four hours after infection.

For in vivo gene targeting, Hspb1 shRNA was designed and cloned by the Iowa Vector Core. The target region in the Hspb1 sequence was analyzed using siSPOTR and potential miRNA target sequences of 21 nucleotides were identified based on low GC content and other factors, as described (Boudreau et al., 2013). Five potential target sequences were cloned in pFBAAV/mU6mcsCMVeGFP. Knockdown efficiency was tested in NIH3T3 cells. The most efficient plasmid was used in producing AAV2/1mU6miHspb1-CMVeGFP triple transfection virus. Non-targeted virus, AAV2/1mU6-miSafe-CMV eGFP, was used as a control. Before injection, virus was dialyzed at 4$^{o}$ C for 3hrs against 7,000 MWCO Slide -A-Lyzer mini-dialysis units (Thermo Scientific) in a custom buffer formulation distributed through the Gene Transfer Vector Core in University of Iowa.

**3.5.9 Stereotaxic cerebellar viral delivery.**

Stereotaxic administration of AAV2 was performed on 7 week-old *Npc1 flox/-, Pcp2-Cre* mice placed under anesthesia using a mixture of $O_2$ and isoflurane (dosage 4% for induction, 1.5% maintenance). Mice received bilateral intracerebellar injections (two sites/hemisphere) of virus. For each injection, ~$1.4 \times 10^{12}$ vg/ml of virus (4 µl) was delivered to the medial or lateral cerebellar nucleus at an infusion rate of 0.5 µl/min using a 10-µl Hamilton syringe (BD). One min after the infusion was completed, the micropipette was retracted 0.3 mm and allowed to remain in place for 4 min prior to complete removal from the mouse brain. Anterior–posterior coordinates were calculated separately for medial and lateral injection into each cerebellar

hemisphere. The coordinates for the medial injection were -6.4 mm anterior-posterior, ±1.3 mm medial-lateral and 1.9 mm dorsal-ventral as measured from bregma. The coordinates for the lateral injection were -6.0 mm anterior-posterior, ± 2.0 mm medial-lateral and 2.2 mm dorsal-ventral as measured from bregma.

### 3.5.10 Immunofluorescence staining

5 μm sections from brains embedded in paraffin were deparaffinized with xylenes and ethanol. Sections were boiled in 10 mM sodium citrate, pH 6, for 10 min for antigen retrieval. After washing with water, sections were blocked with 5% goat serum and 1% BSA in PBS for 1 hr and then incubated in primary antibody (calbindin 1:500, PKCδ 1:50, Hspb1 1:100, HA 1:200, phospho-Hspb1 1:50, GFP 1:100, ubiquitin 1:200) diluted in 1.5% blocking solution overnight at 4$^{o}$ C. Sections were subsequently incubated in secondary antibodies conjugated to Alexa Fluor 594 or 488 for 2 hrs and mounted with mounting medium including DAPI (Vector Lab**,** H-1200). Images were captured on an Olympus FluoView 500 Confocal microscope.

### 3.5.11 Behavioral testing

Motor function was measured by balance beam test. Mice at 4 weeks of age were trained on three consecutive days to cross a 6 mm wide beam suspended at 50 cm. Mice were then tested in triplicate at 5, 10, 15 and 20 weeks of age. Data are reported as average time to traverse the beam, allowing a maximum of 25 sec and scoring falls as 25 sec.

### 3.5.12 Morphological analysis

Purkinje cell density was quantified in midline sagittal sections stained with hematoxylin and eosin or calbindin staining. Purkinje cells were recognized as large cells with amphophilic cytoplasm, large nuclei with open chromatin and prominent nucleoli that were located between the molecular and granular layers or as calbindin positive cells. The number of cells was normalized to the length of the Purkinje layer, as measured by NIH ImageJ software. For analysis of Purkinje cell soma size, calbindin staining was used to define the cell soma. The cell soma was selected and measured by NIH ImageJ, and pixel size was converted to $\mu m^2$ using the scale bar as a calibration standard.

### 3.5.13 Filipin staining

Mouse brain tissue embedded in Optimal Cutting Temperature (OCT) compound (Tissue-Tek) was sectioned at 10 μm in midline. The sections were rinsed with PBS, and fixed with 4% paraformaldehyde for 30 min. After washing with PBS, the sections were incubated with 1.5 mg/ml glycine for 10 min, washed with PBS and stained with 0.05 mg/ml filipin and 10% FBS in PBS for 2 hrs at room temperature. Filipin images were captured with the UV filter set on an Olympus FluoView 500 confocal microscope. Representative images are from one of three mice per genotype.

### 3.5.14 Statistics

Statistical significance was assessed by unpaired Student's *t* test (for comparison of two means) or ANOVA (for comparison of more than two means). The Newman-Keuls post hoc test was performed to carry out pairwise comparisons of group means if ANOVA rejected the null hypothesis. Statistical analyses were performed using the software package Prism 4 (GraphPad

Software). *P* values less than 0.05 were considered significant. Statistical analysis of gene expression data was performed using TM4 MultiExperiment Viewer software (Saeed et al., 2003). For these calculations, statistical significance was determined using Student's *t*-test with Bonferroni correction for multiple comparisons and Significance Analysis of Microarrays (SAM) (Tusher et al., 2001).

### 3.6 Acknowledgements

We thank Dr. Mark Schultz for comments on this manuscript.

This work was performed in collaboration with Matthew Elrick. Dr. Elrick performed the studies described in figures 1-4, while I performed the experiments in figures 5-8.

# Chapter 4

# Conclusion

In this dissertation, I have explored several approaches to understanding the mechanisms leading to severe neurodegeneration in Niemann-Pick type C (NPC) disease. I demonstrated that cystatin B, an endogenous inhibitor of cathepsins B, H, and L, plays a critical role in regulating Purkinje cell degeneration in NPC mice. My data support a model in which NPC1 deficiency increases reactive oxygen species (ROS), leading to lysosomal membrane permeabilization (LMP). Cathepsin leakage through LMP triggered death of Purkinje cells, and inhibition of cytosolic cathepsins protected NPC1-deficient cells from degeneration. Using another approach to understanding neurodegeneration, I identified genes that protect neurons from the toxicity of NPC1 deficiency using a bioinformatics analysis. I determined that one potentially neuroprotective gene, *HSPB1*, promotes survival in cellular models of NPC disease by means of a mechanism involving the inhibition of apoptosis. I showed that HSPB1 protects Purkinje cells in an NPC mouse model using both overexpression and knockdown approaches. In this last chapter, I will discuss relevant questions that remain unanswered and suggest future directions for this work.

### 4.1 Genetic interaction of NPC1 deficiency with cystatin B deletion

In chapter 2, I determined that cystatin B was involved in regulating Purkinje cell degeneration in NPC disease. At the beginning of the project, I expected that reduced cystatin B, an endogenous inhibitor of cathepsin B, L, and H, would modify NPC disease. This expectation was based on previous studies showing that NPC disease is characterized by impaired proteostasis, as reflected by defects in macroautophagy and reduced lysosomal cathepsin activity (Elrick et al., 2012; Sarkar et al., 2013). Ubiquitinated proteins have also been shown to accumulate in the CNS of NPC1 deficient mice (Elrick et al., 2012; Higashi et al., 1993; Liao et al., 2007; Love et al., 1995; Walkley and Suzuki, 2004). Thus, I hypothesized that decreased cystatin B would restore autolysosomal cargo degradation, leading to modification of the disease phenotype. To accomplish this, I diminished expression of cystatin B in NPC1 patient fibroblasts using CSTB siRNA. As expected, cystatin B knockdown rescued lysosomal protease function without decreasing lipid storage.

I therefore sought to determine the effect of enhanced cathepsin activity on NPC mice. To accomplish this, I used *Cstb* null mice. In a prior study, the effects of reversing autophagy dysfunction in a transgenic mouse model of Alzheimer's disease (TgCRND8 mice) was evaluated by generating mice that were deficient in cystatin B. This TgCRND8 mouse was characterized by enlarged autolysosomes, decreased cathepsin activity, and impaired lysosomal turnover of proteins, including the amyloid-β peptide (Yang et al., 2011). Rescue of autophagy dysfunction by *Cstb* deficiency in the Alzheimer's disease mouse ameliorated amyloid pathologies (Yang et al., 2011). Based on this study and NPC cellular data, I anticipated that *Npc1* null mice that were deficient in cystatin B would recover due to enhanced cathepsin activity.

Unexpectedly, *Npc1* and *Cstb* double null mice were born at a very low frequency and showed enhancement of the NPC phenotype. Although the phenotype of these double null mice was unanticipated, they showed that cystatin B could be a pivotally protective gene in neurodegeneration occurring in NPC disease. Because cystatin B null mice were originally generated to model progressive myoclonic epilepsy of the Unverricht-Lundborg type, it might be that cystatin B deficiency would exaggerate neurodegeneration which is caused by NPC1 deficiency due to synthetic lethality. In an attempt to avoid this, I restricted my analysis to mice at a young age. Cystatin B null mice begin to develop disease around 6 months of age. Symptoms include loss of cerebellar granule neurons but not Purkinje cells. At earlier time points, from 1 to 3 months, mutants are normal in body size, weight, behavior, and histopathology compared to wild type littermates (Pennacchio et al., 1998). In this study, I investigated the *Npc1* and *Cstb* double null mice at 4 weeks of age, prior to the onset of neurodegeneration due to cystatin B deficiency.

Since the double null mice displayed severe motor impairment, we looked for neuropathology in the cerebellum and documented marked accentuation of Purkinje neuron loss. To screen for neuropathology in other brain regions, we stained midline sagittal brain sections for GFAP since reactive astrocytes are sensitive indicators of damage in the CNS. Interestingly, marked gliosis and atrophy was restricted to the cerebellum in germ, line double null mice. This result raised a new question: Why does the *Cstb* deficiency affect primarily the cerebellum in global double null mice? We arrived at an answer by looking in the Allen Brain Atlas database. According to information in the database, cystatin B is expressed in the medulla and the cerebellum, especially in Purkinje cells (http://mouse.brain-map.org/experiment/show/1344). Also, reports indicate that most neurons in the adult rat cerebellum do not express detectable

amounts of cystatin B, with the exception of Purkinje cells and some cells of the molecular layer of the cerebellar folia (Riccio et al., 2005). In the human cerebellum, cystatin B is present in only Purkinje cells and Bergmann glial fibers (Riccio et al., 2005). Because cystatin B is mostly expressed in Purkinje cells, germ line deletion of cystatin B was expected to particularly affect Purkinje cells.

The severe Purkinje cell loss in cystatin B and Npc1 deficiency occurred through cell autonomous mechanisms that triggered apoptotic Purkinje cell death. Moreover, our data showed that lysosomal cathepsins are mislocalized within the cytosol of Npc1 deficient Purkinje cells. I provided evidence showing that this may be a consequence of damage to lysosomal membranes by reactive oxygen species (ROS), leading to the leakage of lysosomal contents and culminating in neurodegeneration **(Figure 2.8)**. This model is consistent with reports from NPC and Niemann-Pick type A (NPA) mouse models in which cytosolic (extra-lysosomal) localization of cathepsins was enhanced (Amritraj et al., 2009; Gabande-Rodriguez et al., 2014).

An important, unanswered question is how cytosolic cathepsin mislocalization is increased by NPC1 deficiency. There are several stimuli that have been reported to trigger LMP: lysosomotropic detergents, viral proteins, bacterial toxins, ROS, proteases, lipids, and p53 (Aits and Jaattela, 2013). Interestingly, sphingosine has been found to induce LMP, leading to relocation of lysosomal cathepsins to the cytoplasm (Ullio et al., 2012). Because NPC deficient cells accumulate not only cholesterol but also sphingomyelin (Devlin et al., 2010), gangliosides (particularly GM2 and GM3) (te Vruchte et al., 2004; Zervas et al., 2001; Zhou et al., 2011), sphingosine (Lloyd-Evans et al., 2008), and bis(monoacylglycero) phosphate (Chevallier et al., 2008; Kobayashi et al., 1999) in late endosomes and lysosomes (LE/Lys), accumulated sphingosine may act as an endogenous lysosomotropic detergent. However, the extent to which

sphingosine accumulates in NPC1 deficient cells is incompletely defined. The study reporting sphingosine accumulation in NPC1 deficiency did not use cells deficient in NPC1, but rather treated wild type cells with U18666A, a small molecule that induces an NPC-like defect in intracellular lipid trafficking (Lloyd-Evans et al., 2008). Nonetheless, the possibility that sphingosine contributes to LMP and cathepsin leakage in NPC1 deficiency is intriguing and deserves further close evaluation.

Another factor that may contribute to the induction of LMP is p53. In myeloid leukemia cells, induced p53 is sufficient to cause LMP by lysosomal destabilization, leading to mitochondrial outer membrane permeabilization (Yuan et al., 2002). Phosphorylated p53 binds to LAPF (lysosome-associated and apoptosis-inducing protein containing PH and FYVE domains) and localizes to lysosomes. This complex triggers LMP in a transcription-independent manner, leading to apoptosis (Li et al., 2007). However, in *Npc1* null mice, p53 is efficiently degraded by an Mdm2-dependent mechanism as the result of abnormal p38 MAPK activation (Qin et al., 2010). Due to low levels of p53 in NPC deficiency, I believe that p53 is a less likely candidate for the inducer of LMP in disease.

In chapter 2, I suggested that ROS are an important factor that increases LMP in NPC1 deficient cells. ROS are known to contribute to LMP via a number of oxidative stimuli such as drugs, heavy metals, and ionizing radiation and in conditions such as ischemia, inflammation, and neurodegenerative disorders (Kurz et al., 2008a). In cells treated with hydrogen peroxide, which easily crosses membranes and catalyzes Fenton reactions with lysosomal iron, free radicals destabilize the lysosomal membrane and induce LMP (Kurz et al., 2008b). Also, ROS might trigger LMP by activating $Ca^{2+}$ channels such as transient potential receptor melastatin-2 (TRPM2) (Sumoza-Toledo and Penner, 2011). Indeed, in prior studies, oxidative damage has

been observed in analysis of the NPC mouse brain (Kennedy et al., 2013; Smith et al., 2009; Vazquez et al., 2012) and in different cell models (Zampieri et al., 2009). Also, lipid oxidation products are considered to be specific and sensitive biomarkers for NPC disease (Porter et al., 2010). However, the mechanism leading to ROS production in NPC deficiency is unclear.

One mechanism that could underlie ROS production in NPC1 deficiency is mitochondrial dysfunction due to mitochondrial cholesterol accumulation. In fact, mitochondrial dysfunction appears to be a key element in many neurodegenerative diseases (Caspersen et al., 2005; Manfredi and Xu, 2005; Martin et al., 2006; Takuma et al., 2005). However, the role of mitochondrial dysfunction in NPC disease remains unknown. In previous studies, the level of mitochondrial cholesterol was reportedly elevated in NPC deficient cells (Charman et al., 2010; Kennedy et al., 2014; Lucken-Ardjomande et al., 2007) and in *Npc1* null mice (Fernández et al., 2009; Yu et al., 2005). These data should be interpreted carefully because it is difficult to obtain pure mitochondria, uncontaminated by lysosomes. However, treatment with the cyclodextrin, which removes cholesterol, restores ATP synthesis and mitochondrial function in NPC1 deficient cells (Yu et al., 2005). This supports the idea that increased cholesterol storage impairs mitochondrial function. Also, another laboratory has reported that *Npc1-/-* mouse brains displayed morphologically abnormal mitochondria containing smaller and more rounded figures, with translucent matrices and irregular cisternae. Moreover, the levels of ATP in the brain, muscle, and livers of NPC mice were significantly decreased compared with those in WT mice (Yu et al., 2005). Investigators concluded that mitochondrial dysfunction and subsequent ATP deficiency could be responsible for neuronal impairment in NPC disease (Yu et al., 2005). Therefore, I think that the increase in mitochondrial cholesterol content and dysfunction may contribute to oxidative damage and warrants further exploration.

A related, unresolved and important issue is the intracellular site of action of cystatin B. In chapter 2, I demonstrated that cystatin B protects Purkinje cells from cell death induced by oxidative stress and cytosolic cathepsins. To inhibit cytosolic cathepsins, cystatin B should be localized in cytosol. However, results of a recent study showed that enhanced lysosomal cathepsin activity by cystatin B deletion ameliorated Alzheimer's disease (Yang et al., 2011). This study indicated that cystatin B was located at least partly in lysosomal compartments as well as in cytoplasm (Yang et al., 2011). Previous studies have yielded mixed results regarding the subcellular location of cystatin B to the nucleus, cytosol, and punctate structures within the cytoplasm. These conflicting results may be attributable to the different cell types and antibodies used for analysis. Cystatin B was distributed diffusely throughout the cytoplasm in an embryonic liver cell line and an invasive hepatoma cell line, as detected by staining using a monoclonal antibody (Calkins et al., 1998). Another laboratory reported that cystatin B was found mainly in the nucleus of proliferating cells, and in both the nucleus and the cytoplasm of differentiated cells in nerve growth factor (NGF)-containing media (Riccio et al., 2001). Cystatin B was not only localized in the nucleus and the cytoplasm but also colocalized in lysosomes in COS-1 cells, and human primary myoblasts (Alakurtti et al., 2005). This study showed that differentiated myotubes contained cystatin B localized diffusely in the cytoplasm, but excluded it from the nucleus and lysosomes (Alakurtti et al., 2005). Due to a lack of ER signal sequence in cystatin B, cystatin B may be attached to the cytoplasmic side of the lysosomal membrane rather than within the lysosome. Also, cystatin B is localized in the nucleus of neural stem cells and neurons but in the cytoplasm of astrocytes and in lysosomes of glial cells (Brannvall et al., 2003). These different localizations of cystatin B may suggest other cellular functions for cystatin B, not only cathepsin inhibition but also involvement in apoptosis or transcriptional regulation.

### 4.2 Therapeutic strategies

In chapter 2, I demonstrated that leaked cathepsins trigger neuronal cell death in NPC mice. This work suggested that stabilizing lysosomes or inhibiting cytosolic cathepsins might work as a therapeutic approach. In fact, the approach involving lysosome stabilization is being tested in NPC disease using recombinant heat shock protein 70 (rHSP70). Prior studies have shown that HSP70 binds to the endolysosomal anionic phospholipid bis(monoacylglycero)phosphate (BMP), an essential co-factor for lysosomal sphingomyelin metabolism, leading to enhanced acid sphinogomyelinase (ASM) activity and stabilization of the lysosomal membrane (Kirkegaard et al., 2010). In an NPA model, which is deficient in ASM, rHsp70 enhances ASM activity, stabilizes lysosomes and reverts the lysosomal pathology of NPA fibroblasts (Kirkegaard et al., 2010). Orphazyme, a small biotech company in Europe, is applying these findings to an NPC model and attempting to develop treatments for NPC disease based on this strategy (http://www.niemann-pick.org.uk/orphazyme-phase-1-rhhsp70-for-npc). The company suggests that rHSP70 may correct conditions of lysosomal functional deficiency and concurrent cellular stress. However, I think that it is also possible that rHSP70 may stabilize lysosomes and ameliorate cell death by reducing LMP rather than cellular stress. This idea is based on a study showing that HSP70 promotes cell survival by preventing the release of lysosomal enzymes into cytosol as a result of LMP (Nylandsted et al., 2004).

I inhibited cytosolic cathepsin activity in NPC patient fibroblasts using genetic and small molecule approaches. In the genetic approach, NPC1-deficient fibroblasts were transfected to overexpress cystatin B, an endogenous inhibitor. In the small molecule approach, I used CA-074ME, a specific inhibitor of cathepsin B. Both approaches significantly increased cell viability in NPC1 patient fibroblasts damaged by oxidative stress.

An important future direction will be to test this approach in a mouse model. CA-074ME exhibits membrane permeability, but does not cross the blood brain barrier. In prior studies, it was administered intracerebroventricularly in mouse models of traumatic brain injury and Alzheimer's disease, reducing cathepsin B activity (Hook et al., 2007; Luo et al., 2010). Another candidate small molecule is E64d, which was derived from E64 (1-[L-N-(trans-epoxysuccinyl)leucyl] amino- 4-guanidinobutane), isolated from *Aspergillus japonicas* (Hanada et al., 1978). It is an irreversible inhibitor of cathepsin B, other cysteine peptidases, and calpain (McGowan et al., 1989). Although it is a non-selective cysteine protease inhibitor, orally administered E64d has been shown to be efficacious in animal models. An oral E64d dose is hydrolyzed in the gut to the acid form of E64c, which systemically circulates in the biologically active inhibitor form (Hook et al., 2015). In previous studies, administration of E64d by oral gavage to guinea pigs (1–10 mg/kg/day, 7 days) and feeding E64d (10 mg/kg/day, 2 months) in chow resulted in dose-dependent reductions in brain cathepsin B activity and Aβ deposition (Hook et al., 2011). Moreover, administration of E64d intraperitoneally inhibited brain cathepsin B activity in ischemic rats (5 mg/kg) (Tsubokawa et al., 2006) and epileptic rats (4 μg dose) (Ni et al., 2013), indicating that this might be an interesting molecule to test in NPC mice. Additional small molecules that inhibit cathepsins have been developed for the treatment of osteoporosis, cancer, traumatic brain injury, and Alzheimer's disease (Siklos et al., 2015) . These drugs may have different selectivity, activity, and toxicity. A comprehensive understanding of these inhibitors would be of great value in directing therapies for NPC disease in the future.

### 4.3 Identification of genes that modify neuronal survival and death in NPC1 deficiency

In chapter 3, we identified candidate modifier genes, analyzing gene expression patterns in the cerebellum using bioinformatics tools. This strategy was based on the phenotype exhibited by many models of cerebellar neurodegenerative diseases, including NPC, which show selective Purkinje cell vulnerability in anterior lobules. Of 16 genes identified through this approach, I demonstrated that one potential neuroprotective gene, *HSPB1*, promotes survival in NPC cell culture models through the inhibition of apoptosis. In addition, I showed that the neuroprotective effects of HSPB1 in NPC cell models are mediated by the phosphorylated species. I proposed that PKCδ might be a kinase that phosphorylates HSPB1 in Purkinje cells. This is indirectly supported by data showing that phospho-HSPB1 was observed in the cerebellar posterior lobules, similar to the expression pattern of PKCδ. Consistent with this model, several studies have reported that PKCδ phosphorylates HSPB1 (Gaestel et al., 1991; Lee et al., 2005; Maizels et al., 1998). These results raise several new questions: Is PKCδ the major kinase that targets HSPB1 in Purkinje cells? What is the upstream signaling pathway that regulates activity of HSPB1 and PKCδ? And, does phospho-HSPB1 have another function in NPC disease?

To answer the first question, I checked previous studies of HSPB1 kinases and compared their expression patterns in the Allen Brain Atlas. I initially examined the expression pattern of protein kinase D (PKD). Published studies indicated that phosphorylation of HSPB1 by PKD mediates neuroprotection from ischemic neuronal injury (Stetler et al., 2012). This fits with my findings. However, according to information in the Allen Brain Atlas, PKD1, PKD2, and PKD3 are not expressed in cerebellum. Next, several studies reported that mitogen-activated protein kinase-activated protein kinase-2 and 3 (MAPKAPK2/3) bind to and phosphorylate HSPB1, leading to resistance against oxidative stress (Clifton et al., 1996; Rogalla et al., 1999). According to information in the database, MAPKAPK2 is expressed in all Purkinje cells, while

MAPKAPK3 is not expressed at all. Other studies have demonstrated that HSPB1 is phosphorylated by p38 mitogen-activated protein kinase (p38 MAPK), which is activated by tumor necrosis factor (TNF) (Garrido, 2002; Salinthone et al., 2008). I verified that p38 MAPK is expressed in all Purkinje cells. The mismatch of HSPB1 phosphorylation and kinase expression patterns — except for the case of PKCδ — supports my hypothesis that PKCδ may be an important kinase of HSPB1 in Purkinje cells in NPC disease. To confirm this idea, future studies could use viral vectors to knock down or over-express PKCδ in the NPC mouse cerebellum, and then look for alterations in Purkinje cell survival.

The answer to the second question is suggested by previous research and a candidate gene from our expression analysis. Prior studies demonstrate that PKCδ is activated by diacylglycerol (DAG) and phosphatidylserine (Griner and Kazanietz, 2007; Stahelin et al., 2005). To generate DAG, phosphatidylinositol-specific phospholipase C (PLC) hydrolyzes membrane phosphatidylinositol-4, 5-bisphosphate into inositol-1, 4, 5-trisphosphate ($IP_3$) and DAG (Litosch, 2015). Interestingly, phosphatidylinositol-specific phospholipase C, X domain containing 2 (PLCXD2) was identified through our expression analysis **(Table 3.1)**. This gene is highly expressed in Purkinje cells in posterior lobules, similar to HSPB1 and PKCδ. This observation suggests the expression of regulatory pathway encompassing PLCXD2, PKCδ, and HSPB1 which increases Purkinje cell survival in posterior cerebellar lobules.

The last question raised by my data is whether phospho-HSPB1 has another function in NPC disease. I attempted to gain insight into this question by looking at previously published studies. Phosphorylated HSPB1 forms dimers and tetramers, while dephosphorylated HSPB1 forms multimers of up to 800 kDa. Large complexes of dephosphorylated HSPB1 have chaperone activity (Ehrnsperger et al., 2000; Jakob et al., 1993) and prevent oxidative damage

(Preville et al., 1999). In contrast, smaller, phosphorylated species stabilize the actin cytoskeleton and inhibit apoptosis at multiple levels (Charette and Landry, 2000; Huot et al., 1996; Lavoie et al., 1995; Paul et al., 2010). Because only phosphorylated HSPB1 protected NPC neurons in my study, HSPB1 chaperone or anti-oxidative activities are less likely to be involved in neuroprotection. Additionally, the level of ubiquitinated protein was unchanged in HSPB1 mice that were deficient in *Npc1* only in Purkinje cells **(Figure 3.6)**. Other possible mechanisms by which HSPB1 might increase neuronal survival in NPC1 deficiency is through regulation of key signaling pathways or by influencing lysosomal membrane stability. Prior studies reported that the apoptosome, which is a complex of Apaf-1 and cytochrome c, triggers LMP (Gyrd-Hansen et al., 2006; Huai et al., 2013). Since HSPB1 sequesters cytochrome c by interaction (Bruey et al., 2000), it possible that it could increase lysosomal membrane stability as well as reduce apoptosis by decreasing formation of the apoptosome.

My study confirmed that HSPB1 protects Purkinje cells in an NPC mouse model using both overexpression and knockdown approaches. These data are encouraging and prompt me to suggest investigating this approach in animal models using small molecules. One of the small molecules proven effective at inducing HSPB1 in a rat model is herbimycin A. This small molecule increased arterial HSPB1 (Connolly et al., 2003). It is not yet known whether this small molecule crosses the blood-brain barrier. Another small molecule of interest is 17-allylamino-17-demethoxygeldanamycin (17-AAG). This small molecule is under investigation study for the treatment of several cancers as an HSP90 inhibitor. Because inhibition of HSP90 induces HSPB1, this small molecule can be used as an HSPB1 inducer. Also, it crosses the blood-brain barrier and displays no neuronal toxicity *in vivo* (Egorin et al., 2001; Waza et al., 2005). Because

of these advantages, this small molecule is an attractive candidate for preclinical trials in NPC animal models.

### 4.4 Concluding remarks

Niemann-Pick type C disease is an autosomal recessive lipid storage disorder. Patients develop a clinically heterogeneous phenotype that typically includes childhood onset neurodegeneration and early death. As yet, there is no effective treatment. I believe that an improved understanding of the pathways leading to neurodegeneration in NPC disease will enable us to uncover more effective therapeutic targets. In my thesis, I have helped define a pathway leading to neuron death, yielding targets for a novel therapeutic approach to NPC disease. Further, I have identified several modifier genes that promote neuronal survival in NPC disease. I hope the work described in this thesis contributes to a more comprehensive understanding of neurodegenerative mechanisms and contributes to the discovery of effective treatments for NPC patients.

# References


Ackerley, S., James, P.A., Kalli, A., French, S., Davies, K.E., and Talbot, K. (2006). A mutation in the small heat-shock protein HSPB1 leading to distal hereditary motor neuronopathy disrupts neurofilament assembly and the axonal transport of specific cellular cargoes. Human molecular genetics *15*, 347-354.

Aits, S., and Jaattela, M. (2013). Lysosomal cell death at a glance. Journal of cell science *126*, 1905-1912.

Akbar, M.T., Lundberg, A.M., Liu, K., Vidyadaran, S., Wells, K.E., Dolatshad, H., Wynn, S., Wells, D.J., Latchman, D.S., and de Belleroche, J. (2003). The neuroprotective effects of heat shock protein 27 overexpression in transgenic animals against kainate-induced seizures and hippocampal cell death. The Journal of biological chemistry *278*, 19956-19965.

Alakurtti, K., Weber, E., Rinne, R., Theil, G., de Haan, G.J., Lindhout, D., Salmikangas, P., Saukko, P., Lahtinen, U., and Lehesjoki, A.E. (2005). Loss of lysosomal association of cystatin B proteins representing progressive myoclonus epilepsy, EPM1, mutations. European journal of human genetics : EJHG *13*, 208-215.

Almeida-Souza, L., Asselbergh, B., d'Ydewalle, C., Moonens, K., Goethals, S., de Winter, V., Azmi, A., Irobi, J., Timmermans, J.P., Gevaert, K., *et al.* (2011). Small heat-shock protein HSPB1 mutants stabilize microtubules in Charcot-Marie-Tooth neuropathy. The Journal of neuroscience : the official journal of the Society for Neuroscience *31*, 15320-15328.

Amritraj, A., Peake, K., Kodam, A., Salio, C., Merighi, A., Vance, J.E., and Kar, S. (2009). Increased activity and altered subcellular distribution of lysosomal enzymes determine neuronal vulnerability in Niemann-Pick type C1-deficient mice. The American journal of pathology *175*, 2540-2556.

Andersen, B.B., Gundersen, H.J., and Pakkenberg, B. (2003). Aging of the human cerebellum: a stereological study. J Comp Neurol *466*, 356-365.

Anderson, L., Rossi, D., Linehan, J., Brandner, S., and Weissmann, C. (2004). Transgene-driven expression of the Doppel protein in Purkinje cells causes Purkinje cell degeneration and motor impairment. Proc Natl Acad Sci U S A *101*, 3644-3649.

Armstrong, C.L., Duffin, C.A., McFarland, R., and Vogel, M.W. (2010). Mechanisms of Compartmental Purkinje Cell Death and Survival in the Lurcher Mutant Mouse. Cerebellum.

Armstrong, C.L., Krueger-Naug, A.M., Currie, R.W., and Hawkes, R. (2000). Constitutive expression of the 25-kDa heat shock protein Hsp25 reveals novel parasagittal bands of purkinje cells in the adult mouse cerebellar cortex. The Journal of comparative neurology *416*, 383-397.

Arrigo, A.P. (2007). The cellular "networking" of mammalian Hsp27 and its functions in the control of protein folding, redox state and apoptosis. Adv Exp Med Biol *594*, 14-26.
Arrigo, A.P., and Gibert, B. (2012). HspB1 dynamic phospho-oligomeric structure dependent interactome as cancer therapeutic target. Current molecular medicine *12*, 1151-1163.
Arrigo, A.P., Virot, S., Chaufour, S., Firdaus, W., Kretz-Remy, C., and Diaz-Latoud, C. (2005). Hsp27 consolidates intracellular redox homeostasis by upholding glutathione in its reduced form and by decreasing iron intracellular levels. Antioxidants & redox signaling *7*, 414-422.
Bainton, D.F. (1981). The discovery of lysosomes. The Journal of Cell Biology *91*, 66s-76s.
Barski, J.J., Dethleffsen, K., and Meyer, M. (2000). Cre recombinase expression in cerebellar Purkinje cells. Genesis *28*, 93-98.
Berg, T., Gjoen, T., and Bakke, O. (1995). Physiological functions of endosomal proteolysis. The Biochemical journal *307 ( Pt 2)*, 313-326.
Berry, D.L., and Baehrecke, E.H. (2007). Growth arrest and autophagy are required for salivary gland cell degradation in Drosophila. Cell *131*, 1137-1148.
Biran, V., Heine, V.M., Verney, C., Sheldon, R.A., Spadafora, R., Vexler, Z.S., Rowitch, D.H., and Ferriero, D.M. (2011). Cerebellar abnormalities following hypoxia alone compared to hypoxic-ischemic forebrain injury in the developing rat brain. Neurobiol Dis *41*, 138-146.
Boudreau, R.L., Spengler, R.M., Hylock, R.H., Kusenda, B.J., Davis, H.A., Eichmann, D.A., and Davidson, B.L. (2013). siSPOTR: a tool for designing highly specific and potent siRNAs for human and mouse. Nucleic acids research *41*, e9.
Boya, P., Andreau, K., Poncet, D., Zamzami, N., Perfettini, J.L., Metivier, D., Ojcius, D.M., Jaattela, M., and Kroemer, G. (2003). Lysosomal membrane permeabilization induces cell death in a mitochondrion-dependent fashion. The Journal of experimental medicine *197*, 1323-1334.
Brannvall, K., Hjelm, H., Korhonen, L., Lahtinen, U., Lehesjoki, A.E., and Lindholm, D. (2003). Cystatin-B is expressed by neural stem cells and by differentiated neurons and astrocytes. Biochemical and biophysical research communications *308*, 369-374.
Bruey, J.M., Ducasse, C., Bonniaud, P., Ravagnan, L., Susin, S.A., Diaz-Latoud, C., Gurbuxani, S., Arrigo, A.P., Kroemer, G., Solary, E., *et al.* (2000). Hsp27 negatively regulates cell death by interacting with cytochrome c. Nat Cell Biol *2*, 645-652.
Brunk, U.T., Dalen, H., Roberg, K., and Hellquist, H.B. (1997). Photo-oxidative disruption of lysosomal membranes causes apoptosis of cultured human fibroblasts. Free radical biology & medicine *23*, 616-626.
Bursch, W. (2001). The autophagosomal-lysosomal compartment in programmed cell death. Cell death and differentiation *8*, 569-581.
Butinar, M., Prebanda, M.T., Rajkovic, J., Jeric, B., Stoka, V., Peters, C., Reinheckel, T., Kruger, A., Turk, V., Turk, B., *et al.* (2014). Stefin B deficiency reduces tumor growth via sensitization of tumor cells to oxidative stress in a breast cancer model. Oncogene *33*, 3392-3400.
Buttle, D.J., Murata, M., Knight, C.G., and Barrett, A.J. (1992). CA074 methyl ester: a proinhibitor for intracellular cathepsin B. Archives of biochemistry and biophysics *299*, 377-380.
Byers, R.K., Gilles, F.H., and Fung, C. (1973). Huntington's disease in children. Neuropathologic study of four cases. Neurology *23*, 561-569.

Calkins, C.C., Sameni, M., Koblinski, J., Sloane, B.F., and Moin, K. (1998). Differential localization of cysteine protease inhibitors and a target cysteine protease, cathepsin B, by immuno-confocal microscopy. The journal of histochemistry and cytochemistry : official journal of the Histochemistry Society *46*, 745-751.

Carbon, S., Ireland, A., Mungall, C.J., Shu, S., Marshall, B., and Lewis, S. (2009). AmiGO: online access to ontology and annotation data. Bioinformatics *25*, 288-289.

Carstea, E.D., Morris, J.A., Coleman, K.G., Loftus, S.K., Zhang, D., Cummings, C., Gu, J., Rosenfeld, M.A., Pavan, W.J., Krizman, D.B., *et al.* (1997). Niemann-Pick C1 disease gene: homology to mediators of cholesterol homeostasis. Science (New York, NY) *277*, 228-231.

Caruso, J.A., Mathieu, P.A., Joiakim, A., Leeson, B., Kessel, D., Sloane, B.F., and Reiners, J.J., Jr. (2004). Differential susceptibilities of murine hepatoma 1c1c7 and Tao cells to the lysosomal photosensitizer NPe6: influence of aryl hydrocarbon receptor on lysosomal fragility and protease contents. Molecular pharmacology *65*, 1016-1028.

Caspersen, C., Wang, N., Yao, J., Sosunov, A., Chen, X., Lustbader, J.W., Xu, H.W., Stern, D., McKhann, G., and Yan, S.D. (2005). Mitochondrial Abeta: a potential focal point for neuronal metabolic dysfunction in Alzheimer's disease. FASEB journal : official publication of the Federation of American Societies for Experimental Biology *19*, 2040-2041.

Chang, S.H., Kanasaki, K., Gocheva, V., Blum, G., Harper, J., Moses, M.A., Shih, S.C., Nagy, J.A., Joyce, J., Bogyo, M., *et al.* (2009). VEGF-A induces angiogenesis by perturbing the cathepsin-cysteine protease inhibitor balance in venules, causing basement membrane degradation and mother vessel formation. Cancer research *69*, 4537-4544.

Charette, S.J., and Landry, J. (2000). The interaction of HSP27 with Daxx identifies a potential regulatory role of HSP27 in Fas-induced apoptosis. Annals of the New York Academy of Sciences *926*, 126-131.

Charman, M., Kennedy, B.E., Osborne, N., and Karten, B. (2010). MLN64 mediates egress of cholesterol from endosomes to mitochondria in the absence of functional Niemann-Pick Type C1 protein. Journal of Lipid Research *51*, 1023-1034.

Chen, H., Zheng, C., Zhang, Y., Chang, Y.Z., Qian, Z.M., and Shen, X. (2006). Heat shock protein 27 downregulates the transferrin receptor 1-mediated iron uptake. The international journal of biochemistry & cell biology *38*, 1402-1416.

Cheruku, S.R., Xu, Z., Dutia, R., Lobel, P., and Storch, J. (2006). Mechanism of cholesterol transfer from the Niemann-Pick type C2 protein to model membranes supports a role in lysosomal cholesterol transport. The Journal of biological chemistry *281*, 31594-31604.

Cheung, N.S., Koh, C.H., Bay, B.H., Qi, R.Z., Choy, M.S., Li, Q.T., Wong, K.P., and Whiteman, M. (2004). Chronic exposure to U18666A induces apoptosis in cultured murine cortical neurons. Biochem Biophys Res Commun *315*, 408-417.

Chevallier, J., Chamoun, Z., Jiang, G., Prestwich, G., Sakai, N., Matile, S., Parton, R.G., and Gruenberg, J. (2008). Lysobisphosphatidic acid controls endosomal cholesterol levels. The Journal of biological chemistry *283*, 27871-27880.

Ciesielski, K.T., Yanofsky, R., Ludwig, R.N., Hill, D.E., Hart, B.L., Astur, R.S., and Snyder, T. (1994). Hypoplasia of the cerebellar vermis and cognitive deficits in survivors of childhood leukemia. Arch Neurol *51*, 985-993.

Cirman, T., Oresic, K., Mazovec, G.D., Turk, V., Reed, J.C., Myers, R.M., Salvesen, G.S., and Turk, B. (2004). Selective disruption of lysosomes in HeLa cells triggers apoptosis

mediated by cleavage of Bid by multiple papain-like lysosomal cathepsins. The Journal of biological chemistry *279*, 3578-3587.
Clark, H.B., Burright, E.N., Yunis, W.S., Larson, S., Wilcox, C., Hartman, B., Matilla, A., Zoghbi, H.Y., and Orr, H.T. (1997). Purkinje cell expression of a mutant allele of SCA1 in transgenic mice leads to disparate effects on motor behaviors, followed by a progressive cerebellar dysfunction and histological alterations. J Neurosci *17*, 7385-7395.
Claus, V., Jahraus, A., Tjelle, T., Berg, T., Kirschke, H., Faulstich, H., and Griffiths, G. (1998). Lysosomal enzyme trafficking between phagosomes, endosomes, and lysosomes in J774 macrophages. Enrichment of cathepsin H in early endosomes. The Journal of biological chemistry *273*, 9842-9851.
Clifton, A.D., Young, P.R., and Cohen, P. (1996). A comparison of the substrate specificity of MAPKAP kinase-2 and MAPKAP kinase-3 and their activation by cytokines and cellular stress. FEBS letters *392*, 209-214.
Connolly, E.M., Kelly, C.J., Chen, G., O'Grady, T., Kay, E., Leahy, A., and Bouchier-Hayes, D.J. (2003). Pharmacological induction of HSP27 attenuates intimal hyperplasia in vivo. European journal of vascular and endovascular surgery : the official journal of the European Society for Vascular Surgery *25*, 40-47.
Crooks, R., Mitchell, T., and Thom, M. (2000). Patterns of cerebellar atrophy in patients with chronic epilepsy: a quantitative neuropathological study. Epilepsy Res *41*, 63-73.
Dalet-Fumeron, V., Boudjennah, L., and Pagano, M. (1996). Competition between plasminogen and procathepsin B as a probe to demonstrate the in vitro activation of procathepsin B by the tissue plasminogen activator. Archives of biochemistry and biophysics *335*, 351-357.
Dalet-Fumeron, V., Guinec, N., and Pagano, M. (1993). In vitro activation of pro-cathepsin B by three serine proteinases: leucocyte elastase, cathepsin G, and the urokinase-type plasminogen activator. FEBS letters *332*, 251-254.
Danial, N.N., and Korsmeyer, S.J. (2004). Cell death: critical control points. Cell *116*, 205-219.
Davies, J.P., and Ioannou, Y.A. (2000). Topological analysis of Niemann-Pick C1 protein reveals that the membrane orientation of the putative sterol-sensing domain is identical to those of 3-hydroxy-3-methylglutaryl-CoA reductase and sterol regulatory element binding protein cleavage-activating protein. The Journal of biological chemistry *275*, 24367-24374.
de Duve, C. (1983). Lysosomes revisited. European journal of biochemistry / FEBS *137*, 391-397.
de Duve, C. (2005). The lysosome turns fifty. Nature cell biology *7*, 847-849.
De Duve, C., Pressman, B.C., Gianetto, R., Wattiaux, R., and Appelmans, F. (1955). Tissue fractionation studies. 6. Intracellular distribution patterns of enzymes in rat-liver tissue. The Biochemical journal *60*, 604-617.
De Milito, A., Iessi, E., Logozzi, M., Lozupone, F., Spada, M., Marino, M.L., Federici, C., Perdicchio, M., Matarrese, P., Lugini, L., *et al.* (2007). Proton pump inhibitors induce apoptosis of human B-cell tumors through a caspase-independent mechanism involving reactive oxygen species. Cancer research *67*, 5408-5417.
Deffieu, M.S., and Pfeffer, S.R. (2011). Niemann-Pick type C 1 function requires lumenal domain residues that mediate cholesterol-dependent NPC2 binding. Proceedings of the National Academy of Sciences of the United States of America *108*, 18932-18936.
Dell'Orco, J.M., Wasserman, A.H., Chopra, R., Ingram, M.A.C., Hu, Y.-S., Singh, V., Wulff, H., Opal, P., Orr, H.T., and Shakkottai, V.G. (2015). Neuronal Atrophy Early in Degenerative

Ataxia Is a Compensatory Mechanism to Regulate Membrane Excitability. The Journal of Neuroscience *35*, 11292-11307.
Denton, D., Shravage, B., Simin, R., Mills, K., Berry, D.L., Baehrecke, E.H., and Kumar, S. (2009). Autophagy, not apoptosis, is essential for midgut cell death in Drosophila. Current biology : CB *19*, 1741-1746.
Devlin, C., Pipalia, N.H., Liao, X., Schuchman, E.H., Maxfield, F.R., and Tabas, I. (2010). Improvement in lipid and protein trafficking in Niemann-Pick C1 cells by correction of a secondary enzyme defect. Traffic (Copenhagen, Denmark) *11*, 601-615.
Double, K.L., Reyes, S., Werry, E.L., and Halliday, G.M. (2010). Selective cell death in neurodegeneration: why are some neurons spared in vulnerable regions? Prog Neurobiol *92*, 316-329.
Duchala, C.S., Shick, H.E., Garcia, J., Deweese, D.M., Sun, X., Stewart, V.J., and Macklin, W.B. (2004). The toppler mouse: a novel mutant exhibiting loss of Purkinje cells. The Journal of comparative neurology *476*, 113-129.
Egorin, M.J., Zuhowski, E.G., Rosen, D.M., Sentz, D.L., Covey, J.M., and Eiseman, J.L. (2001). Plasma pharmacokinetics and tissue distribution of 17-(allylamino)-17-demethoxygeldanamycin (NSC 330507) in CD2F1 mice1. Cancer Chemother Pharmacol *47*, 291-302.
Ehrnsperger, M., Gaestel, M., and Buchner, J. (2000). Analysis of chaperone properties of small Hsp's. Methods in molecular biology (Clifton, NJ) *99*, 421-429.
Elrick, M.J., and Lieberman, A.P. (2013). Autophagic dysfunction in a lysosomal storage disorder due to impaired proteolysis. Autophagy *9*, 234-235.
Elrick, M.J., Pacheco, C.D., Yu, T., Dadgar, N., Shakkottai, V.G., Ware, C., Paulson, H.L., and Lieberman, A.P. (2010). Conditional Niemann-Pick C mice demonstrate cell autonomous Purkinje cell neurodegeneration. Human molecular genetics *19*, 837-847.
Elrick, M.J., Yu, T., Chung, C., and Lieberman, A.P. (2012). Impaired proteolysis underlies autophagic dysfunction in Niemann-Pick type C disease. Human molecular genetics *21*, 4876-4887.
Enomoto, A., Fukasawa, T., Takamatsu, N., Ito, M., Morita, A., Hosoi, Y., and Miyagawa, K. (2013). The HSP90 inhibitor 17-allylamino-17-demethoxygeldanamycin modulates radiosensitivity by downregulating serine/threonine kinase 38 via Sp1 inhibition. European journal of cancer (Oxford, England : 1990) *49*, 3547-3558.
Evgrafov, O.V., Mersiyanova, I., Irobi, J., Van Den Bosch, L., Dierick, I., Leung, C.L., Schagina, O., Verpoorten, N., Van Impe, K., Fedotov, V., *et al.* (2004). Mutant small heat-shock protein 27 causes axonal Charcot-Marie-Tooth disease and distal hereditary motor neuropathy. Nat Genet *36*, 602-606.
Fernández, A., Llacuna, L., Fernández-Checa, J.C., and Colell, A. (2009). Mitochondrial Cholesterol Loading Exacerbates Amyloid β Peptide-Induced Inflammation and Neurotoxicity. The Journal of Neuroscience *29*, 6394-6405.
Foghsgaard, L., Wissing, D., Mauch, D., Lademann, U., Bastholm, L., Boes, M., Elling, F., Leist, M., and Jaattela, M. (2001). Cathepsin B acts as a dominant execution protease in tumor cell apoptosis induced by tumor necrosis factor. J Cell Biol *153*, 999-1010.
Friedland, N., Liou, H.L., Lobel, P., and Stock, A.M. (2003). Structure of a cholesterol-binding protein deficient in Niemann-Pick type C2 disease. Proceedings of the National Academy of Sciences of the United States of America *100*, 2512-2517.

Frosch, B.A., Berquin, I., Emmert-Buck, M.R., Moin, K., and Sloane, B.F. (1999). Molecular regulation, membrane association and secretion of tumor cathepsin B. APMIS : acta pathologica, microbiologica, et immunologica Scandinavica *107*, 28-37.

Gabande-Rodriguez, E., Boya, P., Labrador, V., Dotti, C.G., and Ledesma, M.D. (2014). High sphingomyelin levels induce lysosomal damage and autophagy dysfunction in Niemann Pick disease type A. Cell death and differentiation *21*, 864-875.

Gaestel, M., Schroder, W., Benndorf, R., Lippmann, C., Buchner, K., Hucho, F., Erdmann, V.A., and Bielka, H. (1991). Identification of the phosphorylation sites of the murine small heat shock protein hsp25. The Journal of biological chemistry *266*, 14721-14724.

Galluzzi, L., Maiuri, M.C., Vitale, I., Zischka, H., Castedo, M., Zitvogel, L., and Kroemer, G. (2007). Cell death modalities: classification and pathophysiological implications. Cell Death Differ *14*, 1237-1243.

Garrido, C. (2002). Size matters: of the small HSP27 and its large oligomers. Cell death and differentiation *9*, 483-485.

German, D.C., Quintero, E.M., Liang, C.L., Ng, B., Punia, S., Xie, C., and Dietschy, J.M. (2001). Selective neurodegeneration, without neurofibrillary tangles, in a mouse model of Niemann-Pick C disease. The Journal of comparative neurology *433*, 415-425.

Golstein, P., and Kroemer, G. (2007). Cell death by necrosis: towards a molecular definition. Trends in biochemical sciences *32*, 37-43.

Griner, E.M., and Kazanietz, M.G. (2007). Protein kinase C and other diacylglycerol effectors in cancer. Nat Rev Cancer *7*, 281-294.

Groth-Pedersen, L., and Jaattela, M. (2013). Combating apoptosis and multidrug resistant cancers by targeting lysosomes. Cancer letters *332*, 265-274.

Gyrd-Hansen, M., Farkas, T., Fehrenbacher, N., Bastholm, L., Hoyer-Hansen, M., Elling, F., Wallach, D., Flavell, R., Kroemer, G., Nylandsted, J., *et al.* (2006). Apoptosome-independent activation of the lysosomal cell death pathway by caspase-9. Molecular and cellular biology *26*, 7880-7891.

Hanada, K., Tamai, M., Yamagishi, M., Ohmura, S., Sawada, J., and Tanaka, I. (1978). Isolation and Characterization of E-64, a New Thiol Protease Inhibitor. Agricultural and Biological Chemistry *42*, 523-528.

Hang, H.Y., He, L.S., and Fox, M.H. (1995). CELL-CYCLE VARIATION OF HSP70 LEVELS IN HELA-CELLS AT 37-DEGREES-C AND AFTER A HEAT-SHOCK. J Cell Physiol *165*, 367-375.

Havasi, A., Li, Z., Wang, Z., Martin, J.L., Botla, V., Ruchalski, K., Schwartz, J.H., and Borkan, S.C. (2008). Hsp27 inhibits Bax activation and apoptosis via a phosphatidylinositol 3-kinase-dependent mechanism. J Biol Chem *283*, 12305-12313.

Heckroth, J.A., and Abbott, L.C. (1994). Purkinje cell loss from alternating sagittal zones in the cerebellum of leaner mutant mice. Brain Res *658*, 93-104.

Higashi, Y., Murayama, S., Pentchev, P.G., and Suzuki, K. (1993). Cerebellar degeneration in the Niemann-Pick type C mouse. Acta neuropathologica *85*, 175-184.

Hook, G., Hook, V., and Kindy, M. (2011). The cysteine protease inhibitor, E64d, reduces brain amyloid-beta and improves memory deficits in Alzheimer's disease animal models by inhibiting cathepsin B, but not BACE1, beta-secretase activity. Journal of Alzheimer's disease : JAD *26*, 387-408.

Hook, G., Jacobsen, J.S., Grabstein, K., Kindy, M., and Hook, V. (2015). Cathepsin B is a New Drug Target for Traumatic Brain Injury Therapeutics: Evidence for E64d as a Promising Lead Drug Candidate. Frontiers in neurology *6*, 178.

Hook, V., Kindy, M., and Hook, G. (2007). Cysteine protease inhibitors effectively reduce in vivo levels of brain beta-amyloid related to Alzheimer's disease. Biological chemistry *388*, 247-252.

Huai, J., Vögtle, F.-N., Jöckel, L., Li, Y., Kiefer, T., Ricci, J.-E., and Borner, C. (2013). TNFα-induced lysosomal membrane permeability is downstream of MOMP and triggered by caspase-mediated NDUFS1 cleavage and ROS formation. Journal of cell science *126*, 4015-4025.

Huang, L., Min, J.N., Masters, S., Mivechi, N.F., and Moskophidis, D. (2007). Insights into function and regulation of small heat shock protein 25 (HSPB1) in a mouse model with targeted gene disruption. Genesis (New York, NY : 2000) *45*, 487-501.

Huot, J., Houle, F., Spitz, D.R., and Landry, J. (1996). HSP27 phosphorylation-mediated resistance against actin fragmentation and cell death induced by oxidative stress. Cancer Res *56*, 273-279.

Illy, C., Quraishi, O., Wang, J., Purisima, E., Vernet, T., and Mort, J.S. (1997). Role of the occluding loop in cathepsin B activity. The Journal of biological chemistry *272*, 1197-1202.

Infante, R.E., Wang, M.L., Radhakrishnan, A., Kwon, H.J., Brown, M.S., and Goldstein, J.L. (2008). NPC2 facilitates bidirectional transfer of cholesterol between NPC1 and lipid bilayers, a step in cholesterol egress from lysosomes. Proceedings of the National Academy of Sciences of the United States of America *105*, 15287-15292.

Irobi, J., De Jonghe, P., and Timmerman, V. (2004). Molecular genetics of distal hereditary motor neuropathies. Human molecular genetics *13 Spec No 2*, R195-202.

Isaacs, A.M., Oliver, P.L., Jones, E.L., Jeans, A., Potter, A., Hovik, B.H., Nolan, P.M., Vizor, L., Glenister, P., Simon, A.K., *et al.* (2003). A mutation in Af4 is predicted to cause cerebellar ataxia and cataracts in the robotic mouse. J Neurosci *23*, 1631-1637.

Jaattela, M., and Tschopp, J. (2003). Caspase-independent cell death in T lymphocytes. Nature immunology *4*, 416-423.

Jakawich, S.K., Neely, R.M., Djakovic, S.N., Patrick, G.N., and Sutton, M.A. (2010). An essential postsynaptic role for the ubiquitin proteasome system in slow homeostatic synaptic plasticity in cultured hippocampal neurons. Neuroscience *171*, 1016-1031.

Jakob, U., Gaestel, M., Engel, K., and Buchner, J. (1993). Small heat shock proteins are molecular chaperones. The Journal of biological chemistry *268*, 1517-1520.

Jerome, V., Vourch, C., Baulieu, E.E., and Catelli, M.G. (1993). CELL-CYCLE REGULATION OF THE CHICKEN HSP90-ALPHA EXPRESSION. Exp Cell Res *205*, 44-51.

Jiang, C., Baehrecke, E.H., and Thummel, C.S. (1997). Steroid regulated programmed cell death during Drosophila metamorphosis. Development *124*, 4673-4683.

Journet, A., Chapel, A., Kieffer, S., Roux, F., and Garin, J. (2002). Proteomic analysis of human lysosomes: application to monocytic and breast cancer cells. Proteomics *2*, 1026-1040.

Kagedal, K., Zhao, M., Svensson, I., and Brunk, U.T. (2001). Sphingosine-induced apoptosis is dependent on lysosomal proteases. The Biochemical journal *359*, 335-343.

Kalesnykas, G., Niittykoski, M., Rantala, J., Miettinen, R., Salminen, A., Kaarniranta, K., and Uusitalo, H. (2007). The expression of heat shock protein 27 in retinal ganglion and glial cells in a rat glaucoma model. Neuroscience *150*, 692-704.

Katunuma, N. (2010). Posttranslational processing and modification of cathepsins and cystatins. Journal of signal transduction *2010*, 375345.
Kennedy, B.E., LeBlanc, V.G., Mailman, T.M., Fice, D., Burton, I., Karakach, T.K., and Karten, B. (2013). Pre-symptomatic activation of antioxidant responses and alterations in glucose and pyruvate metabolism in Niemann-Pick Type C1-deficient murine brain. PloS one *8*, e82685.
Kennedy, B.E., Madreiter, C.T., Vishnu, N., Malli, R., Graier, W.F., and Karten, B. (2014). Adaptations of energy metabolism associated with increased levels of mitochondrial cholesterol in Niemann-Pick type C1-deficient cells. The Journal of biological chemistry *289*, 16278-16289.
Keppler, D., and Sloane, B.F. (1996). Cathepsin B: multiple enzyme forms from a single gene and their relation to cancer. Enzyme & protein *49*, 94-105.
Khalil, A.A., Kabapy, N.F., Deraz, S.F., and Smith, C. (2011). Heat shock proteins in oncology: diagnostic biomarkers or therapeutic targets? Biochimica et biophysica acta *1816*, 89-104.
Kirkegaard, T., Roth, A.G., Petersen, N.H., Mahalka, A.K., Olsen, O.D., Moilanen, I., Zylicz, A., Knudsen, J., Sandhoff, K., Arenz, C., *et al.* (2010). Hsp70 stabilizes lysosomes and reverts Niemann-Pick disease-associated lysosomal pathology. Nature *463*, 549-553.
Kirschke, H., Barrett, A.J., and Rawlings, N.D. (1995). Proteinases 1: lysosomal cysteine proteinases. Protein profile *2*, 1581-1643.
Ko, D.C., Milenkovic, L., Beier, S.M., Manuel, H., Buchanan, J., and Scott, M.P. (2005). Cell-autonomous death of cerebellar purkinje neurons with autophagy in Niemann-Pick type C disease. PLoS genetics *1*, 81-95.
Kobayashi, S. (2015). Choose Delicately and Reuse Adequately: The Newly Revealed Process of Autophagy. Biological & pharmaceutical bulletin *38*, 1098-1103.
Kobayashi, T., Beuchat, M.H., Lindsay, M., Frias, S., Palmiter, R.D., Sakuraba, H., Parton, R.G., and Gruenberg, J. (1999). Late endosomal membranes rich in lysobisphosphatidic acid regulate cholesterol transport. Nature cell biology *1*, 113-118.
Krenn, M.A., Schurz, M., Teufl, B., Uchida, K., Eckl, P.M., and Bresgen, N. (2015). Ferritin-stimulated lipid peroxidation, lysosomal leak, and macroautophagy promote lysosomal "metastability" in primary hepatocytes determining in vitro cell survival. Free radical biology & medicine *80*, 48-58.
Kume, A., Takahashi, A., Hashizume, Y., and Asai, J. (1991). A histometrical and comparative study on Purkinje cell loss and olivary nucleus cell loss in multiple system atrophy. J Neurol Sci *101*, 178-186.
Kurz, T., Terman, A., Gustafsson, B., and Brunk, U.T. (2008a). Lysosomes and oxidative stress in aging and apoptosis. Biochimica et Biophysica Acta (BBA) - General Subjects *1780*, 1291-1303.
Kurz, T., Terman, A., Gustafsson, B., and Brunk, U.T. (2008b). Lysosomes in iron metabolism, ageing and apoptosis. Histochemistry and cell biology *129*, 389-406.
Kwon, H.J., Abi-Mosleh, L., Wang, M.L., Deisenhofer, J., Goldstein, J.L., Brown, M.S., and Infante, R.E. (2009). Structure of N-terminal domain of NPC1 reveals distinct subdomains for binding and transfer of cholesterol. Cell *137*, 1213-1224.
Lavoie, J.N., Lambert, H., Hickey, E., Weber, L.A., and Landry, J. (1995). Modulation of cellular thermoresistance and actin filament stability accompanies phosphorylation-induced changes in the oligomeric structure of heat shock protein 27. Mol Cell Biol *15*, 505-516.

Lee, C.-Y., Cooksey, B.A.K., and Baehrecke, E.H. (2002). Steroid Regulation of Midgut Cell Death during Drosophila Development. Developmental biology *250*, 101-111.
Lee, Y.J., Lee, D.H., Cho, C.K., Bae, S., Jhon, G.J., Lee, S.J., Soh, J.W., and Lee, Y.S. (2005). HSP25 inhibits protein kinase C delta-mediated cell death through direct interaction. The Journal of biological chemistry *280*, 18108-18119.
Lee, Y.P., Kim, D.W., Kang, H.W., Hwang, J.H., Jeong, H.J., Sohn, E.J., Kim, M.J., Ahn, E.H., Shin, M.J., Kim, D.S., *et al.* (2012). PEP-1-heat shock protein 27 protects from neuronal damage in cells and in a Parkinson's disease mouse model. The FEBS journal *279*, 1929-1942.
Lehtinen, M.K., Tegelberg, S., Schipper, H., Su, H., Zukor, H., Manninen, O., Kopra, O., Joensuu, T., Hakala, P., Bonni, A., *et al.* (2009). Cystatin B deficiency sensitizes neurons to oxidative stress in progressive myoclonus epilepsy, EPM1. The Journal of neuroscience : the official journal of the Society for Neuroscience *29*, 5910-5915.
Lein, E.S., Hawrylycz, M.J., Ao, N., Ayres, M., Bensinger, A., Bernard, A., Boe, A.F., Boguski, M.S., Brockway, K.S., Byrnes, E.J., *et al.* (2007). Genome-wide atlas of gene expression in the adult mouse brain. Nature *445*, 168-176.
Leist, M., and Jaattela, M. (2001). Four deaths and a funeral: from caspases to alternative mechanisms. Nature reviews Molecular cell biology *2*, 589-598.
Levine, B., and Kroemer, G. (2008). Autophagy in the pathogenesis of disease. Cell *132*, 27-42.
Li, N., Zheng, Y., Chen, W., Wang, C., Liu, X., He, W., Xu, H., and Cao, X. (2007). Adaptor protein LAPF recruits phosphorylated p53 to lysosomes and triggers lysosomal destabilization in apoptosis. Cancer research *67*, 11176-11185.
Li, T.R., and White, K.P. (2003). Tissue-specific gene expression and ecdysone-regulated genomic networks in Drosophila. Developmental cell *5*, 59-72.
Lianos, G.D., Alexiou, G.A., Mangano, A., Mangano, A., Rausei, S., Boni, L., Dionigi, G., and Roukos, D.H. (2015). The role of heat shock proteins in cancer. Cancer Letters *360*, 114-118.
Liao, G., Yao, Y., Liu, J., Yu, Z., Cheung, S., Xie, A., Liang, X., and Bi, X. (2007). Cholesterol accumulation is associated with lysosomal dysfunction and autophagic stress in Npc1 -/- mouse brain. The American journal of pathology *171*, 962-975.
Lieberman, A.P., Puertollano, R., Raben, N., Slaugenhaupt, S., Walkley, S.U., and Ballabio, A. (2012). Autophagy in lysosomal storage disorders. Autophagy *8*, 719-730.
Lindquist, S. (1986). The heat-shock response. Annual review of biochemistry *55*, 1151-1191.
Lindquist, S., and Craig, E.A. (1988). The heat-shock proteins. Annual review of genetics *22*, 631-677.
Liscum, L., Ruggiero, R.M., and Faust, J.R. (1989). The intracellular transport of low density lipoprotein-derived cholesterol is defective in Niemann-Pick type C fibroblasts. J Cell Biol *108*, 1625-1636.
Litosch, I. (2015). Regulating G protein activity by lipase-independent functions of phospholipase C. Life Sciences *137*, 116-124.
Lloyd-Evans, E., Morgan, A.J., He, X., Smith, D.A., Elliot-Smith, E., Sillence, D.J., Churchill, G.C., Schuchman, E.H., Galione, A., and Platt, F.M. (2008). Niemann-Pick disease type C1 is a sphingosine storage disease that causes deregulation of lysosomal calcium. Nature medicine *14*, 1247-1255.

Loftus, S.K., Morris, J.A., Carstea, E.D., Gu, J.Z., Cummings, C., Brown, A., Ellison, J., Ohno, K., Rosenfeld, M.A., Tagle, D.A., *et al.* (1997). Murine model of Niemann-Pick C disease: mutation in a cholesterol homeostasis gene. Science (New York, NY) *277*, 232-235.

Love, S., Bridges, L.R., and Case, C.P. (1995). Neurofibrillary tangles in Niemann-Pick disease type C. Brain : a journal of neurology *118 ( Pt 1)*, 119-129.

Lucken-Ardjomande, S., Montessuit, S., and Martinou, J.C. (2007). Bax activation and stress-induced apoptosis delayed by the accumulation of cholesterol in mitochondrial membranes. Cell death and differentiation *15*, 484-493.

Luke, C.J., Pak, S.C., Askew, Y.S., Naviglia, T.L., Askew, D.J., Nobar, S.M., Vetica, A.C., Long, O.S., Watkins, S.C., Stolz, D.B., *et al.* (2007). An intracellular serpin regulates necrosis by inhibiting the induction and sequelae of lysosomal injury. Cell *130*, 1108-1119.

Luo, C.L., Chen, X.P., Yang, R., Sun, Y.X., Li, Q.Q., Bao, H.J., Cao, Q.Q., Ni, H., Qin, Z.H., and Tao, L.Y. (2010). Cathepsin B contributes to traumatic brain injury-induced cell death through a mitochondria-mediated apoptotic pathway. Journal of neuroscience research *88*, 2847-2858.

Maher, K., Jeric Kokelj, B., Butinar, M., Mikhaylov, G., Mancek-Keber, M., Stoka, V., Vasiljeva, O., Turk, B., Grigoryev, S.A., and Kopitar-Jerala, N. (2014). A role for stefin B (cystatin B) in inflammation and endotoxemia. The Journal of biological chemistry *289*, 31736-31750.

Maizels, E.T., Peters, C.A., Kline, M., Cutler, R.E., Jr., Shanmugam, M., and Hunzicker-Dunn, M. (1998). Heat-shock protein-25/27 phosphorylation by the delta isoform of protein kinase C. The Biochemical journal *332 ( Pt 3)*, 703-712.

Manfredi, G., and Xu, Z. (2005). Mitochondrial dysfunction and its role in motor neuron degeneration in ALS. Mitochondrion *5*, 77-87.

Mann, D.M. (1996). Pyramidal nerve cell loss in Alzheimer's disease. Neurodegeneration : a journal for neurodegenerative disorders, neuroprotection, and neuroregeneration *5*, 423-427.

Marschalek, N., Albert, F., Meske, V., and Ohm, T.G. (2014). The natural history of cerebellar degeneration of Niemann-Pick C mice monitored in vitro. Neuropathology and applied neurobiology *40*, 933-945.

Martin, L.J., Pan, Y., Price, A.C., Sterling, W., Copeland, N.G., Jenkins, N.A., Price, D.L., and Lee, M.K. (2006). Parkinson's disease alpha-synuclein transgenic mice develop neuronal mitochondrial degeneration and cell death. The Journal of neuroscience : the official journal of the Society for Neuroscience *26*, 41-50.

Marzban, H., and Hawkes, R. (2011). On the architecture of the posterior zone of the cerebellum. Cerebellum (London, England) *10*, 422-434.

Matsuda, J., Kido, M., Tadano-Aritomi, K., Ishizuka, I., Tominaga, K., Toida, K., Takeda, E., Suzuki, K., and Kuroda, Y. (2004). Mutation in saposin D domain of sphingolipid activator protein gene causes urinary system defects and cerebellar Purkinje cell degeneration with accumulation of hydroxy fatty acid-containing ceramide in mouse. Hum Mol Genet *13*, 2709-2723.

McGowan, E.B., Becker, E., and Detwiler, T.C. (1989). Inhibition of calpain in intact platelets by the thiol protease inhibitor E-64d. Biochemical and biophysical research communications *158*, 432-435.

Milarski, K.L., and Morimoto, R.I. (1986). Expression of human HSP70 during the synthetic phase of the cell cycle. Proceedings of the National Academy of Sciences *83*, 9517-9521.

Millard, E.E., Gale, S.E., Dudley, N., Zhang, J., Schaffer, J.E., and Ory, D.S. (2005). The sterol-sensing domain of the Niemann-Pick C1 (NPC1) protein regulates trafficking of low density lipoprotein cholesterol. The Journal of biological chemistry *280*, 28581-28590.
Mizushima, N., Levine, B., Cuervo, A.M., and Klionsky, D.J. (2008). Autophagy fights disease through cellular self-digestion. Nature *451*, 1069-1075.
Mizutani, T., Maeda, S., Hayakawa, K., Tanaka, U., Hirahata, S., Kamoshita, H., Taketani, T., and Morimatsu, Y. (1988). Paraneoplastic cortical cerebellar degeneration. A neuropathological study of an autopsy case in comparison with cortical cerebellar degeneration in alcoholics. Acta Neuropathol *77*, 206-212.
Morimoto, R.I., and Santoro, M.G. (1998). Stress-inducible responses and heat shock proteins: new pharmacologic targets for cytoprotection. Nature biotechnology *16*, 833-838.
Mort, J.S., and Buttle, D.J. (1997). Cathepsin B. The international journal of biochemistry & cell biology *29*, 715-720.
Mullen, R.J., Eicher, E.M., and Sidman, R.L. (1976). Purkinje cell degeneration, a new neurological mutation in the mouse. Proceedings of the National Academy of Sciences of the United States of America *73*, 208-212.
Musil, D., Zucic, D., Turk, D., Engh, R.A., Mayr, I., Huber, R., Popovic, T., Turk, V., Towatari, T., Katunuma, N., *et al.* (1991). The refined 2.15 A X-ray crystal structure of human liver cathepsin B: the structural basis for its specificity. The EMBO journal *10*, 2321-2330.
Nakanishi, H. (2003). Neuronal and microglial cathepsins in aging and age-related diseases. Ageing research reviews *2*, 367-381.
Naureckiene, S., Sleat, D.E., Lackland, H., Fensom, A., Vanier, M.T., Wattiaux, R., Jadot, M., and Lobel, P. (2000). Identification of HE1 as the second gene of Niemann-Pick C disease. Science (New York, NY) *290*, 2298-2301.
Ni, H., Ren, S.Y., Zhang, L.L., Sun, Q., Tian, T., and Feng, X. (2013). Expression profiles of hippocampal regenerative sprouting-related genes and their regulation by E-64d in a developmental rat model of penicillin-induced recurrent epilepticus. Toxicology letters *217*, 162-169.
Nylandsted, J., Brand, K., and Jaattela, M. (2000). Heat shock protein 70 is required for the survival of cancer cells. Annals of the New York Academy of Sciences *926*, 122-125.
Nylandsted, J., Gyrd-Hansen, M., Danielewicz, A., Fehrenbacher, N., Lademann, U., Hoyer-Hansen, M., Weber, E., Multhoff, G., Rohde, M., and Jaattela, M. (2004). Heat shock protein 70 promotes cell survival by inhibiting lysosomal membrane permeabilization. The Journal of experimental medicine *200*, 425-435.
Ogawa, C., Kihara, A., Gokoh, M., and Igarashi, Y. (2003). Identification and characterization of a novel human sphingosine-1-phosphate phosphohydrolase, hSPP2. J Biol Chem *278*, 1268-1272.
Ohgami, N., Ko, D.C., Thomas, M., Scott, M.P., Chang, C.C., and Chang, T.Y. (2004). Binding between the Niemann-Pick C1 protein and a photoactivatable cholesterol analog requires a functional sterol-sensing domain. Proceedings of the National Academy of Sciences of the United States of America *101*, 12473-12478.
Ollinger, K., and Brunk, U.T. (1995). Cellular injury induced by oxidative stress is mediated through lysosomal damage. Free radical biology & medicine *19*, 565-574.
Ordonez, M.P., Roberts, E.A., Kidwell, C.U., Yuan, S.H., Plaisted, W.C., and Goldstein, L.S. (2012). Disruption and therapeutic rescue of autophagy in a human neuronal model of Niemann Pick type C1. Human molecular genetics *21*, 2651-2662.

Orrenius, S. (2007). Reactive oxygen species in mitochondria-mediated cell death. Drug metabolism reviews *39*, 443-455.
Ostenfeld, M.S., Fehrenbacher, N., Hoyer-Hansen, M., Thomsen, C., Farkas, T., and Jaattela, M. (2005). Effective tumor cell death by sigma-2 receptor ligand siramesine involves lysosomal leakage and oxidative stress. Cancer research *65*, 8975-8983.
Pacheco, C.D., Kunkel, R., and Lieberman, A.P. (2007). Autophagy in Niemann–Pick C disease is dependent upon Beclin-1 and responsive to lipid trafficking defects. Human molecular genetics *16*, 1495-1503.
Pacheco, C.D., and Lieberman, A.P. (2008). The pathogenesis of Niemann-Pick type C disease: a role for autophagy? Expert reviews in molecular medicine *10*, e26.
Pandey, P., Farber, R., Nakazawa, A., Kumar, S., Bharti, A., Nalin, C., Weichselbaum, R., Kufe, D., and Kharbanda, S. (2000). Hsp27 functions as a negative regulator of cytochrome c-dependent activation of procaspase-3. Oncogene *19*, 1975-1981.
Park, W.D., O'Brien, J.F., Lundquist, P.A., Kraft, D.L., Vockley, C.W., Karnes, P.S., Patterson, M.C., and Snow, K. (2003). Identification of 58 novel mutations in Niemann-Pick disease Type C: Correlation with biochemical phenotype and importance of PTC1-like domains in NPC1. Hum Mutat *22*, 313-325.
Patterson, M.C., Hendriksz, C.J., Walterfang, M., Sedel, F., Vanier, M.T., and Wijburg, F. (2012). Recommendations for the diagnosis and management of Niemann-Pick disease type C: an update. Molecular genetics and metabolism *106*, 330-344.
Paul, C., Simon, S., Gibert, B., Virot, S., Manero, F., and Arrigo, A.P. (2010). Dynamic processes that reflect anti-apoptotic strategies set up by HspB1 (Hsp27). Exp Cell Res *316*, 1535-1552.
Pennacchio, L.A., Bouley, D.M., Higgins, K.M., Scott, M.P., Noebels, J.L., and Myers, R.M. (1998). Progressive ataxia, myoclonic epilepsy and cerebellar apoptosis in cystatin B-deficient mice. Nature genetics *20*, 251-258.
Pislar, A., and Kos, J. (2014). Cysteine cathepsins in neurological disorders. Molecular neurobiology *49*, 1017-1030.
Plumier, J.C., Hopkins, D.A., Robertson, H.A., and Currie, R.W. (1997). Constitutive expression of the 27-kDa heat shock protein (Hsp27) in sensory and motor neurons of the rat nervous system. The Journal of comparative neurology *384*, 409-428.
Poirier, S., Mayer, G., Murphy, S.R., Garver, W.S., Chang, T.Y., Schu, P., and Seidah, N.G. (2013). The cytosolic adaptor AP-1A is essential for the trafficking and function of Niemann-Pick type C proteins. Traffic (Copenhagen, Denmark) *14*, 458-469.
Porter, F.D., Scherrer, D.E., Lanier, M.H., Langmade, S.J., Molugu, V., Gale, S.E., Olzeski, D., Sidhu, R., Dietzen, D.J., Fu, R., *et al.* (2010). Cholesterol oxidation products are sensitive and specific blood-based biomarkers for Niemann-Pick C1 disease. Science translational medicine *2*, 56ra81.
Preville, X., Salvemini, F., Giraud, S., Chaufour, S., Paul, C., Stepien, G., Ursini, M.V., and Arrigo, A.P. (1999). Mammalian small stress proteins protect against oxidative stress through their ability to increase glucose-6-phosphate dehydrogenase activity and by maintaining optimal cellular detoxifying machinery. Experimental cell research *247*, 61-78.
Qin, Q., Liao, G., Baudry, M., and Bi, X. (2010). Cholesterol Perturbation in Mice Results in p53 Degradation and Axonal Pathology through p38 MAPK and Mdm2 Activation. PloS one *5*, e9999.

Quigney, D.J., Gorman, A.M., and Samali, A. (2003). Heat shock protects PC12 cells against MPP+ toxicity. Brain research *993*, 133-139.
Quraishi, O., Nagler, D.K., Fox, T., Sivaraman, J., Cygler, M., Mort, J.S., and Storer, A.C. (1999). The occluding loop in cathepsin B defines the pH dependence of inhibition by its propeptide. Biochemistry *38*, 5017-5023.
Raj, L., Ide, T., Gurkar, A.U., Foley, M., Schenone, M., Li, X., Tolliday, N.J., Golub, T.R., Carr, S.A., Shamji, A.F., *et al.* (2011). Selective killing of cancer cells by a small molecule targeting the stress response to ROS. Nature *475*, 231-234.
Renkawek, K., Stege, G.J., and Bosman, G.J. (1999). Dementia, gliosis and expression of the small heat shock proteins hsp27 and alpha B-crystallin in Parkinson's disease. Neuroreport *10*, 2273-2276.
Riccio, M., Di Giaimo, R., Pianetti, S., Palmieri, P.P., Melli, M., and Santi, S. (2001). Nuclear localization of cystatin B, the cathepsin inhibitor implicated in myoclonus epilepsy (EPM1). Experimental cell research *262*, 84-94.
Riccio, M., Santi, S., Dembic, M., Di Giaimo, R., Cipollini, E., Costantino-Ceccarini, E., Ambrosetti, D., Maraldi, N.M., and Melli, M. (2005). Cell-specific expression of the epm1 (cystatin B) gene in developing rat cerebellum. Neurobiology of disease *20*, 104-114.
Rogalla, T., Ehrnsperger, M., Preville, X., Kotlyarov, A., Lutsch, G., Ducasse, C., Paul, C., Wieske, M., Arrigo, A.P., Buchner, J., *et al.* (1999). Regulation of Hsp27 oligomerization, chaperone function, and protective activity against oxidative stress/tumor necrosis factor alpha by phosphorylation. The Journal of biological chemistry *274*, 18947-18956.
Rossi, D., Cozzio, A., Flechsig, E., Klein, M.A., Rulicke, T., Aguzzi, A., and Weissmann, C. (2001). Onset of ataxia and Purkinje cell loss in PrP null mice inversely correlated with Dpl level in brain. The EMBO journal *20*, 694-702.
Saeed, A.I., Sharov, V., White, J., Li, J., Liang, W., Bhagabati, N., Braisted, J., Klapa, M., Currier, T., Thiagarajan, M., *et al.* (2003). TM4: a free, open-source system for microarray data management and analysis. Biotechniques *34*, 374-378.
Salinthone, S., Tyagi, M., and Gerthoffer, W.T. (2008). Small heat shock proteins in smooth muscle. Pharmacology & therapeutics *119*, 44-54.
Santoro, M.G. (2000). Heat shock factors and the control of the stress response. Biochemical Pharmacology *59*, 55-63.
Sarkar, S., Carroll, B., Buganim, Y., Maetzel, D., Ng, A.H., Cassady, J.P., Cohen, M.A., Chakraborty, S., Wang, H., Spooner, E., *et al.* (2013). Impaired autophagy in the lipid-storage disorder Niemann-Pick type C1 disease. Cell reports *5*, 1302-1315.
Sarna, J., Miranda, S.R., Schuchman, E.H., and Hawkes, R. (2001). Patterned cerebellar Purkinje cell death in a transgenic mouse model of Niemann Pick type A/B disease. The European journal of neuroscience *13*, 1873-1880.
Sarna, J.R., and Hawkes, R. (2003). Patterned Purkinje cell death in the cerebellum. Prog Neurobiol *70*, 473-507.
Sarna, J.R., Larouche, M., Marzban, H., Sillitoe, R.V., Rancourt, D.E., and Hawkes, R. (2003). Patterned Purkinje cell degeneration in mouse models of Niemann-Pick type C disease. The Journal of comparative neurology *456*, 279-291.
Schuchman, E.H., and Wasserstein, M.P. (2015). Types A and B Niemann-Pick disease. Best practice & research Clinical endocrinology & metabolism *29*, 237-247.
Schultz, M.L., Tecedor, L., Chang, M., and Davidson, B.L. (2011). Clarifying lysosomal storage diseases. Trends in neurosciences *34*, 401-410.

Settembre, C., Fraldi, A., Medina, D.L., and Ballabio, A. (2013). Signals from the lysosome: a control centre for cellular clearance and energy metabolism. Nature reviews Molecular cell biology *14*, 283-296.

Shimizu, S., Kanaseki, T., Mizushima, N., Mizuta, T., Arakawa-Kobayashi, S., Thompson, C.B., and Tsujimoto, Y. (2004). Role of Bcl-2 family proteins in a non-apoptotic programmed cell death dependent on autophagy genes. Nature cell biology *6*, 1221-1228.

Shimura, H., Miura-Shimura, Y., and Kosik, K.S. (2004). Binding of tau to heat shock protein 27 leads to decreased concentration of hyperphosphorylated tau and enhanced cell survival. The Journal of biological chemistry *279*, 17957-17962.

Siklos, M., BenAissa, M., and Thatcher, G.R.J. (2015). Cysteine proteases as therapeutic targets: does selectivity matter? A systematic review of calpain and cathepsin inhibitors. Acta Pharmaceutica Sinica B *5*, 506-519.

Sistonen, L., Sarge, K.D., Phillips, B., Abravaya, K., and Morimoto, R.I. (1992). Activation of heat shock factor 2 during hemin-induced differentiation of human erythroleukemia cells. Molecular and cellular biology *12*, 4104-4111.

Sleat, D.E., Wiseman, J.A., El-Banna, M., Kim, K.H., Mao, Q., Price, S., Macauley, S.L., Sidman, R.L., Shen, M.M., Zhao, Q., *et al.* (2004). A mouse model of classical late-infantile neuronal ceroid lipofuscinosis based on targeted disruption of the CLN2 gene results in a loss of tripeptidyl-peptidase I activity and progressive neurodegeneration. J Neurosci *24*, 9117-9126.

Smith, D., Wallom, K.-L., Williams, I.M., Jeyakumar, M., and Platt, F.M. (2009). Beneficial effects of anti-inflammatory therapy in a mouse model of Niemann-Pick disease type C1. Neurobiology of disease *36*, 242-251.

Spiegel, S., and Milstien, S. (2003). Sphingosine-1-phosphate: an enigmatic signalling lipid. Nat Rev Mol Cell Biol *4*, 397-407.

Stahelin, R.V., Digman, M.A., Medkova, M., Ananthanarayanan, B., Melowic, H.R., Rafter, J.D., and Cho, W. (2005). Diacylglycerol-induced membrane targeting and activation of protein kinase Cepsilon: mechanistic differences between protein kinases Cdelta and Cepsilon. The Journal of biological chemistry *280*, 19784-19793.

Stetler, R.A., Gao, Y., Zhang, L., Weng, Z., Zhang, F., Hu, X., Wang, S., Vosler, P., Cao, G., Sun, D., *et al.* (2012). Phosphorylation of HSP27 by protein kinase D is essential for mediating neuroprotection against ischemic neuronal injury. The Journal of neuroscience : the official journal of the Society for Neuroscience *32*, 2667-2682.

Sulzer, D., and Surmeier, D.J. (2013). Neuronal vulnerability, pathogenesis, and Parkinson's disease. Movement disorders : official journal of the Movement Disorder Society *28*, 715-724.

Sumoza-Toledo, A., and Penner, R. (2011). TRPM2: a multifunctional ion channel for calcium signalling. The Journal of Physiology *589*, 1515-1525.

Syntichaki, P., Xu, K., Driscoll, M., and Tavernarakis, N. (2002). Specific aspartyl and calpain proteases are required for neurodegeneration in C. elegans. Nature *419*, 939-944.

Takahashi, H., Ikeuchi, T., Honma, Y., Hayashi, S., and Tsuji, S. (1998). Autosomal dominant cerebellar ataxia (SCA6): clinical, genetic and neuropathological study in a family. Acta Neuropathol *95*, 333-337.

Takuma, K., Yao, J., Huang, J., Xu, H., Chen, X., Luddy, J., Trillat, A.C., Stern, D.M., Arancio, O., and Yan, S.S. (2005). ABAD enhances Abeta-induced cell stress via mitochondrial

dysfunction. FASEB journal : official publication of the Federation of American Societies for Experimental Biology *19*, 597-598.
Tavani, F., Zimmerman, R.A., Berry, G.T., Sullivan, K., Gatti, R., and Bingham, P. (2003). Ataxia-telangiectasia: the pattern of cerebellar atrophy on MRI. Neuroradiology *45*, 315-319.
Taylor, R.C., Cullen, S.P., and Martin, S.J. (2008). Apoptosis: controlled demolition at the cellular level. Nature reviews Molecular cell biology *9*, 231-241.
te Vruchte, D., Lloyd-Evans, E., Veldman, R.J., Neville, D.C., Dwek, R.A., Platt, F.M., van Blitterswijk, W.J., and Sillence, D.J. (2004). Accumulation of glycosphingolipids in Niemann-Pick C disease disrupts endosomal transport. The Journal of biological chemistry *279*, 26167-26175.
Terman, A., Kurz, T., Gustafsson, B., and Brunk, U.T. (2006). Lysosomal labilization. IUBMB life *58*, 531-539.
Tissieres, A., Mitchell, H.K., and Tracy, U.M. (1974). Protein synthesis in salivary glands of Drosophila melanogaster: relation to chromosome puffs. Journal of molecular biology *84*, 389-398.
Tolbert, D.L., Ewald, M., Gutting, J., and La Regina, M.C. (1995). Spatial and temporal pattern of Purkinje cell degeneration in shaker mutant rats with hereditary cerebellar ataxia. The Journal of comparative neurology *355*, 490-507.
Torvik, A., and Torp, S. (1986). The prevalence of alcoholic cerebellar atrophy. A morphometric and histological study of an autopsy material. J Neurol Sci *75*, 43-51.
Toth, M.E., Szegedi, V., Varga, E., Juhasz, G., Horvath, J., Borbely, E., Csibrany, B., Alfoldi, R., Lenart, N., Penke, B., *et al.* (2013). Overexpression of Hsp27 ameliorates symptoms of Alzheimer's disease in APP/PS1 mice. Cell stress & chaperones *18*, 759-771.
Towatari, T., Nikawa, T., Murata, M., Yokoo, C., Tamai, M., Hanada, K., and Katunuma, N. (1991). Novel epoxysuccinyl peptides. A selective inhibitor of cathepsin B, in vivo. FEBS letters *280*, 311-315.
Tsubokawa, T., Yamaguchi-Okada, M., Calvert, J.W., Solaroglu, I., Shimamura, N., Yata, K., and Zhang, J.H. (2006). Neurovascular and neuronal protection by E64d after focal cerebral ischemia in rats. Journal of neuroscience research *84*, 832-840.
Tsujimoto, Y., and Shimizu, S. (2005). Another way to die: autophagic programmed cell death. Cell death and differentiation *12 Suppl 2*, 1528-1534.
Turk, B., Bieth, J.G., Bjork, I., Dolenc, I., Turk, D., Cimerman, N., Kos, J., Colic, A., Stoka, V., and Turk, V. (1995). Regulation of the activity of lysosomal cysteine proteinases by pH-induced inactivation and/or endogenous protein inhibitors, cystatins. Biological chemistry Hoppe-Seyler *376*, 225-230.
Turk, B., Dolenc, I., Turk, V., and Bieth, J.G. (1993). Kinetics of the pH-induced inactivation of human cathepsin L. Biochemistry *32*, 375-380.
Turk, B., Dolenc, I., Zerovnik, E., Turk, D., Gubensek, F., and Turk, V. (1994). Human cathepsin B is a metastable enzyme stabilized by specific ionic interactions associated with the active site. Biochemistry *33*, 14800-14806.
Turk, B., Stoka, V., Rozman-Pungercar, J., Cirman, T., Droga-Mazovec, G., Oresic, K., and Turk, V. (2002). Apoptotic pathways: involvement of lysosomal proteases. Biological chemistry *383*, 1035-1044.
Turk, V., and Bode, W. (1991). The cystatins: protein inhibitors of cysteine proteinases. FEBS letters *285*, 213-219.

Turk, V., Stoka, V., Vasiljeva, O., Renko, M., Sun, T., Turk, B., and Turk, D. (2012). Cysteine cathepsins: from structure, function and regulation to new frontiers. Biochimica et biophysica acta *1824*, 68-88.

Tusher, V.G., Tibshirani, R., and Chu, G. (2001). Significance analysis of microarrays applied to the ionizing radiation response. Proc Natl Acad Sci U S A *98*, 5116-5121.

Ullio, C., Casas, J., Brunk, U.T., Sala, G., Fabriàs, G., Ghidoni, R., Bonelli, G., Baccino, F.M., and Autelli, R. (2012). Sphingosine mediates TNFα-induced lysosomal membrane permeabilization and ensuing programmed cell death in hepatoma cells. Journal of Lipid Research *53*, 1134-1143.

Valencia, A., and Moran, J. (2004). Reactive oxygen species induce different cell death mechanisms in cultured neurons. Free radical biology & medicine *36*, 1112-1125.

van der Stappen, J.W., Williams, A.C., Maciewicz, R.A., and Paraskeva, C. (1996). Activation of cathepsin B, secreted by a colorectal cancer cell line requires low pH and is mediated by cathepsin D. International journal of cancer Journal international du cancer *67*, 547-554.

van der Weerd, L., Tariq Akbar, M., Aron Badin, R., Valentim, L.M., Thomas, D.L., Wells, D.J., Latchman, D.S., Gadian, D.G., Lythgoe, M.F., and de Belleroche, J.S. (2010). Overexpression of heat shock protein 27 reduces cortical damage after cerebral ischemia. Journal of cerebral blood flow and metabolism : official journal of the International Society of Cerebral Blood Flow and Metabolism *30*, 849-856.

Vanier, M.T. (2010). Niemann-Pick disease type C. Orphanet journal of rare diseases *5*, 16.

Vanier, M.T. (2013). Niemann-Pick diseases. Handbook of clinical neurology *113*, 1717-1721.

Vanier, M.T., and Millat, G. (2003). Niemann-Pick disease type C. Clin Genet *64*, 269-281.

Varfolomeev, E.E., Schuchmann, M., Luria, V., Chiannilkulchai, N., Beckmann, J.S., Mett, I.L., Rebrikov, D., Brodianski, V.M., Kemper, O.C., Kollet, O., *et al.* (1998). Targeted disruption of the mouse Caspase 8 gene ablates cell death induction by the TNF receptors, Fas/Apo1, and DR3 and is lethal prenatally. Immunity *9*, 267-276.

Vazquez, M.C., Balboa, E., Alvarez, A.R., and Zanlungo, S. (2012). Oxidative stress: a pathogenic mechanism for Niemann-Pick type C disease. Oxidative medicine and cellular longevity *2012*, 205713.

Vleminckx, V., Van Damme, P., Goffin, K., Delye, H., Van Den Bosch, L., and Robberecht, W. (2002). Upregulation of HSP27 in a transgenic model of ALS. Journal of neuropathology and experimental neurology *61*, 968-974.

Wagstaff, M.J., Collaco-Moraes, Y., Smith, J., de Belleroche, J.S., Coffin, R.S., and Latchman, D.S. (1999). Protection of neuronal cells from apoptosis by Hsp27 delivered with a herpes simplex virus-based vector. The Journal of biological chemistry *274*, 5061-5069.

Walkley, S.U., and Suzuki, K. (2004). Consequences of NPC1 and NPC2 loss of function in mammalian neurons. Biochimica et biophysica acta *1685*, 48-62.

Wang, T., and Morgan, J.I. (2007). The Purkinje cell degeneration (pcd) mouse: an unexpected molecular link between neuronal degeneration and regeneration. Brain Res *1140*, 26-40.

Waza, M., Adachi, H., Katsuno, M., Minamiyama, M., Sang, C., Tanaka, F., Inukai, A., Doyu, M., and Sobue, G. (2005). 17-AAG, an Hsp90 inhibitor, ameliorates polyglutamine-mediated motor neuron degeneration. Nat Med *11*, 1088-1095.

Wei, H., Kim, S.J., Zhang, Z., Tsai, P.C., Wisniewski, K.E., and Mukherjee, A.B. (2008). ER and oxidative stresses are common mediators of apoptosis in both neurodegenerative and non-neurodegenerative lysosomal storage disorders and are alleviated by chemical chaperones. Human molecular genetics *17*, 469-477.

Welsh, J.P., Yuen, G., Placantonakis, D.G., Vu, T.Q., Haiss, F., O'Hearn, E., Molliver, M.E., and Aicher, S.A. (2002). Why do Purkinje cells die so easily after global brain ischemia? Aldolase C, EAAT4, and the cerebellar contribution to posthypoxic myoclonus. Adv Neurol *89*, 331-359.

Werneburg, N., Guicciardi, M.E., Yin, X.M., and Gores, G.J. (2004). TNF-alpha-mediated lysosomal permeabilization is FAN and caspase 8/Bid dependent. American journal of physiology Gastrointestinal and liver physiology *287*, G436-443.

Werneburg, N.W., Guicciardi, M.E., Bronk, S.F., and Gores, G.J. (2002). Tumor necrosis factor-alpha-associated lysosomal permeabilization is cathepsin B dependent. American journal of physiology Gastrointestinal and liver physiology *283*, G947-956.

Wilkinson, J.M., and Pollard, I. (1993). Immunohistochemical localisation of the 25 kDa heat shock protein in unstressed rats: possible functional implications. The Anatomical record *237*, 453-457.

Winkelman, M.D., and Hines, J.D. (1983). Cerebellar degeneration caused by high-dose cytosine arabinoside: a clinicopathological study. Ann Neurol *14*, 520-527.

Xu, S., Benoff, B., Liou, H.L., Lobel, P., and Stock, A.M. (2007). Structural basis of sterol binding by NPC2, a lysosomal protein deficient in Niemann-Pick type C2 disease. The Journal of biological chemistry *282*, 23525-23531.

Yakovlev, A.A., Gorokhovatsky, A.Y., Onufriev, M.V., Beletsky, I.P., and Gulyaeva, N.V. (2008). Brain cathepsin B cleaves a caspase substrate. Biochemistry Biokhimiia *73*, 332-336.

Yamamoto, A., Kaji, T., Tomoo, K., Ishida, T., Inoue, M., Murata, M., and Kitamura, K. (1992). Crystallization and preliminary X-ray study of the cathepsin B complexed with CA074, a selective inhibitor. Journal of molecular biology *227*, 942-944.

Yamashima, T. (2000). Implication of cysteine proteases calpain, cathepsin and caspase in ischemic neuronal death of primates. Progress in neurobiology *62*, 273-295.

Yang, C., Trent, S., Ionescu-Tiba, V., Lan, L., Shioda, T., Sgroi, D., and Schmidt, E.V. (2006). Identification of cyclin D1- and estrogen-regulated genes contributing to breast carcinogenesis and progression. Cancer research *66*, 11649-11658.

Yang, D.S., Stavrides, P., Mohan, P.S., Kaushik, S., Kumar, A., Ohno, M., Schmidt, S.D., Wesson, D., Bandyopadhyay, U., Jiang, Y., *et al.* (2011). Reversal of autophagy dysfunction in the TgCRND8 mouse model of Alzheimer's disease ameliorates amyloid pathologies and memory deficits. Brain : a journal of neurology *134*, 258-277.

Yeung, B.H., Huang, D.C., and Sinicrope, F.A. (2006). PS-341 (bortezomib) induces lysosomal cathepsin B release and a caspase-2-dependent mitochondrial permeabilization and apoptosis in human pancreatic cancer cells. The Journal of biological chemistry *281*, 11923-11932.

Yoneshige, A., Suzuki, K., and Matsuda, J. (2010). A mutation in the saposin C domain of the sphingolipid activator protein (Prosaposin) gene causes neurodegenerative disease in mice. J Neurosci Res *88*, 2118-2134.

Yu, L., Alva, A., Su, H., Dutt, P., Freundt, E., Welsh, S., Baehrecke, E.H., and Lenardo, M.J. (2004). Regulation of an ATG7-beclin 1 Program of Autophagic Cell Death by Caspase-8. Science (New York, NY) *304*, 1500-1502.

Yu, T., Chung, C., Shen, D., Xu, H., and Lieberman, A.P. (2012). Ryanodine receptor antagonists adapt NPC1 proteostasis to ameliorate lipid storage in Niemann-Pick type C disease fibroblasts. Human molecular genetics *21*, 3205-3214.

Yu, T., Shakkottai, V.G., Chung, C., and Lieberman, A.P. (2011). Temporal and cell-specific deletion establishes that neuronal Npc1 deficiency is sufficient to mediate neurodegeneration. Human molecular genetics *20*, 4440-4451.

Yu, W., Gong, J.-S., Ko, M., Garver, W.S., Yanagisawa, K., and Michikawa, M. (2005). Altered Cholesterol Metabolism in Niemann-Pick Type C1 Mouse Brains Affects Mitochondrial Function. Journal of Biological Chemistry *280*, 11731-11739.

Yuan, X.-M., Li, W., Dalen, H., Lotem, J., Kama, R., Sachs, L., and Brunk, U.T. (2002). Lysosomal destabilization in p53-induced apoptosis. Proceedings of the National Academy of Sciences *99*, 6286-6291.

Zampieri, S., Mellon, S.H., Butters, T.D., Nevyjel, M., Covey, D.F., Bembi, B., and Dardis, A. (2009). Oxidative stress in NPC1 deficient cells: protective effect of allopregnanolone. Journal of Cellular and Molecular Medicine *13*, 3786-3796.

Zervas, M., Somers, K.L., Thrall, M.A., and Walkley, S.U. (2001). Critical role for glycosphingolipids in Niemann-Pick disease type C. Current biology : CB *11*, 1283-1287.

Zhang, X.M., Ng, A.H., Tanner, J.A., Wu, W.T., Copeland, N.G., Jenkins, N.A., and Huang, J.D. (2004). Highly restricted expression of Cre recombinase in cerebellar Purkinje cells. Genesis (New York, NY : 2000) *40*, 45-51.

Zhao, M., Antunes, F., Eaton, J.W., and Brunk, U.T. (2003). Lysosomal enzymes promote mitochondrial oxidant production, cytochrome c release and apoptosis. European journal of biochemistry / FEBS *270*, 3778-3786.

Zhou, S., Davidson, C., McGlynn, R., Stephney, G., Dobrenis, K., Vanier, M.T., and Walkley, S.U. (2011). Endosomal/lysosomal processing of gangliosides affects neuronal cholesterol sequestration in Niemann-Pick disease type C. The American journal of pathology *179*, 890-902.